TECHNISCHE UNIVERSITÄT MÜNCHEN

Wissenschaftszentrum Weihenstephan für Ernährung, Landnutzung und Umwelt

Lehrstuhl für Mikrobiologie

Insights into trophic connectivities and carbon flow through bacterial members of a belowground food web

Lu Zhang

Vollständiger Abdruck der von der Fakultät Wissenschaftszentrum Weihenstephan für Ernährung, Landnutzung und Umwelt der Technischen Universität München zur Erlangung des akademischen Grades eines Doktors der Naturwissenschaften genehmigten Dissertation.

Vorsitzende(r):   Prof. Dr. Jürgen P. Geist

Prüfer der Dissertation:

1. Priv.-Doz. Dr. Tillmann Lueders
2. Prof. Dr. Ingrid Kögel-Knabner

Die Dissertation wurde am 10.04.2018 bei der Technischen Universität München eingereicht und durch die Fakultät Wissenschaftszentrum Weihenstephan für Ernährung, Landnutzung und Umwelt am 21.06.2018 angenommen.

Abstract

An enormous diversity of organisms thrives in soil, controlling geochemical processes and considerably impacting global carbon cycle. Particularly in plant-influenced soil, bacteria are the primary decomposers of carbon inputs of various quality and complexity and channel them into multi-trophic soil food webs. Despite their fundamental importance in soil carbon turnover and ecosystem services, the role of bacteria, their biodiversity, function and dynamics are still rather poorly understood, especially in comparison to organisms of higher trophic levels, such as protozoa, nematodes and other soil fauna. Moreover, while population-level activities and functions of soil eukaryotes are adequately reflected, in existing models of soil food webs and carbon cycling, specific soil microbiota still await a more general and quantitative consideration. My thesis aims to provide comprehensive insights into the specific roles of distinct bacterial populations in an exemplary soil food web of an arable soil cropped with maize, by addressing the following fundamental research questions:

i) Importance of intra-bacterial predation. Besides acting as primary decomposers of soil organic matter at the base of soil food webs, some bacteria can prey on other bacteria and thus constitute a secondary trophic link in competition to that of protozoa. Intra-bacterial predation in soil has received little attention up to date, and its ecological relevance remains to be elucidated. I conducted a laboratory microcosm experiment to investigate the predation of amended bacterial prey by pro- and eukaryotic micropredators. I query how soil compartment (rhizosphere vs. bulk soil) and nature of prey (Gram-positive vs. Gram-negative) influence predation outcomes of ^{13}C-labelled biomass of *Pseudomonas putida* and *Arthrobacter globiformis*. *P. putida* was consumed much more rapidly than *A. globiformis*. Using rRNA-SIP, I identified an array of predatory bacteria and microeukaryotes utilising carbon derived from the amended biomass. Amongst the bacteria, only one defined lineage of the *Myxococcales* (*Hallangium* spp.) was able to sequester ^{13}C from amended *A. globiformis*, whereas a considerable diversity of predatory bacteria incorporated ^{13}C derived from *P. putida*. Diverse groups of heterotrophic protists, especially amoeba, were observed to incorporate ^{13}C from both strains, but with pronounced niche differentiation between rhizosphere and bulk soil. This provides novel insights into

niche partitioning between bacterial and eukaryotic micropredators in soil, driven not only by the nature of bacterial prey itself, but also by soil compartments.

ii) Vertical transport of bacteria with seepage water. Bacteria translocated from top soils have been speculated to be an important source of biomass for subsoils and groundwater. Upon strong precipitation, substantial amounts of mobile organic matter are transported from plant-associated top soil layers to deeper zones and microbes are assumed to constitute part of this carbon flux. Using lysimeters installed at the field site, I characterised bacterial populations mobilised from rooted top soil triggered by strong rain events, to uncover potential taxon-specific distinctions in mobilisation and to address seasonal variation in vertical bacterial transport. I sampled fresh seepage water directly after natural and artificial rainfall, with the latter also under addition of defined pulses of fluorescently-labelled *A. globiformis* cells to the top soil. A specific subset of plant-associated bacterial populations was found to be mobilised after natural rain, with a more pronounced shift observed in mobilised communities in summer compared to a previous study in winter. Time-resolved analyses of seepage water after simulated rain revealed intriguing temporal patterns in the mobilisation of distinct members of the *Bradyrhizobiaceae*, *Comamonadaceae*, and also of candidate phyla including *Microgenomates* and *Parcubacteria*. The recovery of amended bacterial cells was low (0.2-0.6%), but mobilised bacteria could potentially exert influence on bacterial activity and shifts in communities in subsoils. These findings are important for the understanding of general connectivities between microbial metacommunities and carbon pools in soil.

iii) Distribution and dynamics of key bacterial populations at an experimental maize field. Detailed knowledge about soil bacterial pool sizes, diversity as well as distribution patterns is a prerequisite for a quantitative modelling of microbial carbon flows in the soil food web. At a joint experimental maize field near Göttingen, Germany, a long-term field experiment was established with the following treatments: Corn Maize (maize + maize litter, CM), Fodder Maize (maize without litter, FM), Wheat + maize Litter (WL) and Wheat without litter (W). This was a joint initiative of the DFG FOR-918, as a part of which this thesis was conducted. Annual sampling was performed between 2009 and 2013 at 10, 50 and 70 cm of depth. I hypothesized that depth-dependant bacterial community distinction as well as plant and litter effects would become more and more apparent over time. T-RFLP fingerprinting,

quantitative PCR and amplicon sequencing were applied to trace development of overall soil bacterial communities and specific bacterial populations. Soil depth was found to be the most important driver of distinctions in both quantity and composition of bacterial communities. Furthermore, litter amendments affected the bacterial communities in top soil, which became increasingly apparent over time. Difference in bacterial community structure and overall quantity in root-associated horizon was also observed between maize and wheat treatments. Interestingly, some bacterial lineages previously identified in laboratory labelling experiments to actively degrade rhizosphere or detritusphere carbon substrates, like *Arthrobacter* spp. and *Flavobacterium* spp. were found to display consistent distribution patterns in the field, substantiating their ecological importance in the investigated soil. This reveals a long-term selection of specific bacterial populations by distinct plant-derived substrate inputs in the field.

In summary, my thesis provides important insights into intrabacterial predation in the investigated soil and proposes a niche differentiation between micropredators driven by prey nature and by soil compartments. The results on selective event-driven vertical transport of indigenous soil microbes improve our current understanding of the organismic carbon flow between soil compartments. Finally, long-term patterns of bacterial community response to distinct carbon inputs and the distribution of keystone bacterial food web constituents at an actual field site provide important cues for the incorporation of population-specific distribution patterns and carbon fluxes into up-to-date food web models. This will allow for a more integrative perspective of the involvement of distinct microbial populations in central ecosystem functions, and advance our capacities for predictive processes understanding.

Zusammenfassung

Böden beherbergen eine große Diversität an Organismen. Diese kontrollieren maßgebliche geochemische Prozesse und üben einen großen Einfluss auf den globalen Kohlenstoffkreislauf aus. In durch Pflanzen beeinflussten Böden sind es insbesondere die Bakterien, die primär an der Zersetzung von Kohlenstoffeinträgen unterschiedlicher Qualität und Komplexität beteiligt sind, die dadurch in ein multi-trophisches Nahrungsnetz innerhalb des Bodens eingeleitet werden. Trotz ihrer großen Bedeutung für den Kohlenstoffkreislauf und für viele andere Ökosystem-Dienstleistungen, ist die Bedeutung der Bakterien, ihrer Biodiversität und ihrer Dynamiken noch gering verstanden. Dies trifft insbesondere im Vergleich zu höheren Organismen der Nahrungskette zu, wie zum Beispiel den Protozoen, Nematoden, und andere Organismen der Bodenfauna. Des Weiteren sind die Bodenmikroorganismen bisher nicht ausreichend in quantitativen Modellen des Bodennahrungsnetzes oder der Kohlstoffkreisläufe berücksichtigt. Die vorliegende Dissertation hat zum Ziel, umfassende Einblicke zur spezifischen Funktion unterschiedlicher bakterieller Populationen innerhalb eines Bodennahrungsnetzes zu erarbeiten. Dies erfolgt exemplarisch für einen mit Mais bepflanzten landwirtschaftlichen Boden. Die folgenden grundlegenden Fragen wurden eruiert:

i) Die Bedeutung intra-bakterieller Prädation. Bestimmte Bakterien sind in der Lage, andere Bakterien als Nahrungsquelle zu nutzen, wodurch sie mit den Protozoen auf der nächsthöheren Ebene des Nahrungsnetzes konkurrieren. Die Prädation von Bakterien untereinander wurde im Boden bisher nur wenig untersucht. In dieser Arbeit wurde die Prädation durch prokaryotische und eukaryotische Mikroprädatoren durch die Zugabe von ^{13}C-markierter bakterieller Biomasse von *Pseudomonas putida* und *Arthrobacter globiformis* erstmals untersucht. Im speziellen wurde hinterfragt, wie das Kompartiment (Rhizosphäre vs. normalem Boden) und der Beutetyp (Gram-positiv vs. Gram-negativ) die Prädation beeinflussen. *P. putida* wurde deutlich schneller verwertet als *A. globiformis*. Mittels RNA-SIP konnte eine Vielzahl von bakteriellen Prädatoren und Protozoen identifiziert werden, die die zugegeben Biomasse als Kohlenstoffquelle genutzt hatten. Nur eine Mitglied der *Myxococcales* (*Hallangium* spp.) schien allerdings in der Lage, die Biomasse von *A. globiformis* zu verwerten. Dagegen war eine beachtliche Diversität an bakteriellen Prädatoren an der Verwertung von *P. putida* beteiligt. Diverse Gruppen von Protisten,

insbesondere Amöben, assimilierten ^{13}C von beiden zugegebenen Beutebakterien, allerdings wurden deutlich unterschiedliche Markierungsmuster zwischen Rhizosphäre und dem undurchwurzelten Boden festgestellt. Diese Ergebnisse liefern neue Erkenntnisse zur Definition der ökologischen Nischen zwischen bakteriellen und eukaryotischen Mikroprädatoren im Boden, welche nicht allein durch den Beutetyp, sondern auch durch das Bodenkompartiment gesteuert werden.

ii)   Vertikaler Transport von Bakterien im Sickerwasser. Seit längerem wird angenommen, dass Bakterien aus dem Oberboden einen wichtigen Eintrag für tiefere Bodenzonen und das Grundwasser darstellen können. Nach Starkregenereignissen werden beträchtliche Mengen an organischem Material aus dem Oberboden in tiefere Zonen transportiert. Es wird zudem vermutet, dass Mikroorganismen einen wichtigen Teil dieses Kohlenstoffflusses ausmachen. Mit Hilfe von Feld-Lysimetern wurden in dieser Arbeit bakterielle Gemeinschaften im Sickerwasser charakterisiert. Ziel war es, mögliche populationsspezifische Unterschiede im Mobilisierungsverhalten aufzudecken. Frisches Sickerwasser wurde unmittelbar nach natürlichen und experimentellen Starkregenereignissen beprobt. Bei den simulierten Regenfällen wurden zusätzlich ein definierter Puls an fluoreszenzmarkierten Bakterien hinzugegeben. Es konnte gezeigt werden, dass im Sickerwasser ganz spezifische, aus der Rhizosphäre stammende bakterielle Gemeinschaften zu finden waren. Eine zeitlich aufgelöste Analyse des Sickerwassers ergab klare zeitliche Muster der Mobilisierung, besonders für Arten innerhalb der *Bradyrhizobiaceae* und *Comamonadaceae*, sowie der Candidate-Phyla *Microgenomates* und *Parcubacteria*. Die Wiederfindungsrate der zugegebenen Zellen betrug lediglich 0.2 - 0.6%. Dennoch könnten die mobilisierten Bakterien aus dem Oberboden die Aktivität und Zusammensetzung bakterieller Gemeinschaften im Unterboden durchaus beeinflussen. Diese Ergebnisse liefern einen wichtigen Beitrag zum Verständnis der Konnektivität zwischen räumlich getrennten bakteriellen Gemeinschaften und Kohlenstoff-Pools im Boden.

iii)   Dynamik bakterieller Schlüsselpopulationen im Feld. Ein genaues Verständnis der Diversität und räumlichen Verteilung von am Bodennahrungsnetz beteiligten Mikroben ist eine Voraussetzung für die Verbesserung quantitativer Modelle des Kohlenstoffflusses. Diese Arbeit war eingebettet in ein Langzeit-Feldexperiment der DFG-Forschergruppe FOR-918, innerhalb derer verschiedene landwirtschaftliche

Treatments realisiert wurden: Mais + Maisstreu (CM), Mais ohne Streu (FM), Weizen + Maisstreu (WL) und Weizen ohne Streu (W). Zwischen 2009 und 2013 wurden gemeinsame jährliche Beprobungen durchgeführt, wobei Bodenproben aus 10, 50 und 70 cm Tiefe entnommen wurden. Eine grundlegende Hypothese war, dass die unterschiedlichen Pflanzenarten und Streu-Behandlungen über die Zeit klare Unterschiede der bakteriellen Gemeinschaften im Boden selektieren würden. Die Bodentiefe erwies sich als stärkster Treiber der Artenzusammensetzung und Abundanz der bakteriellen Gemeinschaften im Feld. Des Weiteren wurde ein Einfluss der Streuzugabe auf die bakteriellen Gemeinschaften im Oberboden festgestellt, welcher sich mit der Zeit verstärkte. Klare Unterschiede in der Zusammensetzung der bakteriellen Gemeinschaften ließen sich zudem zwischen der Rhizosphäre von Mais und Weizen erkennen. Besonders interessant war, dass bestimmte Bakterienarten, für die bereits vorher in Laborexperimenten eine Beteiligung an bestimmten Kohlenstoffflüssen der Rhizosphäre oder Detritusphäre nachgewiesen werden konnte, auch im Feld konsistente räumliche Verteilungsmuster aufzeigten. Dies unterstrich deren ökologische Bedeutung in dem untersuchten Boden. Diese Ergebnisse belegen eine langfristige Selektion von spezifischen bakteriellen Populationen durch den Eintrag bestimmter pflanzenbürtiger Substrate im Feld.

Zusammengefasst liefert diese Dissertation wichtige Einblicke zur spezifischen Rolle und Nischenverteilung an einem exemplarischen Bodennahrungsnetz beteiligter bakterieller Populationen. Die Relevanz intrabakterieller Prädation wird erstmals systematisch für verschiedene Beute-Spezies und Bodenkompartimente hinterfragt. Der aufgezeigte vertikale Transport von Rhizosphärenbakterien nach Starkregenereignissen und die räumliche Selektion spezifischer bakterieller Population durch pflanzenbürtigen Kohlenstoff verbessert das gegenwärtige Verständnis der Konnektivität und Kohlenstoffflüsse zwischen den Bodenzonen im Feld. Dies ist ein wichtiger Schritt hin zu einer besseren Einbindung von populationsspezifischen und quantitativen mikrobiellen Informationen in aktuelle Nahrungsnetzmodelle. Ein besseres Verständnis und eine robustere Vorhersage zentraler Ökosystem-Dienstleistungen wird dadurch ermöglicht.

Table of content

List of figures

List of tables

Abbreviations

CFDA/SE	5-(and-6)-carboxyfluorescein diacetate, succinimidyl ester	*Msp*I	restriction enzyme of *Moraxella* sp. ATCC 49670
16S rRNA	prokaryotic ribosomal RNA, small subunit	OTU	operational taxonomic unit
		PBS	phosphate buffered saline
18S rRNA	eukaryotic ribosomal RNA, small subunit	PC1	first principal component
		PC2	second principal component
bp	base pairs	PCA	principal component analysis
DFG	Deutsche Forschungsgemeinschaft	PCR	polymerase chain reaction
		PEG	polyethylene glycol
DNA	deoxyribonucleic acid	POC	particulated organic carbon
dNTP	deoxyribonucleotide	qPCR	quantitative polymerase chain reaction
dw	dry weight		
DOC	dissolved organic carbon	RDA	redundancy analysis
EC	electrical conductivity	RNA	ribonucleic acid
EDTA	ethylenediaminetertraacetic acid	rRNA	ribosomal RNA
		RT	reverse transcription
EF	enrichment factor	SIP	stable isotope probing
EOC	extractable organic carbon	SOM	soil organic matter
		sp(p).	species (plural)
e.g.	exempli gratia	*Taq*I	restriction enzyme of *Thermus aquaticus*
et al.	et alii	T-RF	terminal restriction fragment
FAM	carboxyfluorescein	T-RFLP	terminal restriction fragment length polymorphism
FOR-918	DFG Research uint 918 "Carbon flow in belowground food webs assessed by isotope tracers"	U	unit of enzyme activity, $1\mu mol\ min^{-1}$
		vs.	versus
		w/v	weight/volume
GC	gas chromatography		
MS	mass spectrometry		
i.e.	id est		
IRMS	isotope-ratio mass spectrometry		
MANOVA	multivariate analysis of variance		

1. Introduction

1.1. Soil carbon pools and soil food webs

1.1.1. Role of soil organisms in terrestrial carbon cycling

Soil represents the third largest carbon pool on our planet, next to ocean and fossil fuels. It comprises both soil organic carbon (SOC) and soil inorganic carbon (SIC) pools (Lal, 2008). The pool size of soil carbon and its close interaction with atmospheric carbon results in the fact that even small fractions of carbon released from or entering the soils can have considerable impacts on global climate change (Heimann & Reichstein, 2008). Thus, researchers have accumulated detailed knowledge about total amounts, individual pools and turnover of carbon in soil (Amundson, 2001, Janzen, 2004, Pendall & King, 2007, Marschner *et al.*, 2008, von Lützow *et al.*, 2008, Bol *et al.*, 2009, Todorovic *et al.*, 2010, Schmidt *et al.*, 2011). In contrast, the enormous diversity of soil (micro-) biota, their complex interactions and influence on soil carbon cycling remain poorly understood.

The total size of soil carbon pools is controlled by the critical balance between primary production and decomposition. Plants serve as the primary carbon input to many terrestrial systems. While abiotic factors, such as soil water content, pH and temperature, can influence carbon decomposition rates and cycling, the activity of soil biota largely determines the decomposition of soil organic matter, particularly plant-derived carbon (Gessner *et al.*, 2010, Nielsen *et al.*, 2011, Schimel & Schaeffer, 2012, Gougoulias *et al.*, 2014). Soils harbor a huge diversity of living organisms, including bacteria, fungi, protozoa, nematodes, mesofauna and macrofauna. Species richness and community structure of soil biota play a role in carbon cycling (Nielsen *et al.*, 2011), especially in the rhizosphere and the detritusphere (Schimel & Schaeffer, 2012). It is therefore of prominent importance to generate a profound understanding of soil biodiversity and biotic interactions as regulators of carbon fluxes and ecosystem functioning in soil.

1.1.2. Multi-trophic food webs in plant-influenced soils

Plants introduce a vast amount of carbon into the soil organic carbon pool (Cebrian, 1999), and soil biota are directly responsible for the decomposition and sequestration of plant-derived organic matter. Soil organisms are engaged in dynamic trophic

interactions, i.e. predator-prey interactions amongst each other resulting in complex networks: soil food webs. A conceptual scheme of organismic trophic interactions in soil food webs is given in Figure 1, with diverse soil organisms involved at multiple trophic levels.
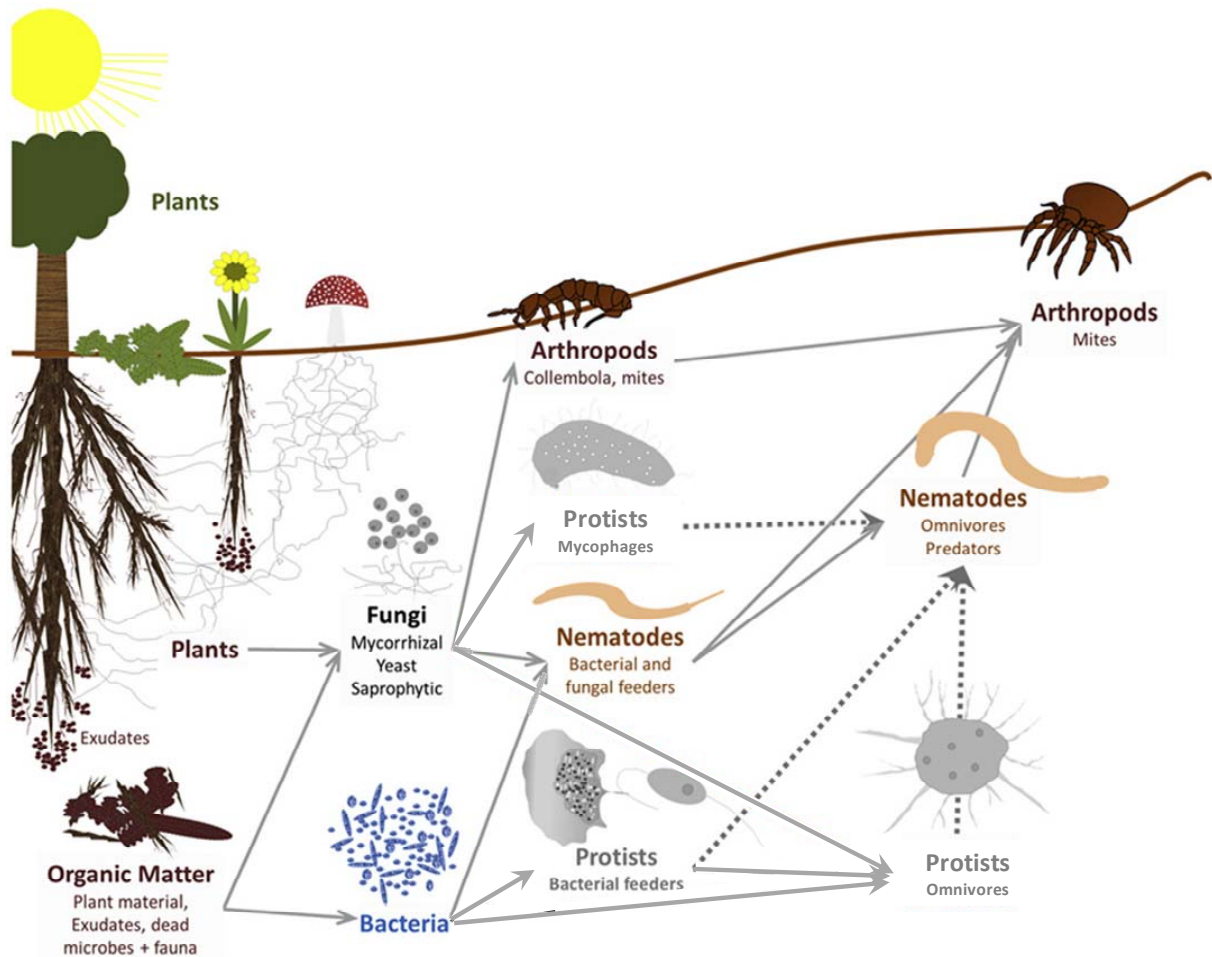
Figure 1. An exemplary food web in soil, as driven by plant inputs and trophic interactions, adapted from Geisen *et al.*, 2016.

In plant-influenced soils, two types of plant-derived carbon inputs prevail: rhizodeposits, the more labile carbon resource, and plant litter, the more recalcitrant and slowly decomposable substrate. Soil microbes, as the primary decomposers of plant rhizodeposits and residues, with their specific enzymes capable of breaking down organic matter, play a major role in channeling plant-derived carbon into belowground food webs. Carbon is subsequently transferred to other groups of soil organisms by predation, through their metabolic products (i.e. crossfeeding), or via their dead biomass being consumed.

16

Involved soil animals comprise the microfauna (e.g. protozoa and nematodes), mesofauna (e.g. Collembola and mites) and macrofauna (e.g. earthworms and isopods). The microfauna dominate the consumption of bacterial biomass and are thus discussed as "the bacterial energy channel", whereas fungi, fungal feeders (predominantly mesofauna) and higher predators form the "fungal energy channel" (Moore & Walter, 1988, Wardle & Yeates, 1993). Soil fauna can largely alter the activity and composition of microbiota in soil, usually with important feedbacks to plant growth (Rønn *et al.*, 2002, Scheu, 2002, Bonkowski, 2004, Scheu *et al.*, 2005, Murase *et al.*, 2006, Bell *et al.*, 2010, Anderson *et al.*, 2013). The extraordinarily high biological diversity and prevalence of generalist feeders and omnivory determine the exceptionally complex nature of soil food webs (Scheu & Setälä, 2002, Scheu *et al.*, 2005). Therefore, it is of fundamental importance to study the diversity and activity of bacteria, and their interaction with bacteria-feeding predators as base of soil food webs to understand the entire networks.

1.2. Distribution and dynamics of bacterial populations in plant-influenced soils

1.2.1. Plant-derived carbon inputs of distinct quality for soil microbes

Plants are the most important primary providers of carbon inputs to soil systems. Plant-derived carbon enters soil food webs through two major pathways, via 1) rhizodeposits, the easily degradable carbon resource, and 2) litter, the slowly decomposable plant debris (Figure 2). Plants modify the chemical and physical conditions in soil surrounding the roots by rhizodeposits. Rhizodeposits generally consist of labile carbon substrates, like sugars, carboxylic and amino acids, whereas plant litter comprises recalcitrant carbon compounds, such as lignin and cellulose. Rhizodeposits and plant residues differ in complexity and availability to soil microbes, and are therefore considered to sustain distinct microbial and soil animal consumer communities (Ruess & Ferris, 2004, Elfstrand *et al.*, 2008, Paterson *et al.*, 2008). Root-derived carbon is assumed to enter soil food web predominantly through the arbuscular mycorrhizal fungi (AMF) for mycorrhizal plants (Olsson & Johnson, 2005, Vandenkoornhuyse *et al.*, 2007, Drigo *et al.*, 2010). The AMF subsequently release carbon gradually to associated rhizosphere bacteria and decomposer fungi. Plant carbon input into rhizosphere can also directly flow to non-symbiotic bacterial and

fungal communities via exudate consumption (Drigo *et al.*, 2010). The bacterial energy channel is known to predominate in the degradation of easily decomposable carbon substrates (Moore *et al.*, 2005, Holtkamp *et al.*, 2011).
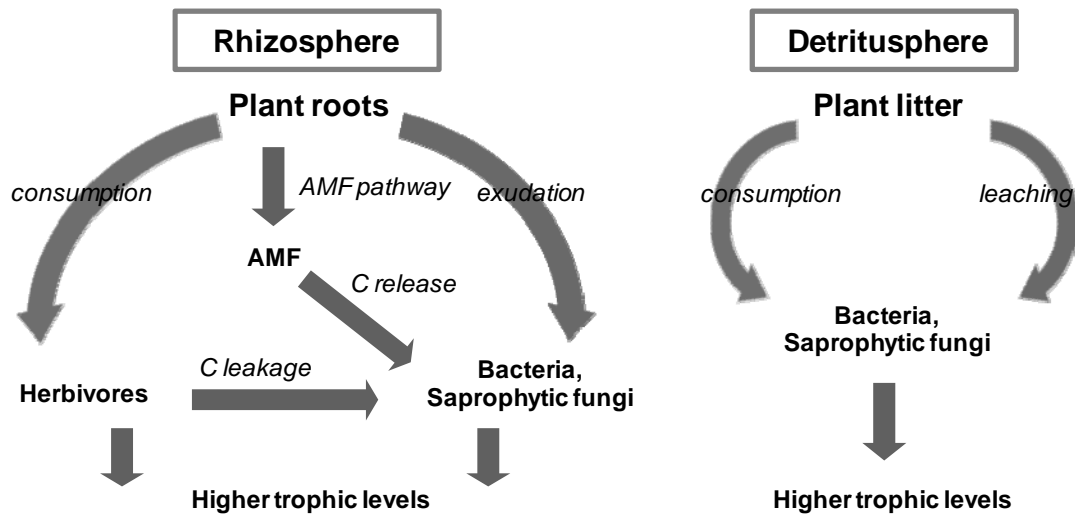
Figure 2. Conceptual model of carbon flow in the soil food web in plant rhizosphere vs. the detritusphere, adapted from Scheu *et al.*, 2005.

In the detritusphere, carbon from plant residues entering into soil is principally considered to be regulated by a distinct array of primary decomposers, also involving bacteria and fungi (Drigo *et al.*, 2010), whereas the fungal channel is favored. Fungal decomposers are taken to contribute more to the decomposition of recalcitrant soil organic matter (SOM) with a wide span of C/N ratios (Frankland, 1998, Dilly *et al.*, 2001). The successive transfer of carbon to higher trophic levels in both systems involves the interactions of these primary decomposers with soil fauna (Fox *et al.*, 2006, Pollierer *et al.*, 2007, Milcu *et al.*, 2008). In addition, living roots can serve as a resource for herbivores, and root herbivory in turn contributes to the regulation of microbial communities via altered root exudation and induction of cell leakage (Poll *et al.*, 2007).

In summary, soil microbes are the fundamental decomposers of plant rhizodeposits and residues, and form the basis of all belowground food webs. While the activities, functions and importance of microeukaryotes in the belowground ecosystem are fairly understood (Bonkowski, 2004, Christensen *et al.*, 2007), the identities of relevant

bacteria and the associated trophic links only start to become uncovered in the recent years (Vandenkoornhuyse *et al.*, 2007, Haichar *et al.*, 2008, Drigo *et al.*, 2010, Lee *et al.*, 2011, Kramer *et al.*, 2016, Hünninghaus *et al.*, submitted). Despite the fundamental roles of the microbial communities in soil carbon flow, their distinct activities in food webs are still rarely represented in carbon cycling models.

1.2.2. Distribution of bacterial communities between soil compartments

It is well-known that microbial communities in soil are shaped by combined abiotic and biotic factors, available energy resources and soil structural properties (Fierer *et al.*, 2003). Labile and recalcitrant carbon substrates are assumed to be consumed by distinct microbial communities (Orwin *et al.*, 2006, Kramer & Gleixner, 2008, Paterson *et al.*, 2008). Other soil characteristics which affect bacterial community composition include pH, nutrient availability, water content and oxygen concentration (Eichorst, et al., 2007, Will, et al., 2010, Gelsomino & Azzellino, 2011). Different soil compartments therefore constitute distinct environmental niches, populated by specific microbiomes (Figure 3; Hartmann *et al.*, 2009, Schimel & Schaeffer, 2012).

Soil microbes are not evenly distributed across soil layers, but are highly concentrated in the top soil horizons. Especially, bacteria and fungi have been observed to display a strong decline in biomass and diversity with altered community compositions over depth (Fierer *et al.*, 2003, LaMontagne *et al.*, 2003, Agnelli *et al.*, 2004, Hansel *et al.*, 2008). The depletion in total amounts of bioavailable organic carbon with depth is suggested to be the major driver of depth-dependent microbial community distribution (Fierer *et al.*, 2003, Hartmann *et al.*, 2009). Not only is a decrease in total carbon amounts observed along soil profiles, but also differences in carbon substrate quality and availability. Specifically in cropped soils, litter input from aboveground can actually be dominating in top soils. In the deeper rooted zone, root exudates and residues represent the dominant energy source. Thus, the changes in microbial communities with soil depth can be attributed to the distinct soil organic matter availability as well as to varied physical and chemical conditions (Kramer & Gleixner, 2006, Hansel *et al.*, 2008, Kramer & Gleixner, 2008).
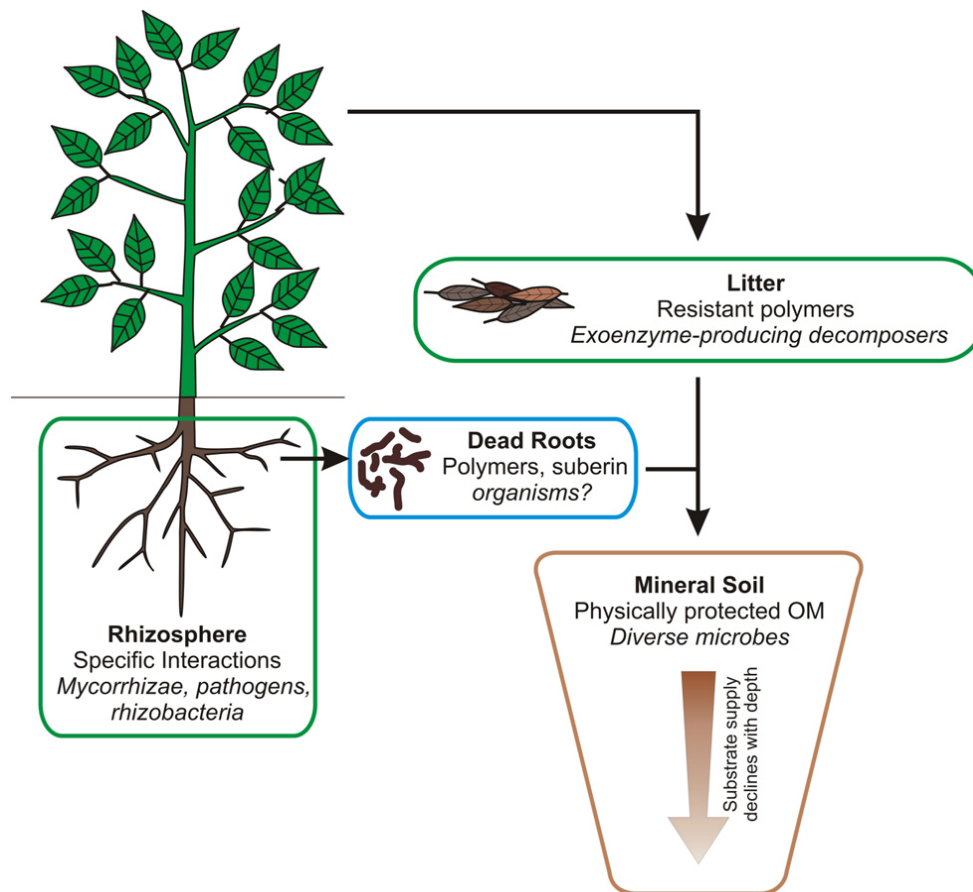
Figure 3. The main compartments in plant-influenced soil, the characteristics controlling microbial function within respective compartment and the dominant organisms therein (from Schimel & Schaeffer, 2012).

As a result, bacteria at depth may function differently from those in the top soil, because microbial communities are generally assumed to be specifically adapted to their local environments (Fritze *et al.*, 2000, Blume *et al.*, 2002). Reflecting the variation in communities of these fundamental components of the belowground food web, biomass and diversity of soil animals also decline with depth, most remarkably observed for the meso- and macrofauna (Ekelund *et al.*, 2001, Sadaka & Ponge, 2003). Particularly, as meso- and macrofauna are scarcely present in subsoil, protozoa and nematodes become the dominant food web members at higher trophic levels therein (Scharroba *et al.*, 2012). Therefore, soil biota have been suggested to constitute structurally distinct and spatially separated food webs over depth, with different energy availability and disconnected metacommunities involved (Scharroba *et al.*, 2012). However, comprehensive studies on soil food webs including all trophic

levels remain rare, and mechanisms of interplay in the networks, especially the predator-prey interaction, remain poorly understood.

1.3. Predation in soil food webs

1.3.1. General role of predation in belowground food webs

Predation is an important regulatory force in all food webs. Classical theories and extensive knowledge about predator-prey interactions are mainly based on studies of plant and animals in aboveground systems, whereas their relevance for microorganisms in belowground food webs remains largely unknown. Due to the uniqueness of belowground systems, an improved understanding of biological interactions therein can certainly enrich current ecological concepts (Scheu & Setälä, 2002). Theory suggests that body size is a fundamental factor determining feeding interactions in food webs (Warren & Lawton, 1987, Cohen *et al.*, 1993), which has also been demonstrated for interaction between microbes and soil invertebrates (Figure 4; Scheu & Setälä, 2002, Scheu *et al.*, 2005). Size-associated features actually influence the trophic status as well as resource-partitioning within food webs (Cohen & Newman, 1985, Woodward & Hildrew, 2002). Bacterial feeders are necessarily small, as small body size enables the predators to access the pore space colonized by bacteria. Therefore the microfauna, which are dominated by protozoa and nematodes, can most effectively predate on bacteria.

Principally, the prey range of predators, i.e. generalists or specialists, influences the relative importance of top-down control vs. bottom-up control of prey populations (Jiang & Morin, 2005). Top-down control refers to the regulation of lower trophic levels by their consumers, whereas with bottom-up control, resource and productivity regulates ecosystem structure. Most soil animals are considered to be generalists rather than specialists in grazing (Scheu *et al.*, 2005), possibly due to the highly packed potential prey and the opaque habitat which makes it difficult to locate specific prey. Top-down control is therefore assumed to be of limited importance in belowground systems (Scheu & Setälä, 2002), in contrast to food webs, for example, in aquatic ecosystems. Nevertheless, top-down control can still be important in certain conditions or for certain prey populations in soils. For instance, bacteria are

assumed to be strongly top-down regulated by protozoa in the rhizosphere (Bonkowski, 2004).
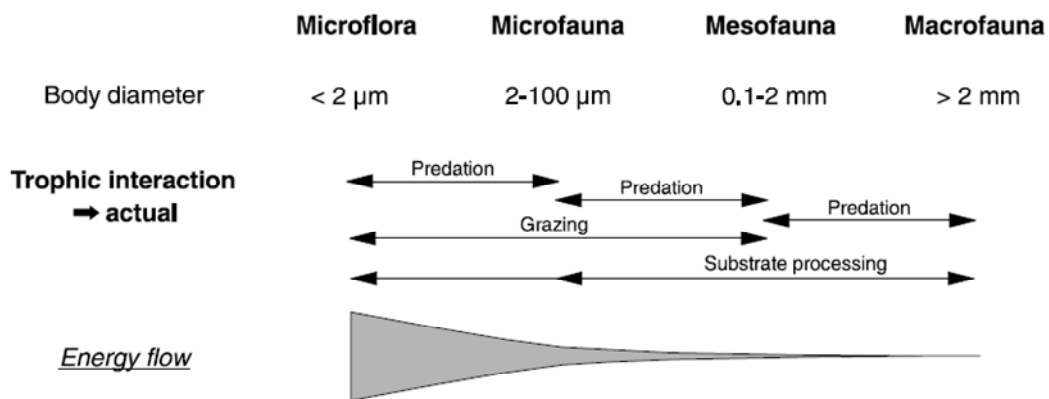
Figure 4. Size-dependent trophic interactions among soil organisms (from Scheu & Setälä, 2002).

An important aspect which adds to the complexity of predation interactions is the occurence of intraguild predation (IGP). IGP refers to the consumption of one predator species by another predator, which also compete for shared prey (Polis *et al.*, 1989). IGP is actually a form of omnivory, and is widespread in soil food webs (Scheu *et al.*, 2005). Ubiquitous in both natural and artificial ecosystems, IGP impacts the suppression of prey populations by multiple predators, while the effect varied across different ecosystems (Vance-Chalcraft *et al.*, 2007).

1.3.2. Bacterial micropredators in terrestrial systems

The three key groups of micropredators predating on bacteria in soil include protists, predatory bacteria and bacteriophages, with distinct predation strategies and community-level impacts (Johnke *et al.*, 2014). While the importance of predation by protozoa on soil bacteria is well understood (Bonkowski, 2004), there has been increasing evidence that also intrabacterial predations may be important in soil food webs and play a role in carbon turnover (Lueders *et al.*, 2006, Murase & Frenzel, 2007, Banning *et al.*, 2010).

Bacterial micropredators that are capable of growing on living bacterial prey as a sole or co-substrate have been found in and cultured from a large variety of habitats, with diverse phylogenetic affiliation (Martin, 2002, Jurkevitch, 2007). Known bacterial micropredators include *Bdellovibrio* spp. (and-like-organisms, BALOs), the myxobacteria (*Deltaproteobacteria*) or relatives of *Lysobacter* spp. (*Gammaproteobacteria*) (Jurkevitch *et al.*, 2000, Morgan *et al.*, 2010, Johnke *et al.*, 2014, Seccareccia *et al.*, 2015). Bacterial micropredators utilise distinct predation mechanisms. Myxobacteria, for example, prey on living bacteria by producing lytic exoenzymes (Harcke *et al.*, 1972), whereas *Bdellovibrio* spp. normally invade Gram-negative periplasms (Stolp & Starr, 1963). Intrabacterial predation by diverse prokaryotic micropredators has been suggested to be of higher prevalence and greater ecological importance than currently perceived (Reichenbach, 1999, Lueders *et al.*, 2006). Little direct evidence, however, is available for the actual activity of bacterial micropredators in complex soil systems (Lueders *et al.*, 2006, Murase & Frenzel, 2007, Morgan *et al.*, 2010, Kramer *et al.*, 2016); and competitive niche partitioning between bacterial and protistan micropredators in different soil compartments has not been elucidated.

Although protists are considered as generalists in predation of bacteria, marked prey preferences have been reported for different groups (Jezbera *et al.*, 2005, Bell *et al.*, 2010). Also bacterial micropredators show feeding preferences. For example, preferential or obligate predation on Gram-negative bacteria has been reported for myxobacteria (Morgan *et al.*, 2010) and different BALOs (Rogosky *et al.*, 2006, Rotem *et al.*, 2014). Still, little is known how such prey preferences are reflected in complex soil microbial food webs, and how they influence carbon flow under competitive predation by bacteria and protozoa. It also remains to be established whether the activity of different micropredators could be distinct in different soil compartments when distinct substrates and environmental conditions prevail.

The tracing of stable isotope-labelled prey cells has been suggested as a promising means to unravel complex predator-bacteria interactions in soil (Johnke *et al.*, 2014). As a powerful tool to address specific biological processes, stable isotope probing (SIP) of nucleic acids has been widely applied to trace organismic carbon flow in a number of soil food webs (Lueders *et al.*, 2006, Murase & Frenzel, 2007, Drigo *et al.*, 2010, Murase *et al.*, 2012, Chatzinotas *et al.*, 2013, Kramer *et al.*, 2016). Also, time-

resolved SIP analyses have provided valuable information on the trophic succession and connectivities of food webs in soil. Although evidence for the comparative labelling of both bacterial and protistan micropredators in the same soil is still scarce (Lueders *et al.*, 2004, Murase & Frenzel, 2007, Kramer *et al.*, 2016), a significant potential of SIP to resolve predatory niche partitioning in complex communities is undisputed. Advanced knowledge on niche segregation between micropredators in different soil compartments will improve our current understanding of structure and interaction mechanisms in the potentially separated soil food webs.

1.4. Vertical transport of bacteria in soil during seepage events

1.4.1. Transport of bacteria in soil

An important aspect of a holistic understanding of bacterial distribution and functioning in soil ecosystem is their mobility. In soil, bacteria can either migrate actively when they are capable of moving (Sen, 2011), or otherwise they can be mobilised passively by water flow (Wang *et al.*, 2013), nematodes (Knox *et al.*, 2004), along growing plant roots (Feeney *et al.*, 2006) or fungal hyphae (Simon *et al.*, 2015). Prediction of bacterial mobility in soil is extremely difficult due to the diverse processes associated to their transport, the various factors influencing mobilisation and the large number of routes for bacteria to migrate through soil (Bradford *et al.*, 2013). At the pore scale, interactions between bacterial cells and soil particle surfaces play a critical role in release, aggregation and retention processes which influence transport. These interactions are largely influenced by the surface charge of cells which can be dynamic and unevenly distributed, and depends on strains and growth phase (Foppen & Schijven, 2006). The level of complexity is further enhanced in unsaturated soil by the presence of gas phases and soil heterogeneity.

Preferential flow is well established as an important mechanism which can trigger rapid bacterial transport bypassing the soil matrix (Bradford *et al.*, 2012). A diverse array of preferential-flow mechanisms is shown in Figure 5. In heterogeneous soils, preferential water flow can occur in presence of macropores such as root channels, earthworm burrows and cracks. Particularly upon intensive precipitation events when water flow intensity exceeds the infiltration capacity of the soil, larger and more

conductive preferential flow paths tend to become activated (Cey & Rudolph, 2009). This can enable the transport of considerable amounts of colloids and microorganisms with seepage water (Bradford *et al.*, 2013).
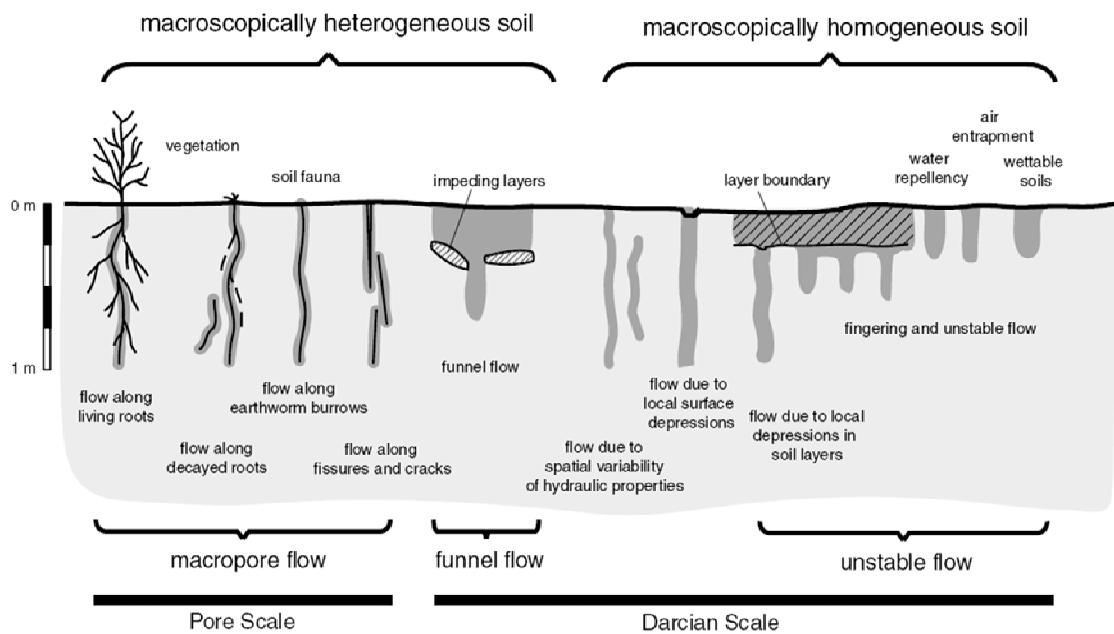
Figure 5. Schematic of different preferential flow mechanisms (adapted from Hendrick & Flury, 2001).

An extensive amount of research has been conducted to elucidate the environmental and biological factors controlling bacterial transport and fate in soil, largely focusing on pathogenic bacteria, such as *E. coli* and other fecal indicator bacteria after being released to soil. The transport and survival of microbial pathogens in agricultural systems largely determines the health risks they pose to humans via food and water. Factors that influence the survival of those artificially amended bacteria include pH, temperature, nutrient availability, soil moisture and predation (Mawdsley *et al.*, 1995, Ishii *et al.*, 2006, Franz *et al.*, 2008), whereas microbial mobilisation depends highly on soil type (Aislabie *et al.*, 2011) and bacterial features, like cellular shape (Weiss *et al.*, 1995), hydrophobicity (Kim *et al.*, 2009), surface charge (Bolster *et al.*, 2009), but also bacterial interactions (Stumpp *et al.*, 2011).

1.4.2. Vertical transport of natural bacterial populations by seepage

Due to the distinctions in resource quality, environmental characteristics and accordingly biomass and community structure of living organisms along soil profile, it is considered that separate soil food webs are sustained across depth (Scharroba *et al.*, 2012). Nevertheless, the mobilisation of viable microbes from top soil mediated by preferential flow after strong precipitation events could act as an important influx of diversity to subsoils, where the translocated microbes may contribute to local microbial activities (Kieft *et al.*, 1998, Jaesche *et al.*, 2006, Küsel *et al.*, 2016). After weather events producing large amounts of seepage water, such as rainfall or snowmelt, substantial fluxes of SOM from top soil can be translocated to deeper soil layers with seepage water (Totsche *et al.*, 2007). This carbon flow across soil compartments is assumed to be one important component of carbon fluxes in soil, representing a significant contribution of fresh inputs of OM to subsoil and even to the groundwater (Rumpel & Kögel-Knabner, 2011, Küsel *et al.*, 2016). The contribution of living microorganisms to this inter-compartment carbon flux, however, has received little attention to date. Efforts are still needed to characterise the nature of translocated microbial biomass and to trace whether these microorganisms merely fuel the food webs at depth or adapt themselves to the local environment. From this perspective, it is of particular interest to understand the transport mechanisms of intrinsic microorganisms, besides pathogenic indicator strains in soil.

While central aspects of the transport of selected bacterial strains in soil have been intensively investigated, current understanding of the behavior of complex indigenous microbiota transported with seepage water remains scarce. Dibbern and colleagues (2014) have addressed this knowledge gap by characterising natural bacterial communities mobilised with seepage water after snowmelt and rainfall in late winter on an experimental maize field in Germany. The findings suggested that specific subsets of bacteria associated to the decaying roots were selectively mobilised, and preferential flow along root channels played an important role in the transport of topsoil bacteria to deeper soil layers (Figure 6; Dibbern *et al.*, 2014). This study provided valuable first insights into the mobilisation of natural bacterial communities at the field scale. However, a critical aspect needed to generalise such findings remains at lack, such as seasonality and whether and how the mobilisation behavior of intrinsic microbiota could vary after precipitation events for living rhizosphere

systems during the growing season. Furthermore, a quantitative assessment of bacterial transport from top soil to deeper horizons is essential to understanding the role of bacteria in carbon flow across soil compartments and organismic connections between metacommunities across soil compartments.
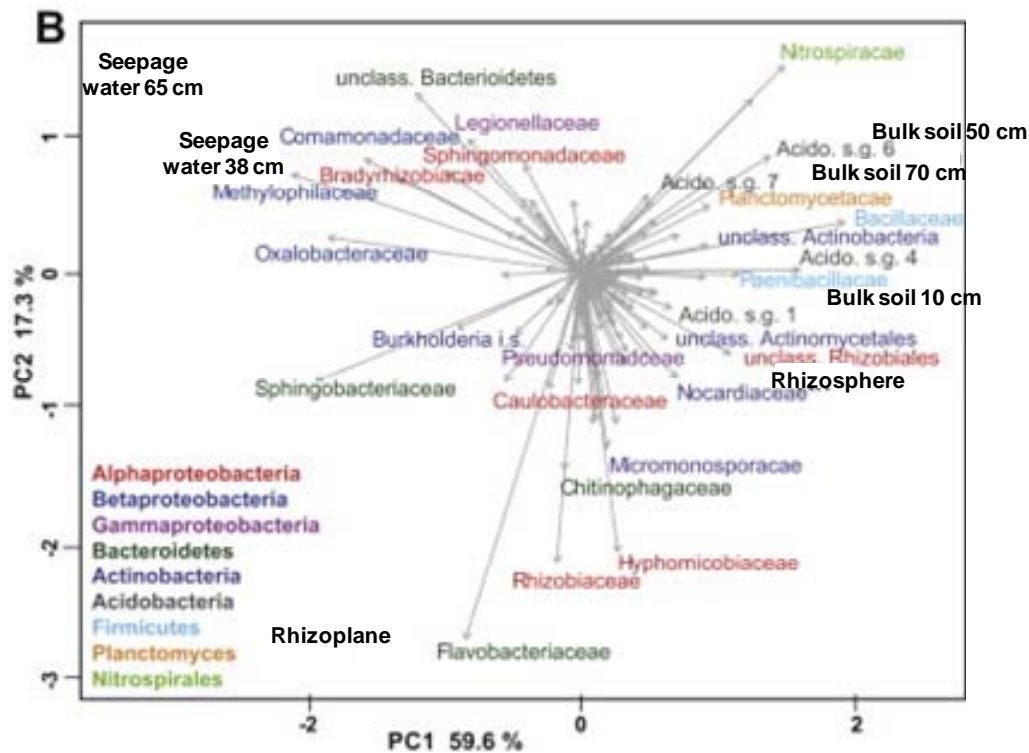
Figure 6. PCA biplot showing translocated bacterial communities with seepage water after a natural rainfall in comparison to bulk soil at different depths, rhizosphere and rhizoplane communities (modified from Dibbern *et al.*, 2014).

1.5. Introduction to the DFG FOR-918 "Carbon flow in belowground food webs assessed by isotope tracers"

1.5.1. Concept and overarching research questions

My thesis work was part of the second phase of the joint DFG Research Unit FOR-918 "Carbon flow in belowground food webs assessed by isotope tracers". The project aimed to address pathways and fluxes of carbon flow through an exemplary

soil food web by using (stable) isotope methods as tracers across disciplines and organismic groups. The Research Unit used an arable soil cropped with maize and wheat as a model system and set up a long-term field experiment. Four treatments representing substrate inputs with different quality and complexity were set up in the field: corn maize (CM, carbon inputs from maize root and aboveground shoots), fodder maize (FM, maize root inputs only), wheat with maize litter (WL) and wheat only (W). Joint efforts were invested to identify key groups of soil biota, quantify carbon fluxes and establish food web models. Pool size, structure and interaction covering all the relevant components of the entire soil food web were evaluated. The obtained data shall ultimately be integrated into a quantitative food web model, conceptualising all food chains and trophic levels occurring *in situ* in the arable field soil.

1.5.2. Labelling strategies in the Research Unit

Recent years have seen enormous development and application of a suite of (stable) isotope tracer methods to investigate dynamics of soil carbon pools. The Research Unit employed an array of labelling strategies to estimate carbon pools, quantify carbon fluxes and identify key populations involved in the specific soil food webs.

C_3 vs. C_4 plant

The experimental field site was previously run solely with C_3 crops. After the joint field experiment started, a natural and somewhat "heavier" ^{13}C signature was introduced to the food web by growing the C_4 plant *Zea mays* and by adding maize litter to the soil. Thus, the carbon flow from maize roots and litter into different soil carbon pools could be assessed by tracing the shift in carbon stable isotope ratios associated with the switching from a C_3 to a C_4 plant (Kramer *et al.*, 2012, Müller *et al.*, 2016).

$^{13}CO_2$ incubation and ^{13}C-plant litter amendment

A $^{13}CO_2$ pulse labelling experiment was applied in the field to quantitatively characterise carbon pools and fluxes within the entire investigated soil food web (Pausch *et al.*, 2016). Pool sizes of and ^{13}C incorporation into biomass of bacteria, fungi, meso- and macrofauna were quantified by analysing bulk tissues and compound-specific carbon isotope ratios. Two targeted stable isotope probing (SIP) experiments were also conducted, one with maize plants incubated under pulse

labelling of $^{13}CO_2$ (Hünninghaus *et al.*, submitted) and the other with soil microcosms under amendment of ^{13}C-labelled detritusphere substrates (Kramer *et al.*, 2016). These SIP studies were aimed to trace the flow of rhizosphere and detritusphere carbon into microbes, and generate comprehensive level of details on key microbial populations (bacteria, also fungi and protists) involved in distinct carbon flows in the investigated soil.

SIP has been previously employed as a powerful tool to provide insights into food web dynamics. SIP is a culture-independent approach that allows the identification of microbes involved in a given biogeochemical process in a complex environment (Dumont & Murrell, 2005). This method involves the incubation of environmental samples with substrate that is highly enriched in stable isotopes, for example via specific ^{13}C or ^{15}N-substrates. The identification of active microorganisms is achieved by assessing the label incorporation into cellular biomarkers including phospholipid fatty acids (PLFAs), DNA and RNA. Specifically, nucleic acid-based SIP is capable of providing unprecedented details in identity and diversity of microbial populations linked to specific function (Lueders *et al.*, 2016). RNA-based SIP displays higher sensitivity which enables the identification of active populations at a faster rate, whereas DNA-SIP is advantageous in metagenomic studies (Manefield *et al.*, 2002, Lueders *et al.*, 2004, Dumont & Murrell, 2005, Coyotzi *et al.*, 2016).

Nucleic acid-based ^{13}C-SIP has indeed facilitated tracking fluxes of plant-derived carbon into soil biota, and detection of organisms actively involved in rhizosphere (Leake *et al.*, 2006, Vandenkoornhuyse *et al.*, 2007, Drigo *et al.*, 2010, Drigo *et al.*, 2013) and detritusphere food webs (Bernard *et al.*, 2007, Lee *et al.*, 2011, Murase *et al.*, 2012). Moreover, SIP-based time-course experiments can provide valuable information on microbial interactions and food web links. With the extension of amended carbon resources in SIP to microbial biomass itself, more insights can be provided into microbial predation. rRNA-SIP has revealed the substantial contribution of *Lysobacter* spp, *Myxococcales* and some *Bacteroidetes* species to carbon sequestration and turnover of ^{13}C-labelled *Escherichia coli* biomass added to a soil microbial food web (Lueders *et al.*, 2006). The extensive application and success of SIP also initiated variants based on the traditional methods. For example, by switching ^{13}C-labelled substrate to a natural abundance substrate part way through

the incubation, carbon dynamics, including uptake, turnover and decay in a given system can be investigated simultaneously and in more details (Maxfield *et al.*, 2012).

$^{14}CO_2$ assimilation

A ^{14}C-labelling experiment was conducted under controlled conditions to unravel the ratio between rhizodeposited C to root-C (Pausch *et al.*, 2012). Assuming this ratio should stay constant, rhizodeposition carbon pool *in situ* can be inferred via root biomass carbon measured in the field. Maize plants were pulse-labelled with $^{14}CO_2$, and the soil $^{14}CO_2$ efflux was separated into root and rhizomicrobial respiration. The latter, together with the ^{14}C activity remaining in the soil, was taken as total rhizodeposition. A rhizodeposition-to-root ratio was calculated and then applied to the root biomass carbon measured in the field to estimate rhizodeposition under field conditions.

1.5.3. Overview of findings on soil food webs within the Research Unit

Soil carbon pools

Based on a field experiment with $^{13}CO_2$ labelling, the pool size of and incorporation of maize root-derived carbon into all major compartments and food web members in top soil (0-10 cm depth) were assessed, as summarized in Figure 7 (Pausch *et al.*, 2016). Approximately 20% of the carbon assimilated by the maize plant was transferred to belowground carbon pools. Root-derived carbon was predominantly incorporated into rhizosphere microbiota rather than into those of the bulk soil. Moreover, saprotrophic fungi showed a much higher ^{13}C incorporation and turnover rate than bacteria, which was suggested by the higher incorporation of ^{13}C into fungal-feeding nematodes vs. bacterial feeders, indicating an unexpectedly important flux of fresh plant root-derived carbon through the fungal energy channel. Limited amounts of plant-derived carbon was traced to higher trophic levels, dominated by fungal-feeding nematodes and macrofauna decomposers (Pausch *et al.*, 2016).

In addition to the pulse labelling, analyses of shifts in natural carbon isotope values in food web components after switching from C_3 to C_4 plants completed the picture. Root-derived carbon was found to be consumed more efficiently than shoot litter-derived resources by the soil microorganisms (Kramer *et al.*, 2012). Albeit much later than for top soil, maize-derived carbon was also detected in food webs of the deeper

rooted zone (40-50 cm depth) and the root-free zone (60-70 cm depth) (Müller *et al.*, 2016). Plant carbon incorporation was lower in subsoil carbon pools than in top soil, and saprotrophic fungi incorporated more maize-derived carbon than bacteria in all soil depths (Müller *et al.*, 2016).
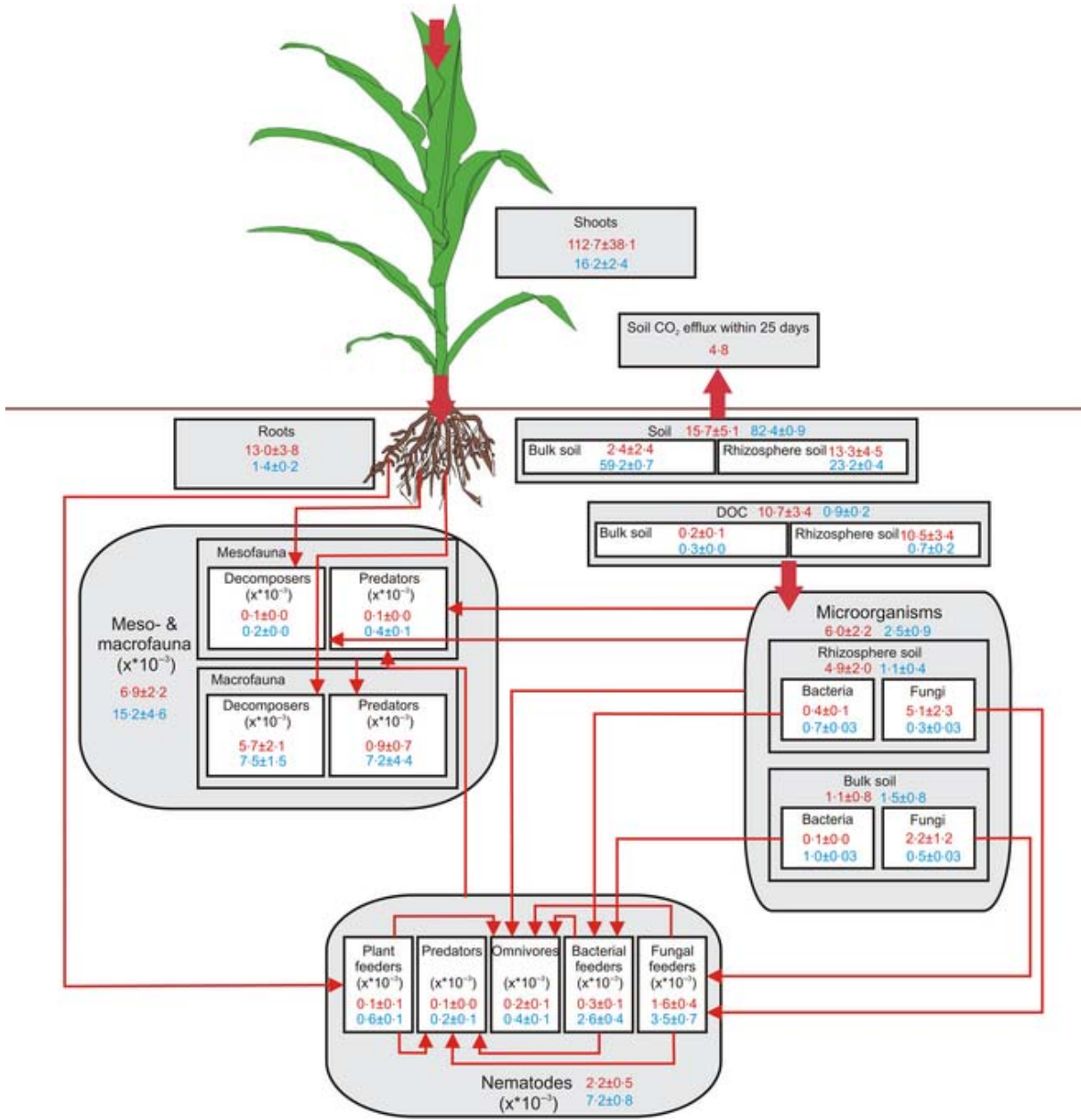
Figure 7. Carbon budget within the investigated soil food web in the upper 10 cm and net tracer incorporation into each carbon pool. Carbon budget is represented as percentage of total carbon per m^2 (blue values), and tracer incorporation was determined 25 days after $^{13}CO_2$ pulse labelling of maize (red values). From Pausch *et al.*, 2016.

Distribution and dynamics of soil (micro-) biota

A time- and depth-resolved monitoring of the bacterial, fungal and faunal communities in the experimental field was performed to provide a scaffold for more detailed food web investigations and modelling. In addition, plant-derived carbon resource quality and availability was manipulated in the field. The community composition of soil organisms and the response to resource supply were assessed.

The distribution of bacterial populations in the field appeared mostly affected by soil compartment and depth (Dibbern *et al.*, 2014), while the effects of experimental treatments was much less apparent (Scharroba *et al.*, 2012), at least in the first years of the experiment. In contrast, fungal community structure were largely influenced by litter amendment in top soil, whereas fungal community composition and biomass in the rooted zone mainly depended on plant species (Moll *et al.*, 2015). Protozoan morphotypes showed a clear vertical distribution, with flagellates and ciliates most abundant in top soil and naked amoeba predominant at depth (Scharroba *et al.*, 2012). In the plough layer in summer, addition of plant litter elevated the density of fan-shaped amoeba as well as that of bacterial and fungal feeding nematodes (Scharroba *et al.*, 2012). The density of omnivores and carnivores in nematodes was low, and their presence was restricted to top soil, indicating the depletion in trophic levels of the food web in the investigated soil at depth (Scharroba *et al.*, 2012). Last, neither diversity nor abundance of soil arthropods was affected by litter addition. In stark contrast, wheat sustained much more soil arthropods than maize, which highlights the importance of rhizodeposition in shaping soil arthropod communities in arable systems (Scheunemann *et al.*, 2015). Overall, depth-dependent community distribution of soil organisms indicates varied total biodiversity in different soil layers and therefore potentially separate food webs (Scharroba *et al.*, 2012).

Microbial food web members

The rRNA-SIP experiments traced bacterial carbon flows in the rhizosphere and detritusphere food webs of the investigated soil and identified the label-assimilating microbial key players. It was shown that the flow of fresh ^{13}C-labelled rhizodeposits was dominated by arbuscular mycorrhizal fungi (AMF) and resulted in labelling of distinct *Verrucomicrobia*, *Planctomycetes* and other bacteria in the hyphosphere of the investigated soil, more rapidly and pronounced than direct exudation to typical

rhizosphere bacteria (Hünninghaus *et al.*, submitted). This was in stark contrast to the assumed dominance of the bacterial energy channel in the rhizosphere.

In the detritusphere, the diversity of primary substrate degraders hardly increased with substrate complexity (Kramer *et al.*, 2016). However, consumer succession and secondary trophic labelling increased with substrate complexity. Protists were not only active as bacterivores, but also as fungivores and even as primary saprotrophs. And interestingly, hints arose towards a predatory role of members of the myxobacteria in the detritusphere. Moreover, carbon flow from both labile and complex substrates involved a marked activity of both bacteria and fungi, challenging the hypothesis of separate bacterial and fungal energy channels for the investigated soil (Kramer *et al.*, 2016).

1.6. Objectives for this thesis

Within the framework of the FOR-918 Research Unit, my specific project aimed to identify and quantify some of the most relevant bacterial populations involved in carbon flow within the investigated soil food web and across soil compartments. Specifically, I attempted to close the following knowledge gaps:

I)   Within the soil food web at the investigated site, which bacteria are capable of preying on other bacteria? Which factors influence the relevance of intrabacterial predation in comparison to predation by protozoa?

II) Between the microbiota and food webs in plant-associated top soil vs. deeper horizons, does bacterial transport triggered by strong precipitation represent a significant flux of organisms and carbon across compartments? What are the mechanisms of mobilisation and transport of this efflux?

III) Back in the field, how are bacterial populations distributed, especially the bacterial key players identified to be actively involved in detritusphere and rhizosphere carbon flows? Does distribution of these key players *in situ* reflect their functions assigned from microcosm experiments?

I hypothesized that

I) Intrabacterial predation should be more important in bulk soil than in rhizosphere soil, and that the nature of prey (Gram-positive or Gram-negative) and soil compartment can be factors contributing to micropredator niche differentiation.

II) Transport of bacteria via preferential flow along root channels after strong precipitation events in summer enables rapid and selective mobilisation of specific rhizosphere bacterial populations from top soil to deeper horizons. Compositon of mobilised bacterial communities vary during the transport.

III) Resource quality and quantity (driven by plant rhizodeposition and litter input) regulate biomass and community composition of bacteria, and the impact becomes increasingly apparent over the years.

To address these hypotheses, I have applied a series of field as well as laboratory experiments based on the joint experimental arable field site (Figure 8). A SIP experiment with ^{13}C-labelled bacterial biomass used soil from the field site, so that the pro- and eukaryotic key players and trophic interactions identified in this experiment should be readily linked to data generated from direct field surveys. Transported bacterial communities obtained after natural and artificial rain were analysed to investigate precipitation-driven bacterial transport which can open a link between food webs in separate soil compartments. Finally, annual sampling of soil across depths under treatments with manipulated resource complexity over a period of four years allowed me to unravel the distribution pattern of bacterial populations and their long-term response to rhizodeposition and litter inputs under field conditions. Moreover, the distribution of key bacterial food web members identified in the SIP experiment (this thesis and previous studies) was examined in the field. In summary, this thesis includes the following three sub-projects:
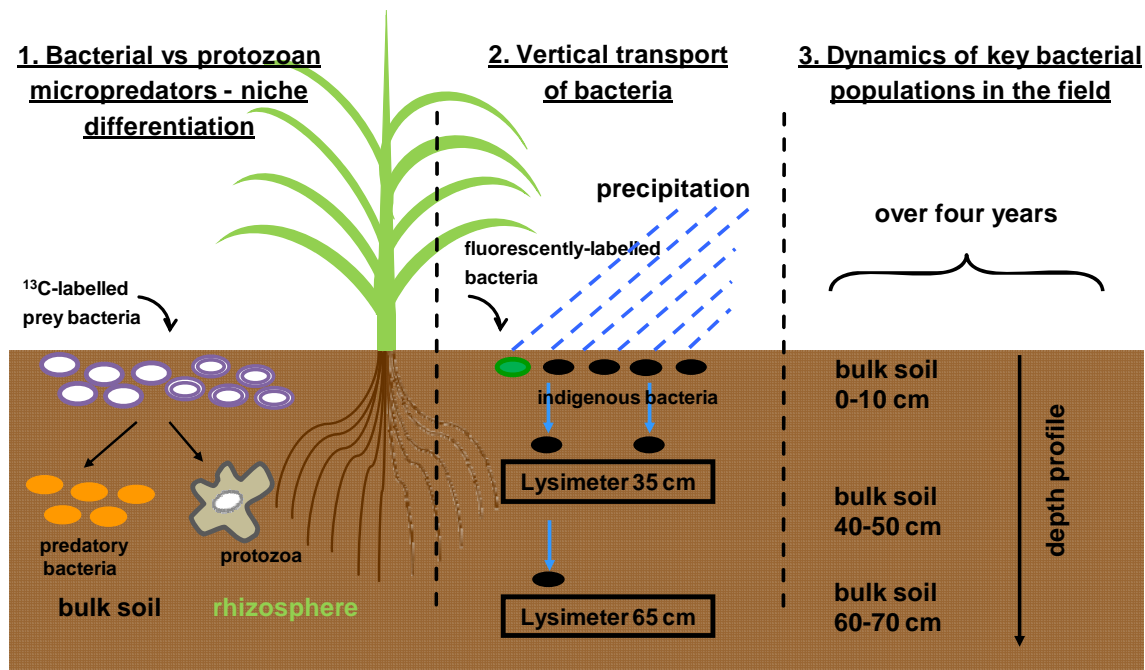
Figure 8. Overview of experimental setup and approaches in my thesis with aim to address three aspects of bacterial populations in soil food web: predation, distribution, and transport *in situ*.

I) Predation of bacteria by pro- and eukaryotic micropredators in relation to prey and soil compartment *(Zhang & Lueders, 2017)*

Using the maize soil as a model system, I investigated the predation of amended ^{13}C-labelled bacterial prey by pro- and eukaryotic micropredators. Influence of soil compartment (rhizosphere vs. bulk soil) and nature of prey (Gram-positive vs. Gram-negative) on predation outcomes were investigated. The assimilation and mineralization of signal derived from ^{13}C-labelled biomass of *Pseudomonas putida* and *Arthrobacter globiformis* added to soil microcosms was tracked over time. By combining rRNA-SIP and amplicon pyrosequencing, I identified bacteria and microeukaryotes that had incorporated carbon from the biomass amendments. Potential niche partitioning driven by prey species and habitat was disentangled.

II) Transport of bacterial populations from top soil to deeper layers upon precipitation events in summer *(Zhang et al., 2018)*

To characterise bacterial populations mobilised from rooted top soil to deeper horizons after strong precipitation events particularly in summer in presence of living

roots, I sampled seepage water from lysimeters installed (by the group of Kai-Uwe Totsche, Institute of Geosciences, University of Jena) in the field at 35 cm and 65 cm depth after a natural rainfall in Sept. 2012 and conducted an artificial rain experiment in Sept. 2014. In the latter experiment, defined pulses of fluorescently-labelled *A. globiformis* cells were added to the top soil as a bacterial tracer to enable a better quantitative grasp of the bacterial transport mechanism. The controlled condition in artificial rain experiment also allowed for time-resolved sampling of seepage water to elucidate potential taxon-specific and temporal distinctions in mobilisation and transport behavior. Bacterial transport mechanisms as revealed here were compared with previous findings concerning bacterial transport in winter with decayed roots above lysimeters. Transport of key bacterial food web constituents was also examined.

III) Four-year tracking of soil bacterial populations in the field *(Zhang et al.,* in prep.)

To acquire quantitative data of bacterial populations *in situ*, bacterial abundance, diversity and distribution was monitored in the field across soil profile of depth (0-10, 40-50 and 60-70 cm) over four years (between 2009 and 2013). As plant species (maize vs. wheat) and litter input (with vs. without litter) were manipulated in the field, I was able to address the long-term response of bacterial communities to distinct carbon resource quality and availability. 16S RNA gene terminal restriction fragment length polymorphism (T-RFLP) fingerprinting was first applied to the samples to obtain an overview of the distribution and diversity of bacteria in relation to depth, plant type, litter amendment and year. qPCR was employed to quantify the overall bacterial 16S RNA gene abundance. Moreover, the maize soil samples were subjected to amplicon pyrosequencing, with which I identified the prevalent bacteria in respective libraries and lineages specifically responsive to biotic and abiotic factors. Key bacterial food web members identified in this thesis and previous SIP experiments were traced back in the field for their abundance and distribution in the natural habitat. These three inter-connected sets of experiments and analyses jointly generated a unique array of qualitative and quantitative data concerning the populations, fluxes and interaction mechanisms associated to soil bacteria, together providing essential basis for a population-based understanding and modelling of soil carbon flow.

2. Materials and methods

2.1. The arable field site and experimental setup

2.1.1. Site description

The research in my thesis was conducted at an experimental agricultural field site installed by the Research Unit FOR-918, or relates to samples taken from there. The field site was located in Holtensen, in the north-west of Göttingen (Lower-Saxony, Germany). The region has a temperate climate with a mean annual temperature of 7.9 °C and a mean annual precipitation of 651 mm y^{-1}. The mean monthly precipitation sums (1981-2010, Göttingen weather station, 167 m above sea level; source: Deutscher Wetterdienst 2017, aggregated) ranged between 39-46 mm (minima in February, April and October) and 66 mm (maxima in June). Extreme precipitation event thresholds were determined by rarity (99th percentile; cf. Beniston & Stephenson, 2004) as 16.6 mm d^{-1} for summer (April - September) and 22.0 mm d^{-1} for winter (October - March).

The dominant soil types are Luvisols (87.2% silt, 7.0% clay and 5.8% sand) with occasional stagnic properties (Kramer *et al.*, 2012). The albic horizon typically found for these soils is not detectable, attributed to the long-term agricultural management with intensive tillage. Two plough layers were found at 20 cm and 30 cm below surface with strong compaction below the second layer. Further geological information about the field site and details on the soil properties are given in Kramer *et al.*, 2012 and Müller *et al.*, 2016.

2.1.2. Treatments

In April 2009, the field experiment was set up with maize (*Zea mays* L.) and wheat (*Triticum aestivum* L.) planted in ten plots each (24 × 24 m) in two adjacent rows (Figure 9). Maize and wheat plots were arranged in two rows to allow for standard agricultural management. In autumn, crops were harvested and removed from the field, and maize shoots (without corncobs) were chopped into small pieces and applied to topsoil of randomly chosen half of both maize and wheat plots (0.8 kg dry weight m^{-2} equivalent to 0.35 kg C m^{-2}). Thus, four treatments each with five replicates were established: corn maize (CM, maize with maize litter), fodder maize

(FM, no litter), wheat with maize litter (WL) and wheat only (W). The CM and WL plots received rhizodeposition during the growing season and additional litter inputs after harvest, while the FM and W plots received only rhizodeposits. In April from 2010 to 2013, after tillage with a chisel plough to a depth of 12 cm for all plots, wheat and maize were sown on the same plots as in 2009. Details about agricultural practices from 2009 to 2013 (sowing, fertilization and herbicide application) are given in Müller *et al.*, 2016.
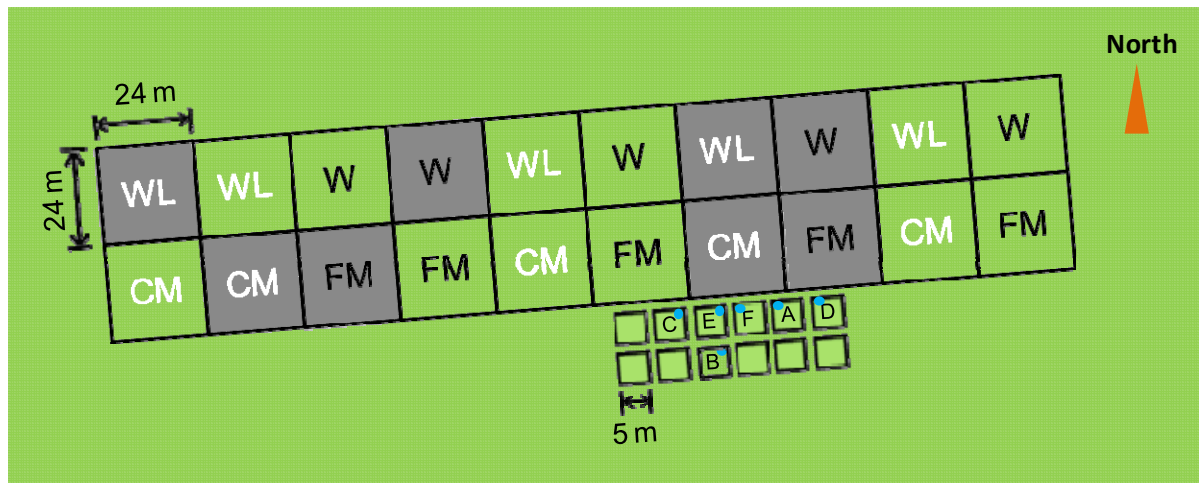
Figure 9. Map of the experimental field site showing the 20 plots of the long-term field experiment and locations of the lysimeters. CM: corn maize, FM: fodder maize, WL: wheat with maize litter, W: wheat. Each treatment has five replicates, while plots grey-colored in the map were not analysed in my thesis. Blue dots indicate where the lysimeters were installed, by the group of Kai-Uwe Totsche, Institute of Geosciences, University of Jena.

2.1.3. Soil sampling

Joint annual sampling campaigns of the Research Unit took place in September, shortly before crop harvest, from 2009 to 2013. Out of five replicated plots for each treatment, three plots were repetitively sampled and analysed for this study (Figure 9). Ten soil cores (diameter 2.5 cm; length ~ 80 cm) were randomly taken from each plot between the crop rows and split into 10-cm sub-cores. The three analysed soil horizons were i) 0-10 cm, topsoil within the plough layer, ii) 40-50 cm, rooted zone below the plough layer, and iii) 60-70 cm, subsoil below the rooted zone. Ten soil samples from the same depth within each plot were homogenized manually as a composite sample, distributed among members of the Research Unit. Samples for

the present thesis were transported in cooling boxes to the laboratory, frozen and stored at -20 °C until further analysis.

2.1.4. Lysimeters at the field site

The lysimeters used in this thesis were located south to the plots for the long-term experiment (Figure 9). Here, in May 2012, another joint field experiment was established with 12 plots (5 × 5 m) to trace the inputs of rhizosphere- vs. detritusphere-derived carbon to the soil food web. Details on this experiment and agricultural practices can be found in Loeppmann *et al.*, 2016a, Loeppmann *et al.*, 2016b and Glavatska *et al.*, 2017. Lysimeters were installed in rooted plots by the group of Kai-Uwe Totsche (Institute of Geosciences, University of Jena), underneath growing maize plants. Tension controlled lysimeters (KL2-100, UMS) were installed directly below the plough horizon (35 cm depth) and below the main rooted zone (65 cm depth), as described previously (Dibbern *et al.*, 2014).

The lysimeters were composed of a stainless-steel ring (diameter: 30 cm; height: 14 cm) filled with inert glass beads (size/diameter: 1-2 mm) and a porous plate (pore size of 10 µm, SIC275, UMS) at the bottom. There, suction was applied via a vacuum station (VS-twin, UMS) regulated by the prevailing soil water potential that was constantly measured with a tensiometer (T8, UMS) installed at 35 cm depth.

2.2. Laboratory SIP experiment with ^{13}C-labelled bacterial prey

2.2.1. Rhizosphere soil preparation

The soil used for the SIP experiment to investigate consumption of ^{13}C-labelled bacterial prey by bacterial and eukaryotic micropredators was taken from the experimental field site described above. Representative composite top soil (0-10 cm) was sampled from a FM plot under maize in March 2015. To obtain fresh rhizosphere soil for the SIP experiment conducted in August 2015, young maize plants were grown in a greenhouse. Maize seeds were germinated on agar plates prepared with Miller LB broth (Sigma-Aldrich) at 30 ºC and transferred after germination to plastic pots (diameter = 9.5 cm, height = 14.5 cm) filled with sieved (4 mm mesh) soil from the field in a greenhouse for over 12 weeks. Plants received natural sunlight and

were kept at 25 ºC during the day and at 20 ºC at night. Watering was applied daily in the first two weeks and two times every week afterwards. Fertilization was not applied. After 12 weeks of growth, planted pots were densely filled by maize roots. For the SIP incubation, fresh rhizosphere soil was directly harvested by loosely shaking the roots to collect all readily detachable soil and manually removing remaining fine roots (Buddrus-Schiemann *et al.*, 2010). For the bulk soil treatments, pots of soil with no plants were kept next to the planted pots in the greenhouse, under identical climatic conditions and water treatment. Water content of rhizosphere and bulk soil was determined by drying ~30 g of soil in an oven at 105°C for 48 h.

2.2.2. Cultivation of ^{13}C-labelled bacteria

The bacterial strains used in this SIP experiment were the Gram-negative *Pseudomonas putida* (DSM 6125) and Gram-positive *Arthrobacter globiformis* (DSM 20124). For both strains, closely related taxa are abundant in the investigated soil (Dibbern *et al.*, 2014, Kramer *et al.*, 2016) and can therefore be considered as representative components of the intrinsic soil microbial food web. Strains were originally obtained from the DSMZ (Braunschweig, Germany). Labelled bacteria were grown in M9 minimal medium, prepared with 5x M9-Minimal salts (Serva), containing 4 g L^{-1} 99% ^{13}C$_6$-glucose (Santa Cruz Biotechnology, Inc.) as sole carbon source. In parallel, the same strains were grown in M9 medium with unlabelled glucose (Sigma Aldrich). After approximately 24 h of cultivation and two transfers, cells were collected as prey for the SIP experiment by centrifugation at 3345 rcf for 15 min, washed five times with fresh, glucose-free M9 media, and was finally resuspended in 15 ml M9 medium.

Bacterial cell concentrations in the washed suspensions were determined using flow cytometry as will be explained in 2.4.6. ^{13}C-labelling of the harvested bacterial cells was determined using elementary analysis - isotope-ratio mass spectrometry (IRMS) by Ramona Brejcha (Research Unit of Environmental Isotope Chemistry, IGÖ), with an elemental analyser (EURO EA, Euro Vector Instruments) coupled to an IRMS (MAT 253, ThermoFischer). Approximately 30 mg of harvested bacterial cells were weighed into tin capsules for each measurement. Each sample was measured at least twice, similarly as done before (Lueders *et al.*, 2006).

2.2.3. Microcosm setup

The SIP-microcosm experiment was designed as follows: microcosms contained 30 g of maize rhizosphere (Rh) or bulk soil (Bs), amended with same amount of either ^{13}C-labelled or unlabelled *P. putida* and *A. globiformis*, set up in duplicates per each of the eight treatments. First, for the cell amendment, 250 g of freshly retrieved rhizosphere soil or bulk soil were transferred into sterile 1000-ml beakers. 7.5 ml of bacterial cell suspensions at ~ 9.6×10^8 cells ml^{-1} concentration, adjusted after cell counting, were slowly added in droplets with a 1000-µl pipette while manually stirring the soil. Afterwards, soil with bacterial amendment was manually distributed to eight sterile 500-ml glass bottles per treatment (64 bottles in total), each with 30 g of soil, and bottles were closed with rubber stoppers and aluminium screw caps, and incubated over 16 d at 20°C. The SIP microcosms were sampled at successive time points: at time 0 (directly after bacterial amendment), after 6 h, 1 d, 2 d, 4 d, 8 d and 16 d. At each time point, 15 g of soil were sampled from two of the eight bottles per treatment as duplicates, i.e. two replicate microcosms were fully sacrificed after every second sampling time point. The two microcosms per treatment reserved for the final time point (16 d) were also used for CO_2 measurement during the incubation. Control microcosms without bacterial amendments were also set up, run and sampled in parallel. For each time point, ~2 g of fresh soil from the sampled 15 g were immediately frozen in liquid nitrogen and stored at -80 °C for subsequent RNA extraction. The remaining soil was stored at -20 °C.

2.2.4. CO_2 measurements

$^{13}CO_2$ production derived from ^{13}C-labelled bacterial biomass in microcosms was measured daily with GC/MS (Finnigan TRACE DSQ GC/MS, Thermo Electron). 20 µl headspace gas samples were withdrawn with a gas-tight glass syringe and injected into the GC/MS. Gases were first separated by gas chromatography with a GS-Q column at 50 °C (8 min) with helium as carrier gas (flow rate 3 ml min^{-1}). Then molecular masses 44 Da ($^{12}CO_2$) and 45 Da ($^{13}CO_2$) were quantified with the Trace DSQ MS detector under selected ion mode (SIM). Data were analysed using the software Xclibur (version 1.4.2, Thermo Scientific). The relative abundance of $^{13}CO_2$ in the headspace was calculated as the ratio of $^{13}CO_2$ to total CO_2 ($^{13}CO_2$ plus $^{12}CO_2$).

Calibration was performed with a standard gas consisting of 1% CO_2 with $^{13}CO_2$ at natural relative abundance.

2.3. Field bacterial transport experiments

To unravel transport patterns of bacteria driven by extreme precipitation events in summer in rooted soil, seepage water was sampled after a natural rainfall in September 2012. Furthermore, an experiment with simulated precipitation and fluorescently-labelled bacteria added to top soil were conducted in September 2014, aimed for time-resolved seepage water sampling and possible quantitative estimation of bacterial transport.

2.3.1. Sampling after a natural rain event

An extreme rainfall event of 30.2 mm occurred on 11.09.2012, followed by several successive precipitation events (0.2-0.4 mm) over the next days. The soil water content and soil temperature were measured with sensors (5TM, Decagon Devices) installed at 48 cm (n = 5) and 58 cm (n = 5) below soil surface in a soil hydraulic pit. On 19 September, a further 2.8 mm rain event occurred before the actual sampling. Directly before sampling, empty sterilized glass bottles were installed to collect seepage water from four lysimeters, i.e. two pairs of co-localized 35-cm and 65-cm lysimeters in two different field plots (L35A, L65A and L35B, L65B) , which were ~25 m apart. Fresh seepage water was sampled within 24 h. Immediately after retrieval, subsamples of seepage water ~120 ml in volume was filtered for bacterial analyses (0.2 μm, Corning). The remaining water was subject to physicochemical analysis as described in 2.3.4. For each water sample, DNA was extracted in duplicates from two sectioned filter quarters. Filters with retained microbial biomass were frozen at -20 °C until further processing.

On the same day, depth-resolved composite soil samples were taken from the field plots where the lysimeters were installed as described in 2.1.3. Furthermore, two live root balls were extracted from each plot. All soil and root samples were frozen and stored at -20 °C until further analyses. Rhizosphere (Rh) and rhizoplane (Rp) samples were obtained as previously described (Dibbern *et al.*, 2014). The root balls were first thawed and manually shaken to get rid of all readily detachable soil. Root

subsamples were then washed twice with 25 ml 1x PBS buffer (pH 7.4) in a 50-ml centrifuge tube. The washed roots were cut into small fragments and used for DNA extraction. Buffer with suspended particles after washing was collected in a fresh 50-ml tube and rhizosphere soil was collected by centrifugation at 3345 rcf for 10 min. All bulk soil, rhizosphere and rhizoplane samples were obtained and processed in biological triplicates, whereas water samples were processed in biological duplicates.

2.3.2. Artificial rain experiment

To investigate the mobilisation and transport of bacterial populations from top soil under controlled experimental conditions, an artificial rain experiment was conducted in September 2014. The artificial rain experiment was set up for six lysimeters, all installed at 35 cm depth, but located in different replicate field plots planted with maize. Defined spikes of fluorescently labelled bacterial cells were amended to the top soil of four lysimeters (L35A, L35B, LC and LD; Figure 9). Further two lysimeters (LE and LF; Figure 9) were intended as controls without bacterial amendment. Here, the strain *A. globiformis* DSM 20124 was again used as amendment to be added to the soil and tracked for mobilisation with seepage water. The strain, as explained above, closely related to abundant *Arthrobacter* populations in the investigated soil. Labelling of *A. globiformis* cells with a fluorescent dye is described below in 2.3.3.

The artificial rain water comprised of 6.86 mg L^{-1} $NaNO_3$ (Carl Roth), 1.64 mg L^{-1} $KHCO_3$ (Carl Roth) and 33.97 mg L^{-1} $CaSO_4$ x 2 H_2O (VWR), dissolved in ultrapure, degassed water (Milli-Q®; Integral System, Merck; equipped with a 0.22-µm membrane filter). As a non-reactive tracer, 2 mM KBr was additionally added to the artificial rain water to identify the predominant water flow regimes in the soil compartments, resulting in a Br^- concentration of 151 mg L^{-1}. The electrical conductivity was 335 µS cm^{-1} and the pH was 6.1. Although utmost cleanliness was applied during all procedures, the artificial rain water was not prepared or handled under sterile conditions. Two days before the artificial rain experiment, two 2.9- and 4.5-mm rain events occurred, respectively. Two rainfall simulators units (emc) were used to generate extreme and constant sprinkling irrigation at a uniform rate of 8 mm h^{-1} over ~8 h per lysimeter at the actually irrigated area of 50 × 50 cm. This resulted in an artificial extreme rain event of 64 mm (per 8h, a total of 16 L) per lysimeter.

Fluorescently labelled cells of *A. globiformis* in 1× PBS buffer were prepared ~48 h before amendment and transported to the field under cooling. One hour after the simulated irrigation started, 50 ml of cell suspension was added to the top soil above each of four lysimeters (L35A, L35B, LC and LD). Two other lysimeters (LE and LF) intended as controls, did not receive labelled bacterial amendment. Cell suspensions were first transferred to a 50-ml sterile syringe and injected at ~2 cm soil depth to ten random spots on top soil above the lysimeters.

Empty sterilized glass bottles were installed to collect seepage water from lysimeters. For each sampling, bottles were exchanged and samples were collected when approximately > 250 ml seepage water had accumulated, which was the minimum amount required for all analyses. However, seepage water collection was successful only for two of the lysimeters with bacterial amendment (LC and LD). No seepage water accumulated from the other two lysimeters amended with labelled *A. globiformis* and the two control lysimeters. Sampling was conducted until no more seepage water was received, which lasted ~27 h for LC and ~23 h for LD. In the end, six time-resolved seepage water samples were collected for LC, and seven for LD, respectively. At least half of each water sample was immediately filtered and stored for nucleic acid extraction as described above. Furthermore, 10 ml of each seepage water sample was fixed with glutardialdehyde (2.5% final conc.) for cell counting (described in 2.4.6) and stored at 4 °C. In addition, bulk soil, rhizosphere and rhizoplane samples were again obtained as described above. All bulk soil, rhizosphere and rhizoplane samples were obtained and processed in biological triplicates, whereas water samples were analysed in biological duplicates.

2.3.3. Labelling of bacteria with a fluorescent dye CFDA/SE

A. globiformis cells added to top soil to be tracked for transport with seepage water were fluorescently labelled to be distinguished from the indigenous *Arthrobacter* populations. Cultures of *A. globiformis* were grown in liquid DSMZ medium 53 (*Corynebacterium* agar) for 24 h at 30 °C. Before staining, cells were harvested by centrifugation at 3345 rcf for 15 min, washed twice with 1× PBS buffer, and resuspended in 60 ml 1× PBS. Thereafter, the cells were labelled with a fluorescent protein stain, CFDA/SE (5-(and-6)-carboxyfluorescein diacetate, succinimidyl ester; Life Technologies), which has been shown to uniformly stain bacterial cells for up to

five months, with no apparent influence on cell viability or transport behaviour (Fuller *et al.*, 2000, Fuller *et al.*, 2001).

The staining was performed following a procedure modified from Fuller *et al.*, 2000. Cell suspensions were evenly distributed to 2-ml Eppendorf tubes. CFDA/SE (50 mM in dimethyl sulfoxide) was then added to cell suspension to a final concentration of 100 µM. Cells were incubated on a thermomixer (Eppendorf) at 450 rpm for approximately 50 min, with temperature being cycled between 25 ºC and 39 ºC over five cycles. Afterwards, cells were harvested by centrifugation at 10,000 rcf for 10 min, washed three times with 1× PBS buffer, and resuspended in 200 ml of 1× PBS. 100 µl of these cell suspensions was then removed and cell concentrations were determined using flow cytometry as described in 2.4.6. Labelled cell suspension was evenly distributed to four 50-ml Falcon tubes for four lysimeters

2.3.4. Physicochemical analyses of seepage water

Seepage water sampled from both experiments was analysed for physicochemical parameters. Electrical conductivity (EC) and pH were determined with electrochemical probes (Cond 197i, Sentix 41, WTW) and meters (LF 197 and pH 197, WTW). Seepage water analyses also included dissolved (DOC) and total organic carbon (TOC), measured by catalytic high-temperature combustion and non-dispersive infrared (NDIR) detection (multi N/C 2100S, Analytic Jena). DOC samples were filtered with 0.45 µm PES syringe filters prior to measurements (Supor, Pall). Sulfate, nitrate and the tracer bromide (for the artificial rain experiment) were quantified by ion chromatography (IC 20, Dionex). Turbidity was determined by UV-Vis spectroscopy (Cary 50 Conc, Varian) as spectral absorption at 860 nm and converted to formazine attenuation units (FAU). To characterise the mobile colloidal inventory of the seepage water, the hydrodynamic diameter as well as the zeta potential were measured by dynamic light scattering (DLS; Nano ZS, Malvern Instruments).

2.4. Microbiological and molecular methods

2.4.1. DNA and RNA extraction

The nucleic acid extraction protocol used in this thesis was modified from Lueders *et al.*, 2004.

DNA and RNA co-extraction

~0.4 g (wet weight) of bulk and rhizosphere soil, ~0.5 g of roots or quarter of a water filter (Corning) with retained microbial biomass was used for extraction. Roots and water filters were cut into small ~5 mm^2 pieces beforehand, using sterile scalpels. Samples were added to bead beating cups filled with 0.2 ml of a 1:1 (v/v) mixture of sterile 0.1 mm zirconia/silica beads and 0.7 mm zirconia beads (Biospec Products, Inc.). Cells were lysed by bead beating in presence of 750 μl NaPO$_4$ (pH 8), 250 μl TNS buffer (500 mM Tris, 100 mM NaCl, 10% (w/v) sodium dodecyl sulphate; pH 8), as well as 250 μl phenol-chloroform-isoamylalcohol (PCI; 25:24:1, pH 8). Bead beating was performed on a FastPrep-24 cell disruptor (MP Biomedicals) at 6.5 m s^{-1} for 45 s, followed by centrifugation at 4 ºC and 15,294 rcf for 4 min. The supernatant (~750 μl) was mixed with an equal volume of PCI (25:24:1, pH 8) in a fresh vial and centrifuged at 4 ºC and 20,817 rcf for 4 min. The aqueous supernatant was then transferred to a 2-ml Phase Lock Gel Heavy vial (5 Prime), mixed with an equal volume of chloroform-isoamylalcohol (24:1), and centrifuged again at 4 ºC and 20,817 rcf for 4 min. Afterwards, the separated aqueous phase was transferred to another fresh 2-ml vial and nucleic acids were precipitated by mixing with two volumes of PEG solution (30% (w/v) polyethylene glycol 6000, 1.6mM NaCl) and centrifugation at 4 ºC and 20,817 rcf for 30 min. Extracted nucleic acid pellets were washed with 70% (v/v) ethanol (-20 ºC) and dissolved in 80 μl EB buffer (Qiagen).

Bulk soil, rhizosphere and rhizoplane samples were always obtained and processed in biological triplicates, while water samples were processed in biological duplicates, i.e. extraction was applied in duplicates from two sectioned filter quarters.

As the nucleic acid extracts from soil (bulk and rhizosphere) samples were rich in humic substances, purification was performed for these samples prior to subsequent analyses using silica gel columns from the DyeEx 2.0 Spin Kit (Qiagen) following the

manufacturer's instructions. Purity and integrity of DNA and RNA were checked by gel electrophoresis.

RNA extraction

In this thesis, RNA extraction was done for soil samples obtained from SIP microcosms. DNA and RNA were first extracted simultaneously and purified following the procedures as described above. Then, DNA was removed to produce a total RNA extract, using RQ1 RNAse-free DNAse (DNAse I, Promega). 80 µl DNA/RNA extracts were mixed with 50 µl DNAse I, 20 µl buffer and 50 µl H_2O and incubated at 37 °C for 2 h. Afterwards, RNA was re-extracted with PCI and CI as described above with minor modifications. Equal volumes of acid PCI (pH 4.8; Carl Roth) and normal CI were used for extraction prior to precipitation with two volumes of PEG solution and centrifugation. Washed RNA pellets were resuspended in 50 µl EB buffer (Qiagen). RNA purity and integrity were checked by gel electrophoresis.

RNA extraction was done for soil sampled from all the treatments for time 0 and day 8, but only from the ^{13}C-microcosms for the remaining time points. Soil RNA was extracted from duplicate soil microcosms per time point and treatment and stored at -80 °C until further analyses.

2.4.2. Stable isotope probing (SIP) gradient centrifugation and fractionation

RNA-SIP analyses were carried out as previously published (Kleindienst *et al.*, 2014, Kramer *et al.*, 2016) with minor modifications. RNA extracts of day 8 (for all treatments) were selected for SIP based on substrate mineralization data. Soil RNA extracted from duplicate soil microcosms per treatment was pooled before analyses. Total RNA was first quantified with the Quant-iT RiboGreen RNA Assay Kit (Invitrogen) according to the manufacturer's instructions but in 100 µl volume per assay and with a customized standard curve (2.5, 2.0, 1.5, 1.0, 0.5, 0.1, 0.05 and 0 µg ml^{-1}). Samples were measured in three dilutions, each with duplicates on a Stratagene MX3000P qPCR cycler (Agilent) in "quantitative plate read" mode.

500 ng of ^{13}C-labelled or unlabelled RNA were mixed with 185 µl of formamide and loaded onto 5 ml of cesium trifluoroaetate (CsTFA; ~ 2.0 g ml^{-1}; GE Healthcare Life Sciences). Additionally, up to 1 ml of gradient buffer (GB; 0.1 M Tris-HCl at pH 8, 0.1

M KCl, 1mM EDTA) was added to a final volume of 6185 µl (RNA volume was subtracted from GB). Afterwards, density of the prepared gradients was checked by measuring the refractory index with a refractometer (AR200, Reichert technologies), and adjusted to 1.80 g ml^{-1} by adding small volumes of CsTFA or GB when necessary. The mixture was then transferred to a polyallomer QuickSeal tube (Beckman Coulter) and centrifugation was performed at 125,000 rcf on an Optima XE-90 ultracentrifuge (Beckman Coulter) with a Vti-65.2 vertical rotor (Beckman Coulter) for ~65 h.

After isopycnic centrifugation, gradients in tubes were fractionated from bottom to top by displacing the gradient medium with water from the top of the tubes through a needle at a constant flow rate of 1 ml min^{-1} controlled by a Perfusor V syringe pump (B. Braun Melsungen). 13 density–resolved RNA fractions were collected from each gradient, each of ~400 µl. To compare density fractions of corresponding ^{13}C-labelled and unlabelled gradients, density of each fraction was determined using the refractometer. RNA was precipitated from the fractions by mixing with an equal volume of isopropanol and precipitation at 4 °C and 20,817 rcf for 30 min. Precipitates were washed with 70% (v/v) ethanol (-20 °C) and re-eluted in 25 µl EB buffer (Qiagen). Fractionated RNA was stored at -80 °C until further analyses.

2.4.3. Terminal restriction fragment length polymorphism (T-RFLP) fingerprinting

First, terminal restriction fragment length polymorphism (T-RFLP) fingerprinting was applied to analyse bacterial and eukaryotic community structure in different samples following published protocols (Euringer & Lueders, 2008, Pilloni *et al.*, 2011, Dibbern *et al.*, 2014).

Polymerase chain reaction (PCR)

Bacterial community structure in field soil, root and seepage water samples was first characterised by 16S rRNA gene-targeted T-RFLP fingerprinting. For this, polymerase chain reaction (PCR) was performed with the primers Ba27f and Ba907r (Table 1) on a Mastercycler ep gradient thermal cycler (Eppendorf). For T-RFLP, the forward primer was labelled with 6-FAM (6-carboxyfluorescein) at the 5' end. Each 50 µl PCR reaction consisted of 5 µl of 10× PCR buffer, 3 µl of 25 mM MgCl$_2$, 0.5 µl of

10 mM dNTPs, 0.25 µl of recombinant Taq polymerase (5 U µl^{-1}) (all from Thermo Fisher Scientific), 0.5 µl of 20 µg µl^{-1} bovine serum albumin (BSA; Roche), 0.3 µl of each primer (50 µM, Biomers) and 1 µl of template DNA. The cycling conditions were as follows: initial denaturation (94 ºC, 5 min) was followed by 26 cycles of denaturation (94 ºC, 30 s), annealing (52 ºC, 30 s) and elongation (70 ºC, 60 s), and final elongation (70 ºC, 5 min).

Table 1. Bacterial 16S and eukaryotic 18S rRNA gene-specific PCR primers used in this thesis

Primer	Sequence (5'-3')	Reference
Ba27f	AGA GTT TGA TCM TGG CTC AG	(Suzuki & Giovannoni, 1996)
Ba519f	CAG CMG CCG CGG TAA NWC	(Lane, 1991)
Ba519r	TAT TAC CGC GGC KGC TG	(Lane, 1991)
Ba907r	CCG TCA ATT CCT TTG AGT TT	(Amann *et al.*, 1992)
Euk20f	TGC CAG TAG TCA TAT GCT TGT	(Euringer & Lueders, 2008)
Euk519r	ACC AGA CTT GYC CTC CAA T	(Euringer & Lueders, 2008)

Prior to PCR reactions, DNA was diluted 100-fold for rhizosphere, 0-10-cm and 40-50-cm soil samples, and diluted 10-fold for rhizoplane and 60-70-cm soil samples. DNA extracts from seepage water samples were not diluted for PCR.

Reverse transcription polymerase chain reaction (RT-PCR)

Bacterial and eukaryotic rRNA in unfractionated total RNA extracts and density-resolved SIP fractions (fractions 2 to 11 of all day 8 gradients) was first analysed by 16S and 18S rRNA-targeted T-RFLP fingerprinting. For bacterial 16S rRNA, reverse transcription polymerase chain reaction (RT-PCR) was carried out using the one-step AccessQuick^{TM} RT-PCR System (Promega) with also the primers FAM-Ba27f and Ba907r (Table 1). 2 µl of RNA was used for each 50-µl reaction containing 25 µl of 2× Master Mix, 0.8 µl of avian myeloblastosis virus (AMV) reverse transcriptase (RT) (both from the kit), 0.5 µl of 20 µg µl^{-1} BSA (Roche) and 0.3 µl of each primer (50 µM, Biomers). Reverse transcription was performed at 45 ºC for 30 min, followed by PCR amplification comprised of initial denaturation (95 ºC, 5 min), (30 for unfractionated rRNA, and 16-30 for SIP fraction rRNA depending on quantity) cycles of denaturation

(95 ºC, 30 s), annealing (52 ºC, 30 s) and elongation (68 ºC, 60 s), and final elongation (68 ºC, 5 min).

For eukaryotic 18S rRNA, RT-PCR was performed with the Brilliant III Ultra-Fast SYBR Green QRT-PCR Master Mix (Agilent) and the primers FAM-Euk20f and Euk519r (Table 1). Each 50-µl one-step reaction was composed of 25 µl of 2× SYBR Green Master Mix, 0.5 µl of 100 mM dithiothreitol (DTT), 2.5 µl of RT/RNase block (all from the kit), 0.3 µl of each primer (50 µM, Biomers) and 2 µl of RNA template. Reverse transcription was done at 50 ºC for 15 min, and the subsequent PCR amplification included initial denaturation (95 ºC, 5 min), (26 for unfractionated rRNA, and 22-32 for SIP fraction rRNA depending on quantity) cycles of denaturation (95 ºC, 30 s), annealing (55 ºC, 30 s) and elongation (68 ºC, 60 s), and final elongation (68 ºC, 5 min). In addition to "no RNA" template controls, "no RT" controls were also included for each RT-PCR run to check for DNA contamination.

After checking with gel electrophoresis, amplified DNA of expected size, with sufficient yield and without contamination was purified with PCR Extract Kit (5Prime) following the manufacturer's protocol. Purified amplicons were quantified with Nanodrop spectrophotometer (ND-1000, Thermo Fisher Scientific).

Amplicon digestion and fragment analysis

80 ng of DNA amplicons was used for restriction, mixed with 0.3 µl of restriction enzymes (10 U µl^{-1}) and 1 µl of buffer (all from Thermo Fisher Scientific) in a total reaction volume of 10 µl, and incubated at 37 ºC for 2 h. The restriction enzymes were *Msp*I for bacteria and *Bsh*1236I for eukaryotes. After digestion, amplicons were desalted using DyeEx 2.0 Spin Kit (Qiagen). 1 µl of desalted digests was then mixed with 13 µl of Hi-Di formamide (Applied Biosystems) containing 400-fold diluted 6-carboxy-X-rhodamine-labelled MapMarker 1000 ladder (BioVentures) and denatured at 95 ºC for 5 min.

The fragments were separated by capillary electrophoresis on a 3730 DNA analyser (Applied Biosystems). Electrophoresis was carried out with POP-7 polymer in a 50-cm capillary array, and the electrophoretic conditions were as follows: 10 s injection time, 2 kV injection voltage, 7 kV run voltage, 66 ºC run temperature and 63 min analysis time.

The electropherograms were first evaluated with the GeneMapper software (version 5.1, Applied Biosystems), and then analysed with the T-REX online software (Culman *et al.,* 2009). True peaks were identified by peak heights with the noise filtering factor set to 1. T-RFs were defined by aligning peaks and the clustering threshold was set to 1. T-RF frequencies were inferred from peak heights.

2.4.4. Amplicon pyrosequencing

Amplicon pyrosequencing was performed to identify relevant microbial lineages in soil, root and water samples, as well as a selection of SIP gradient fractions. Based on rRNA fingerprinting of gradient fractions, the fractions 3, 6, and 9 of all gradients, corresponding to buoyant densities of ~1.82, 1.80 and 1.78 g ml^{-1} CsTFA respectively, were selected as representative for "heavy", "medium", and "light" rRNA and subjected to sequencing.

Barcoded amplicon PCR and RT-PCR

For the 2009 soil samples of the long-term field experiment and natural rain event samples (water, soil and root samples) of the lysimeter experiment, barcoded amplicons were prepared following a bidirectional strategy, using bacterial primers Ba27f/519r (Table 1) extended with the respective A or B adapters and multiplex identifiers (MIDs). Tagged PCR was performed with the same conditions as described above for T-RFLP fingerprinting in 2.4.3.

For the DNA extracts from the 2010-2013 soil samples of the long-term field experiment and the artificial rain experiment samples, as well as for unfractionated RNA extracts and selected gradient-fractionated RNA of the SIP experiment, barcoded amplicons for a unidirectional sequencing were amplified using the bacterial 16S rRNA primers Ba27f/907r (Table 1) and the eukaryotic 18S rRNA primers Euk20f/519r (only for RT-PCR of the SIP experiment RNA samples; Table 1) with Lib-L adapters and MIDs attached to the forward primer. Barcoding PCR and RT-PCR were performed with the same conditions as described in 2.4.3.

Amplicons of expected size, with sufficient yield and lack of contamination verified by gel electrophoresis were then purified with PCR Extract Kit (5Prime) following the manufacturer's protocol. Purified amplicons were checked for primer

dimers using the Bioanalyzer 2100 and High Sensitivity DNA assay chips (both from Agilent) according to the manufacturer's instructions. Purified amplicons were quantified with the Quant-iT PicoGreen dsDNA Assay Kit (Invitrogen) following the manufacturer's instructions but in 100 µl volume per assay and with an adjusted standard curve (2.5, 2.0, 1.5, 1.0, 0.5, 0.1, 0.05 and 0 ng µl^{-1}). Samples were measured in two dilutions, each with duplicates on a Stratagene MX3000P qPCR cycler (Agilent). Subsequently, samples were diluted for bidirectional sequencing to 1 × 10^9 molecules µl^{-1}, and for unidirectional sequencing to 5 × 10^9 molecules µl^{-1} according to the following equation: molecules µl^{-1} = (sample concentration (ng µl^{-1}) × 6.022 × 10^{23}) / (656.6 × 10^9 × amplicon length (bp)). ~25 samples were then pooled and purified using Agencourt AMPure XP beads (Beckman Coulter) following the manufacturer's protocol, for amplicon sequencing.

Emulsion PCR, emulsion breaking and sequencing were performed applying the GS FLX Titanium chemistry (sequenced on a 454 GS FLX sequencer) for bidirectional sequencing, done by Katrin Hörmann (Group of Molecular Ecology, IGÖ) and Brigitte Schloter-Hai (Comparative Microbiome Analysis, COMI) at the Helmholtz Zentrum München. GS FLX+ sequencing was done using respective chemistry and a GS FLX+ sequencer (all from Roche) for unidirectional sequencing, at IMGM (Martinsried). Sequencing of amplicon mixes was done on PicoTiter plates divided into quarter regions, following the manufacturer protocols.

Data processing

Initial quality filtering of the pyrosequencing reads obtained from both systems was performed using the automatic amplicon pipeline of the GS Run Processor (Roche). Sequences were then extracted as described in Pilloni *et al.*, 2012, generating fasta and qual files, both of which were further used to trim reads using the Trim function of Greengenes (DeSantis *et al.*, 2006) with default settings.

Trimmed reads were subsequently analysed and classified using the SILVAngs data analysis platform (Pruesse *et al.*, 2007, Quast *et al.*, 2013, Yilmaz *et al.*, 2013). Reads were first aligned by SINA (http://www.arb-silva.de/aligner/sina-download/; Pruesse *et al.*, 2007). In this initial quality filtering step, PCR artefacts and non-rDNA sequences were excluded. Furthermore, reads shorter than 250 aligned nucleotides

or with a quality score < 20, and reads with more than 2% of ambiguities or 2% of homopolymers were filtered out and not considered for further processing. Afterwards, the remaining reads were de-replicated: only the longest read of identical reads were retained and subsequently clustered to operational taxonomic units (OTUs) with a threshold of 98% sequence identity. For classification, the representative read of each OTU was compared to the SILVA reference datasets of the 16S/18S rDNA with its corresponding SILVA taxonomy (Quast *et al.*, 2013). The threshold for classification similarity ((sequence identity + alignment coverage) / 2) was set to 93 for the bacterial libraries and 85 for the eukaryotes. The classification of each OTU reference read was mapped onto all reads that were assigned to the respective OTU. Sequencing raw data have been deposited with the NCBI sequence read archive under the SRA accession numbers SRP100422 (SIP experiment), SRP103676 (lysimeter experiments) and SRP125518 (long-term field experiment).

2.4.5. Quantitative PCR (qPCR)

Bacterial 16S rRNA gene quantities in the soil samples of the long-term field experiment (samples of all years except 2009, i.e. 2010-2013) were assessed via quantitative PCR (qPCR) on a Stratagene MX3000P qPCR cycler (Agilent) following the procedures described previously (Winderl *et al.*, 2008) with minor modifications. Each of triplicate soil DNA extract was quantified in two dilutions with duplicate measurements. A series of dilutions had been tested for amplification efficiency, from which 50- and 100-fold dilutions were selected and applied to all the investigated soil samples. The primers used for 16S rRNA gene-targeted qPCR were Ba519f and Ba907r (Table 1). 2 µl of DNA template was quantified in each 50-µl reaction containing 0.25 µl of 500-fold diluted fluorescent dye SYBR Green, 0.75 µl of 500-fold diluted reference dye ROX (both from Life Technologies), 5 µl of 10× PCR buffer, 3 µl of 25 mM $MgCl_2$, 0.5 µl of 10 mM dNTPs, 0.25 µl of recombinant Taq polymerase (5 U $µl^{-1}$) (all from Thermo Fisher Scientific), 0.5 µl of 20 µg $µl^{-1}$ bovine serum albumin (BSA; Roche) and 0.3 µl of each primer (50 µM, Biomers). Initial denaturation (94 °C, 3 min) was followed by 40 cycles of denaturation (94 °C, 30 s), annealing (52 °C, 30 s) and elongation (70 °C, 30 s). Afterwards, a melting curve was recorded between 55 °C and 95 °C to verify the specificity of amplification products. *E.coli* 16S rRNA gene (980 bp) fragment covering the primer sites was used as standard (gBlocks,

Integrated DNA Technologies, Leuven, Belgium), in a concentration series between 1.7×10^7 and 1.7×10^1 copies μl^{-1}.

2.4.6. Cell counting with flow cytometry

Concentrations of ^{13}C-labelled and unlabelled *A. globiformis* and *P. putida* cells in the washed suspensions prepared for the SIP-microcosm experiment were determined using flow cytometry. Cell suspensions were diluted in 10-fold series and fluorescently-stained with SYBR Green I (1×; Molecular Probes) for 10 min in the dark. The measurements were performed on a FC 500 cell analyser (Beckman Coulter) using a 488 nm (20 mV) laser. Instrument settings were as follows: forward scatter 178 mV, side scatter 624 mV, B530 (bandpass filter 530 nm) 397 mV, B610 572 mV, signal trigger was set on B530. Parameters were collected as logarithmic signals. Sample flow rate was 30 μl min^{-1}, and for each measurement cells were counted until ~200 events of the internal standard were detected. BD TruCOUNT Tubes (BD Biosciences) were used to provide an internal standard (bead concentration: 6331 ml^{-1}). Data analyses were performed using the CXP software (Beckman Coulter). On the basis of the total cell counts, concentrations of the different cell suspensions were adjusted with 1× PBS to ensure that same amount of ^{13}C-labelled and unlabelled *A. globiformis* and *P. putida* were added to the respective soil microcosms.

Suspensions of CFDA/SE-stained *A. globiformis* cells prepared for the artificial rain experiment were assessed for stained bacterial counts also with flow cytometry prior to amendment to define the amount of bacterial cells added to top soil per lysimeter. 100 μl of these cell suspensions was removed to prepare 10^4-, 10^5- and 10^6-fold dilutions generated in 10-fold dilution series for measurements. Instrument settings and data processing were same as described above, except that Flow-count fluorospheres (Beckman Coulter) were used as quantification standards (bead concentration: 1026 μl^{-1}) for these measurements.

Furthermore, the amount of retrieved CFDA/SE-stained *A. globiformis* cells and total number of bacteria in the collected seepage water samples were also determined via flow cytometry. Before cell counting of fixed seepage water samples, glutardialdehyde was removed from water by centrifugation of the samples at 18,000

rcf for 10 min and resuspending the cell pellets in 1× PBS buffer. Afterwards, density gradient centrifugation was performed to remove remaining soil particles (Grösbacher *et al.,* 2016). 1.5 ml of each sample was transferred into a 10-ml ultra-centrifugation tube and placed on top of 5 ml Nycodenz solution (1.3g ml^{-1}; Axis-Shield Poc) cooled to 4 ºC. Samples were then centrifuged at 15,500 rcf and 4 ºC in a swinging bucket rotor SW 40 Ti (Beckman Coulter) for 1 h. Thereafter, the top second and third 1-cm gradient fractions containing the purified cells were collected. Samples were diluted five-fold in 1× PBS buffer prior to analysis. For total cell counts in seepage water, samples were first stained with 1× SYBR Green I for 10 min in the dark; while for counting of the CFDA/SE-stained cells recovered in seepage water, diluted samples were directly loaded for measurements. Internal standard bead concentration was 992 µl^{-1} for measurements of the seepage water samples.

2.5. Data analyses

2.5.1. Calculating taxon-specific enrichment factors in labelled rRNA for the SIP experiment

To identify bacterial and eukaryotic taxa that were involved in the assimilation of ^{13}C derived from the amended bacterial biomass, sequencing read enrichment factors (EFs) in heavy rRNA fractions were inferred as described previously (Kramer *et al.,* 2016). Briefly, the calculation was done as follows:

$$EF = {}^{13C}heavy/{}^{13C}light - {}^{12C}heavy/{}^{12C}light,$$

where ^{13C}heavy and ^{13C}light are the taxon-specific relative read abundances in heavy and light rRNA fractions of ^{13}C treatments, and ^{12C}heavy and ^{12C}light are the same for unlabelled treatments. EFs were calculated for all taxa with > 1% read abundance in heavy rRNA fractions of at least one treatment. Bacterial and eukaryotic taxa that showed an EF > 0.5 were considered as ^{13}C-labelled (Kramer *et al.,* 2016).

2.5.2. Univariate statistical analyses

All statistical analyses were performed in R version 3.4.1 (R Development Core Team, 2011). For the four-year field experiment, effects of crop plant and litter

amendment on bacterial 16S rRNA gene abundance at each depth and sampling date were analysed by two-way analysis of variance (ANOVA). Two-way ANOVAs were also applied to identify depth and litter effects and their interaction on the relative pyrosequencing read abundances of operational taxonomic units (OTUs) for those higher in relative abundance than 1% in at least one soil sample. ANOVAs were applied using the function 'anova' from the package car (Fox & Weisberg, 2011). The influence of litter input on individual OTUs in top soil was further explored using nonparametric Mann-Whitney U-test.

For the SIP experiment, $^{13}CO_2$ production was compared between rhizosphere and bulk soil treatment, within *P. putida* and *A. globiformis* microcosms separately, using two-way repeated measures ANOVA.

2.5.3. Multivariate statistical analyses

Both the T-RFLP fingerprinting and amplicon sequencing relative abundance data sets of the four-year field experiment were assessed using permutational multivariate analysis of variance (perMANOVA; Anderson, 2001) for potential effects of depth, plant, litter and year. PerMANOVAs were performed based on Bray-Curtis distance with 999 permutations using the function 'adonis' from the package 'vegan' (Oksanen *et al.*, 2016). The two multivariate datasets of the bacterial communities were also visualized by redundancy analysis (RDA). Explanatory variables were depth, plant, litter and year for the T-RFLP RDA, and depth, litter and year for the amplicon sequencing RDA. Depth-resolved sequencing datasets were also visualized via principal component analysis (PCA). RDA and PCA were done using the function 'rda' from the package 'vegan' (Oksanen *et al.*, 2016). Arcsin transformation (arcsin√) was applied for the relative abundance values to improve homogeneity of variance and normality. For visual clarity, only 25 T-RFs or OTUs with largest sum of squares of species scores on the first two axes were shown in each PCA and RDA plot.

PCAs were also applied as described above for the bacterial transport experiments, to compare bacterial community structures obtained from different seepage water samples, bulk soil, rhizosphere and rhizoplane samples, with both the T-RFLP fingerprinting and amplicon sequencing relative abundance data sets.

3. Results

Within the frame of the DFG Research Unit FOR-918 "Carbon flow in belowground food webs assessed by isotope tracers", my thesis aimed to elucidate the diversity, distribution and function of bacteria in a soil microbial food web. The Research Unit established an experimental field site at an arable soil cropped with maize and wheat plants as a model system. Four treatments were set up in the field: corn maize (CM, carbon inputs from maize root and shoot materials), fodder maize (FM, maize root inputs only), wheat with maize litter (WL) and wheat only (W) (Scharroba et al., 2012). Within this general setting, I specifically aimed to resolve the role of predation on bacteria by pro- and eukaryotic micropredators in rhizosphere and bulk soil, and to identify involved keystone food web members. On the basis of previous findings within the Research Unit that identified primary bacterial consumers of plant-derived C in rhizosphere and detritusphere of the soil food web (Kramer et al., 2016, Hünninghaus et al., submitted), I explored the secondary trophic links and identified bacterial as well as protozoan micropredators in the investigated soil. The second part of my thesis engaged in investigating the transport mechanisms of root-associated topsoil bacteria to deeper soil layers with seepage water, as a potentially under-regarded flux of bacterial populations between soil compartments. Moreover, four years of field sampling allowed for investigation of long-term soil bacterial community dynamics in response to carbon resource quality and at different depths. Furthermore, key bacterial food web components identified in SIP were tracked back in the field to reveal their abundance, distribution and dynamics in situ.

3.1. Consumption of bacteria by pro- and eukaryotic micropredators in relation to prey species and soil compartment

Predation of soil bacteria by bacterial and protistan micropredators was investigated in bulk vs. rhizosphere soil. ^{13}C-labelled bacterial biomass of Gram-negative *Pseudomonas putida* and Gram-positive *Arthrobacter globiformis* were added to soil microcosms, and intrinsic pro- and eukaryotic micropredators incorporating ^{13}C label were identified by combining rRNA-stable isotope probing (SIP) and amplicon pyrosequencing.

3.1.1. ^{13}C mineralization during microcosm incubation

^{13}C-labelled bacterial biomass was added to the microcosms at a final concentration of ~3.8 × 10^7 cells per g_{dw} soil. This was intended to correspond to ~2% of the indigenous bacterial biomass of 2.1 × 10^9 cells per g_{dw} soil, as previously estimated for the site (Dibbern *et al.*, 2014). Unlabelled bacterial biomass was amended to the microcosms at the same concentration. ^{13}C-labelled cells amended to the microcosms were determined to be 87 and 70 atom % ^{13}C labelled for *A. globiformis* and *P. putida*, respectively. Gravimetric water content of the soil after amendment was 0.22 for rhizosphere and 0.23 for bulk soil.
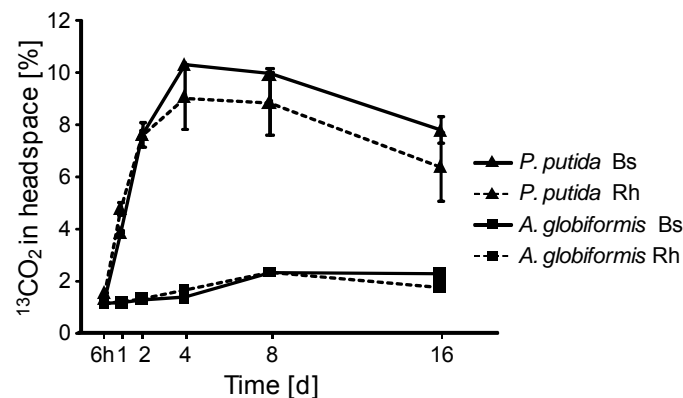
Figure 10. $^{13}CO_2$ production in rhizosphere and bulk soil microcosms amended with ^{13}C-labelled *A. globiformis* and *P. putida* during SIP incubation. Error bars represent standard error ($n = 2$).

Mineralization of ^{13}C-labelled bacterial biomass was tracked for duplicate ^{13}C-microcosms for all the ^{13}C treatments over 16 d (Figure 10). Mineralization of amended ^{13}C-biomass was clearly stronger in treatments with *P. putida* than with *A. globiformis*. The evolution of $^{13}CO_2$ from amended *P. putida* in bulk soil and rhizosphere microcosms peaked at day 4, with 10.3 and 9.0 ^{13}C atom % detectable in headspace CO_2, respectively. In the *A. globiformis* treatments, mixing ratios of formed $^{13}CO_2$ were much lower, but increased slightly until day 8, with 2.3 atom % in both the bulk soil and rhizosphere microcosms. ^{13}C mineralization rate was not significantly different between bulk soil and rhizosphere microcosms over time (Figure 14; soil effect: $F = 0.28$, $p = 0.70$, time effect: $F = 118.9$, $p < 0.001$, for *P. putida*; soil effect: $F = 11.9$, $p = 0.18$, time effect: $F = 13.1$, $p < 0.001$, for *A.*

globiformis), with mineralization of *P. putida* being slightly lower in rhizosphere microcosms after 4 days of incubation.

3.1.2. Bacterial and eukaryotic community dynamics during incubation

T-RFLP analysis of total bacterial 16S rRNA was used to trace the dynamics of bacterial communities in soil microcosms over time, and also to compare communities before and after microcosm incubation as well as between treatments (Figure 11). The T-RFs of amended *P. putida* (490 bp) and *A. globiformis* (61 bp) were clearly visible and at comparable abundance directly after amendment in all treatments. The *P. putida* T-RF was in a range of 60-71% relative abundance, while *A. globiformis* was between 52-60% in respective treatments.

However, while the *A. globiformis* T-RF gradually decreased back to its initial ~10% abundance over the entire experiment, the T-RF of *P. putida* drastically decreased to < 10% already after 1 d of incubation (Figure 11).

The comparison of initial unamended T-RF patterns to that of amended microcosms after 8 or 16 d revealed very similar overall bacterial community composition, suggesting that marked long-term community shifts were not induced by the amendments. Distinctions between soils were apparent, before or after amendment, but more related to different relative abundances of the most important T-RFs than to T-RF distinctions. In contrast, the structure of microeukaryote 18S rRNA patterns was markedly distinct between rhizosphere and bulk soil microcosms (Figure 12). The amendment of bacterial prey did not induce immediate shifts in overall microeukaryotic communities. However, several gradual changes were observed, such as a consistent increase in abundance of the 273 bp T-RF in rhizosphere soils. Apart from that, rhizosphere microeukaryote communities appeared rather stable over the experiment, while specific T-RFs in the bulk soil treatments were of fluctuating abundance.
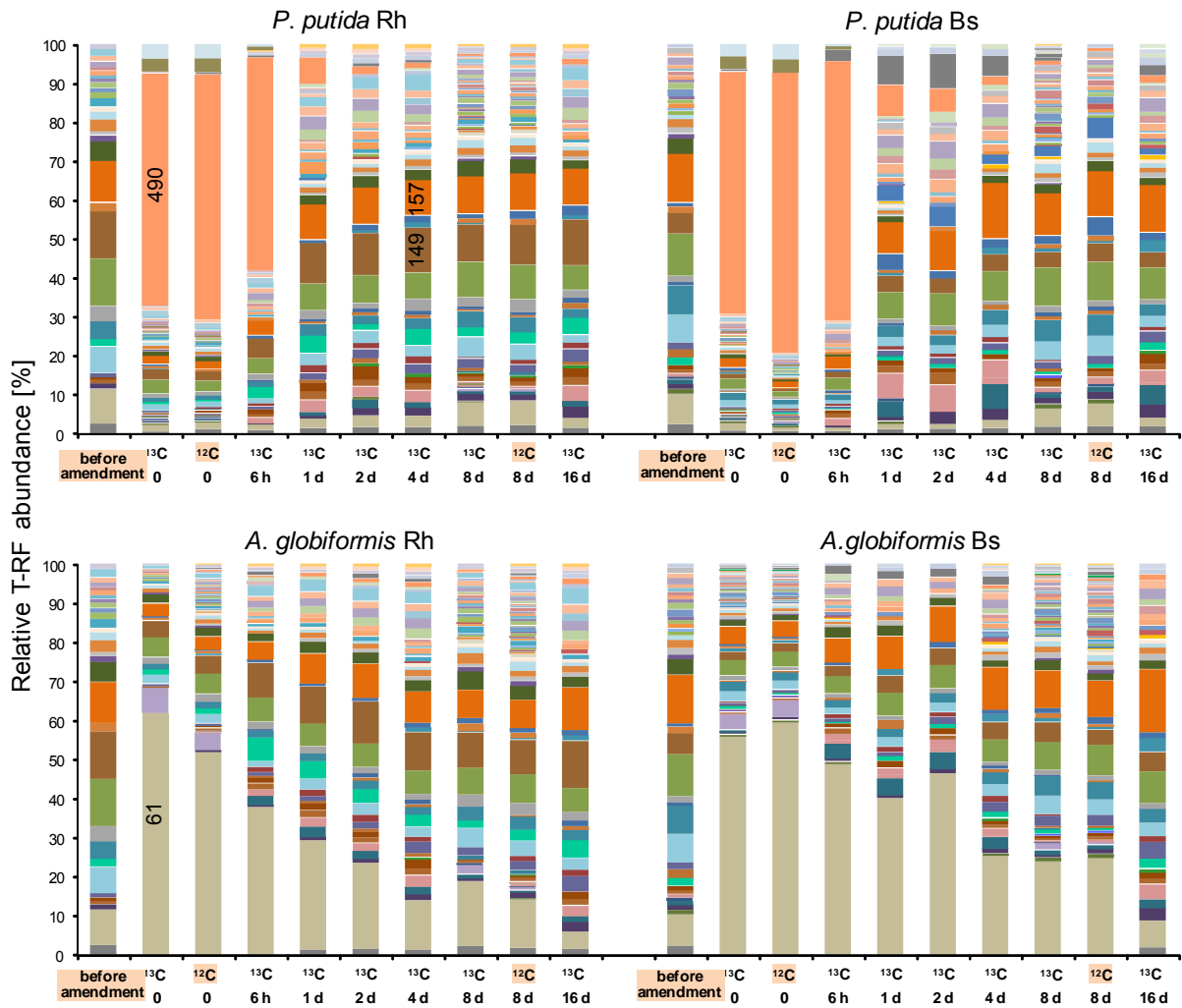
Figure 11. Variation of overall bacterial community structure as revealed by T-RFLP fingerprinting of total rRNA extracts of rhizosphere (Rh) and bulk soil (Bs) microcosms amended with *P. putida* or *A. globiformis* during SIP incubation. The T-RFs of 490 and 61 bp were assigned to *P. putida* and *A. globiformis*, respectively (Kramer *et al.*, 2016). Selected other abundant T-RFs (149 and 159 bp) are also highlighted.
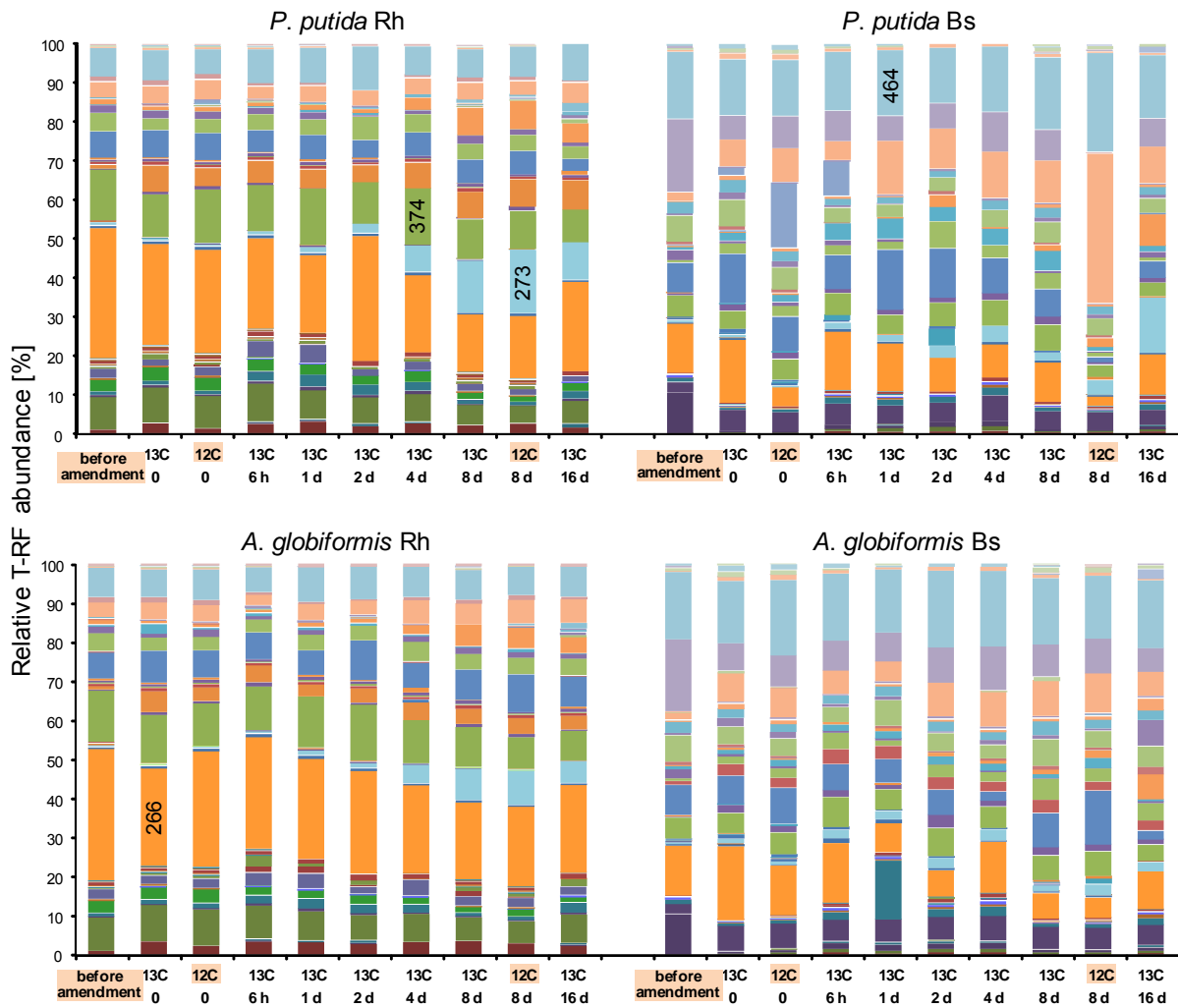
Figure 12. Variation of overall microeukaryotic community structure as revealed by T-RFLP fingerprinting of total rRNA extracts of rhizosphere (Rh) and bulk soil (Bs) microcosms amended with *P. putida* or *A. globiformis* during SIP incubation. Selected abundant T-RFs (266, 273, 374 and 464 bp) are highlighted.

3.1.3. Sequencing of density-resolved rRNA

rRNA extracts from the microcosms sampled after 8 d of incubation were selected for SIP analysis based on ^{13}C mineralization and T-RFLP community dynamics. To identify labelled taxa, but also for more precise information on community assembly in the different treatments, libraries of bacterial and microeukaryotic rRNA from selected heavy, medium and light gradient fractions were sequenced.

61
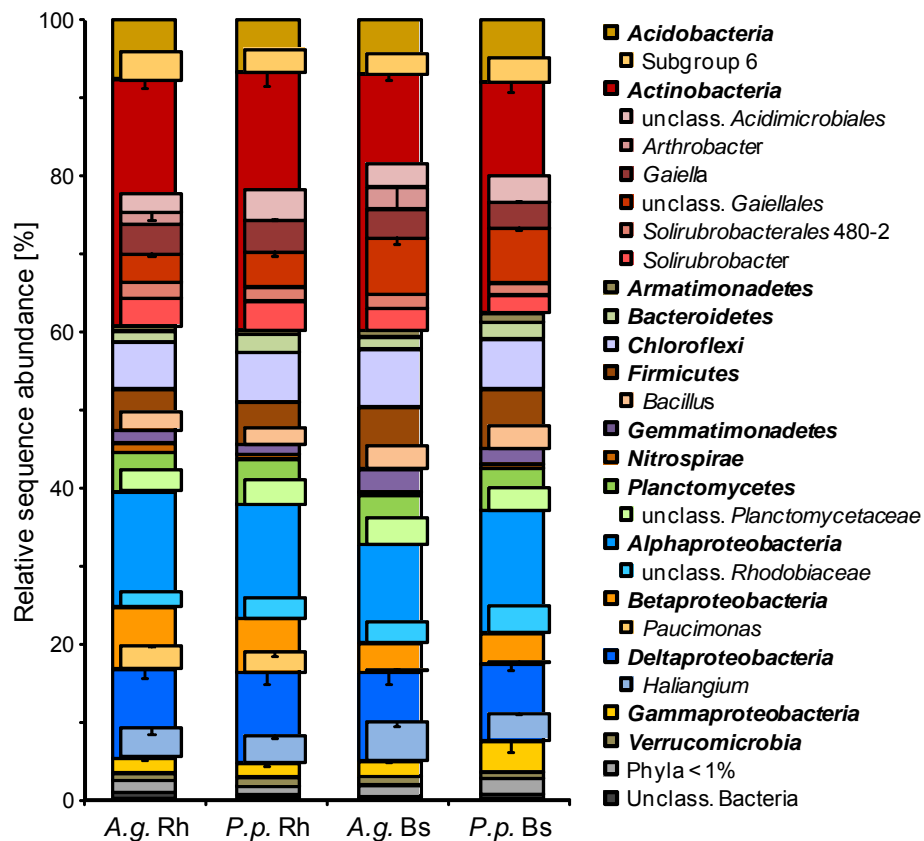
Figure 13. Relative sequence abundance for overall bacterial taxa obtained by amplicon sequencing of light gradient fractions from rhizosphere (Rh) and bulk soil (Bs) microcosms amended with *A. globiformis* (*A.g.*) or *P. putida* (*P.p.*) and after 8 d of incubation. Relative sequence abundances in light fractions were averaged between ^{13}C- and ^{12}C-microcosms. Error bars are given for selected phyla or classes and represent standard errors (*n* = 2). Selected sub-phylum taxa are highlighted.

First, as an indicator of potential compartment effects on total overall community composition, libraries from light rRNA gradient fractions were averaged between isotopic treatments (Figures 13 and 14). Generally, the abundance of bacterial taxa in libraries from light rRNA was highly reproducible, with most of the abundant taxa not showing notable distinctions in relative abundance between rhizosphere and bulk soil (Figure 13). Minor exceptions included reads of *Paucimonas* spp., being consistently detected at 2-3% abundance in rhizosphere only. rRNA of unclassified *Gaiellales* was another example, present at consistently higher relative abundance in bulk soil (~7%) than in the rhizosphere (4-5%).
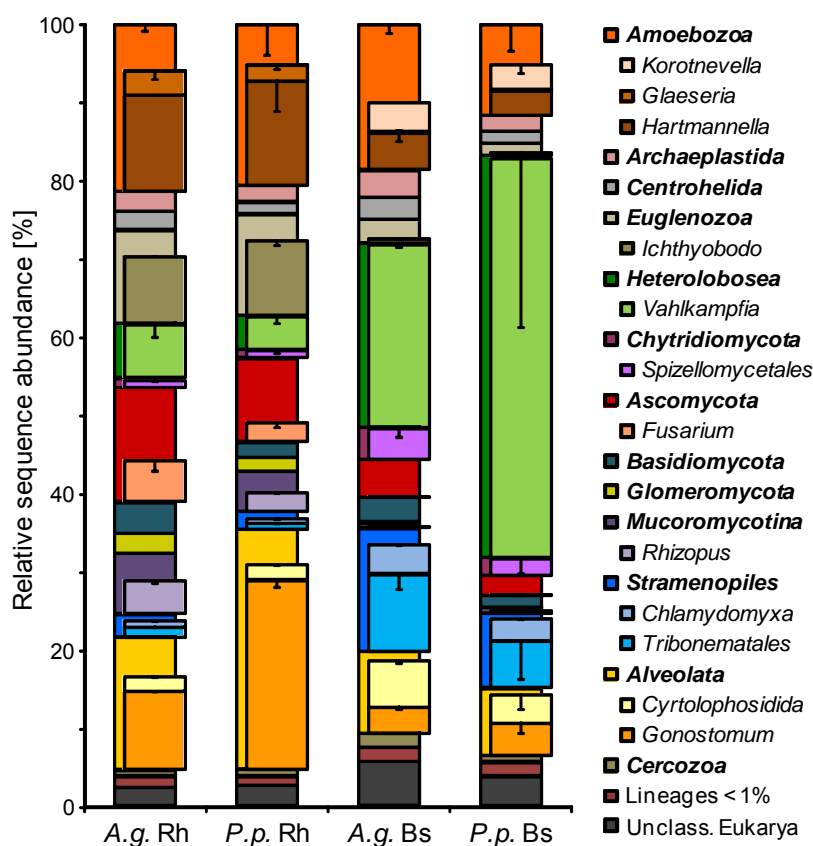
Figure 14. Relative sequence abundance for overall eukaryotic taxa obtained by amplicon sequencing of light gradient fractions from soil microcosms after 8 d of incubation. Codes and other details are as in Figure 13.

In contrast, much more pronounced distinctions in microeukaryotic communities were consistently observed between compartments (Figure 14). Amongst the *Amoebozoa*, rRNA of *Glaeseria* and *Korotnevella* spp. was identified in rhizosphere or bulk soil only, respectively. rRNA of the amoeboid *Hartmannella* spp. was much higher in relative abundance in the rhizosphere (~13% vs. ~3%). Other microeukaryotes enriched in the rhizosphere included protists like *Ichthyobodo* (~9% vs. ~1%) and *Gonostomum* (10-24% vs. ~4%), and different fungi including *Fusarium* and *Rhizopus* spp.. In contrast, rRNA of the amoeboid *Vahlkampfia* spp. appeared highly enriched in bulk soil libraries (23-51%), especially under *P. putida* amendment. Furthermore, ciliates within the *Cyrtolophosidida* (~5% vs. ~2%), fungal *Spizellomycetales* (~3% vs. ~1%), and members of the algal *Stramenopiles* (10-16% vs. ~2%) consistently showed higher relative abundance in bulk soil.

63

3.1.4. Labelled bacterial taxa

A first comparison of sequencing libraries across buoyant densities at phylum- and class-level already revealed the impact of ^{13}C-amendments in comparison to controls (Figure 15). Not unexpectedly, heavy rRNA of *Actinobacteria* was still highly dominant (> 90%) in heavy ^{13}C-rRNA fractions in samples where *A. globiformis* was amended. In contrast, reads of *Gammaproteobacteria* were much less enriched in heavy fractions of the [13]C-*P. putida* amended samples, while actual *P. putida* reads were hardly detected in these libraries. Instead, rRNA reads of the *Deltaproteobacteria* appeared clearly enriched in [13]C-*P. putida* treatments.
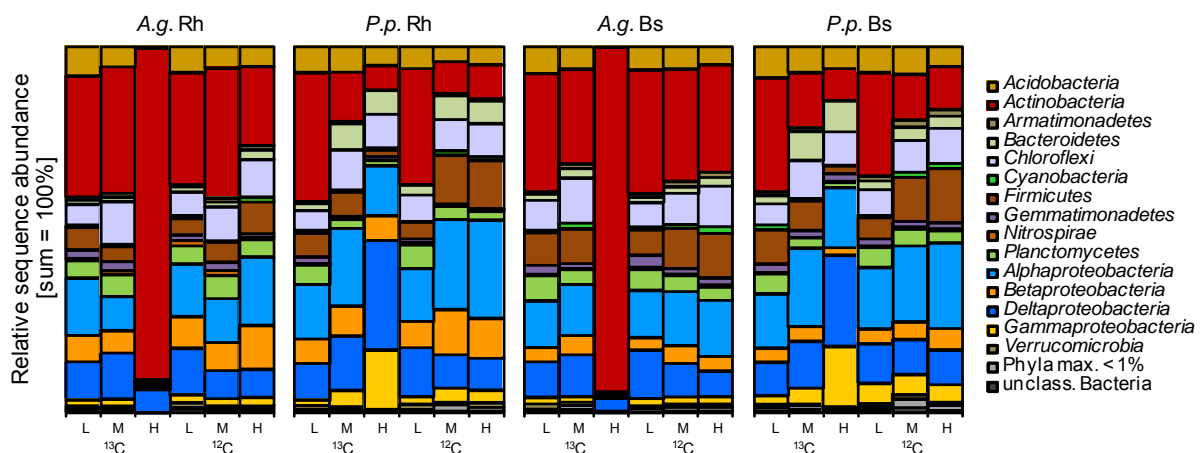
Figure 15. Relative phylum- and class-level community composition of bacterial sequencing libraries obtained from representative light, medium and heavy rRNA gradient fractions after SIP centrifugation. Microcosm codes are as in Figure 13.

The specific bacterial populations incorporating ^{13}C from the amended biomass were identified based on the calculation of taxon-specific enrichment factors (Kramer *et al.*, 2016). The thus identified ^{13}C-labelled bacterial taxa belonged to diverse bacterial phyla, mainly the *Proteobacteria*, and also the *Gemmatimonadetes*, *Chloroflexi*, *Bacteroidetes*, *Actinobateria* and *Acidobacteria* (Figure 16). However, as already suggested by the [13]CO$_2$ and T-RFLP data, ^{13}C-enriched rRNA of the amended *A. globiformis* remained highly detectable after 8 d of incubation, whereas that of the *P. putida* amendment was no longer detectable. Apart from *A. globiformis*, the only intrinsic bacterial taxa that seemed to have incorporated ^{13}C-label in the respective treatments were *Haliangium* spp., as well as a small number of other myxobacterial lineages. Labelling of these *Deltaproteobacteria* was generally more apparent in the rhizosphere than in bulk soil (Figure 16).
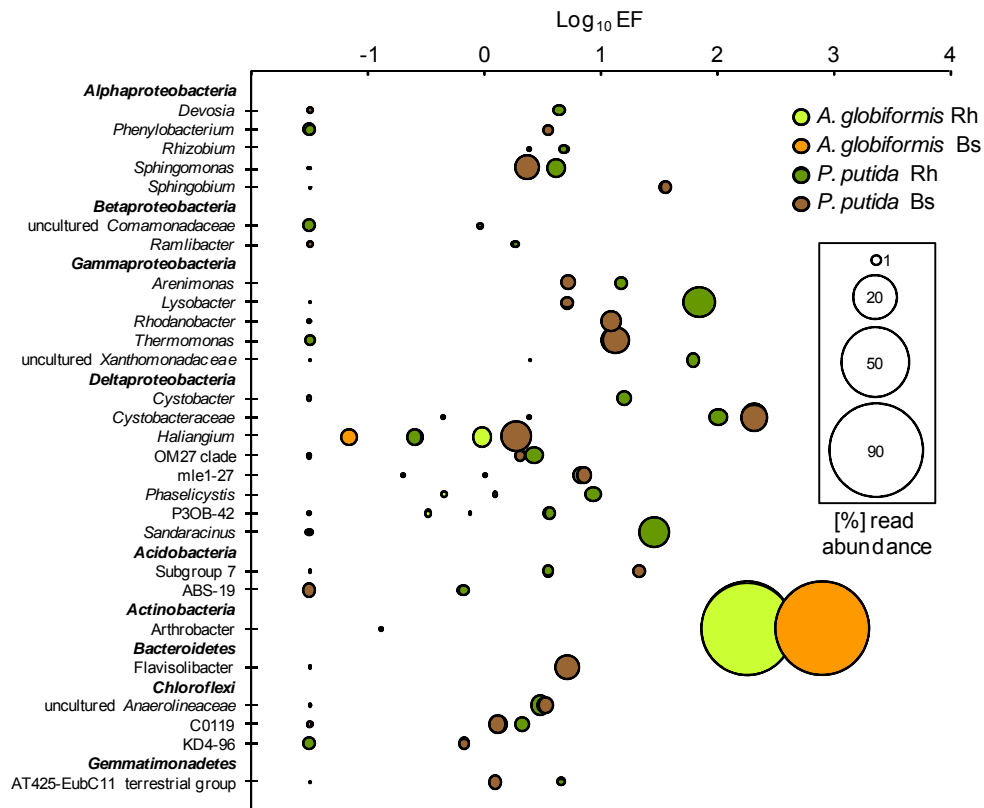
Figure 16. ^{13}C-labelled bacterial taxa identified by SIP in rhizosphere (Rh) and bulk soil (Bs) microcosms amended with *A. globiformis* and *P. putida* after 8 d of incubation. Labelling was inferred based on enrichment factors (EF) calculated from heavy vs. light rRNA gradient fractions of [13]C- and ^{12}C-microcosms. Taxa with an EF > 0.5 in at least one treatment were considered as ^{13}C-labelled. EFs are shown in combination with relative read abundance of labelled taxa in heavy ^{13}C-RNA. The EFs of taxa with a negative read enrichment for given time points or treatments, but labelled in others, was manually set to a $\log_{10}$ of -1.5 for graphical display.

In stark contrast, ^{13}C-label from *P. putida* was suggested to be assimilated by a considerable diversity of bacterial populations in both rhizosphere and bulk soil (Figure 16). Especially, rRNA of unclassified *Cystobacteraceae* (also myxobacteria) was most highly enriched in heavy rRNA from both soils. Other bacterial taxa with marked rRNA enrichment in both compartments included the gammaproteobacterial *Lysobacter* and *Arenimonas* spp., diverse myxobacteria including *Haliangium* spp., the *Bdellovibrionaceae* clade OM27, the alphaproteobacterial *Sphingomonas* spp., as well as unclassified *Chloroflexi*. In addition, several taxa were found to be specifically labelled either in bulk soil or the rhizosphere, such as *Thermomonas* and *Rhodanobacter* spp. (*Gammaproteobacteria*), *Sphingobium* spp. (*Alphaproteobacteria*) and *Flavisolibacter* spp. (*Bacteroidetes*) in bulk soil, or *Sandaracinus* and *Cystobacter* spp. (*Deltaproteobacteria*) as well as unclassified

65

Xanthomonadaceae (*Gammaproteobacteria*), which were strongly ^{13}C-enriched in rhizosphere soil (Figure 16).

3.1.5. Labelled eukaryotic taxa

Same as for bacterial rRNA, the composition of microeukaryotic rRNA libraries across gradient fractions also suggested clear labelling patterns in SIP. rRNA of *Amoebozoa* appeared highly enriched in heavy rRNA fractions of rhizosphere samples in response to both *P. putida* and *A. globiformis* amendments, and to a lesser extent also in bulk soil for the *A. globiformis* amendment (Figure 17). Reads of the amoeboid *Heterolobosea* were generally more abundant in bulk soil than in the rhizosphere, and showed enrichment in the heavy fractions especially for the *P. putida* treatment.
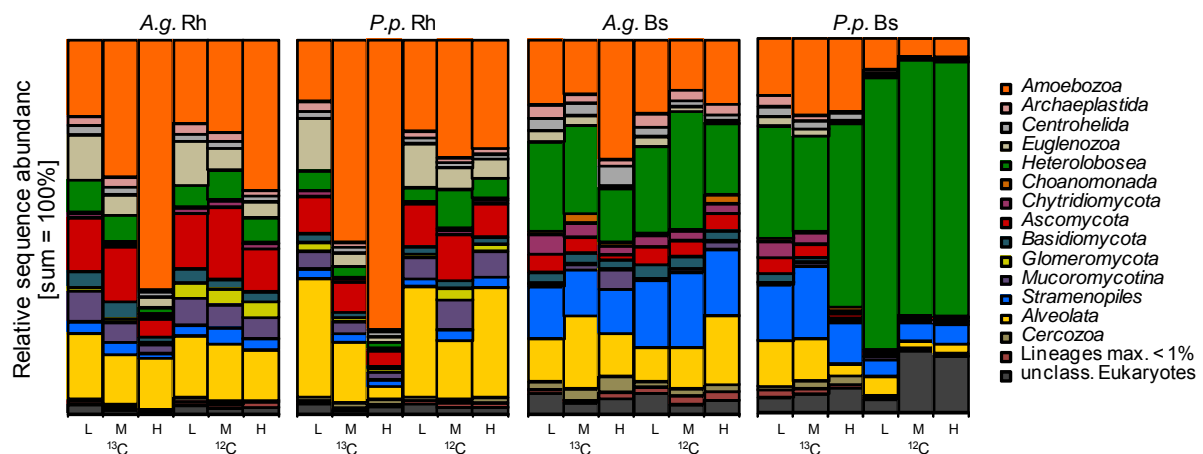
Figure 17. Community composition of eukaryotic sequencing libraries obtained from representative light, medium and heavy rRNA gradient fractions after SIP centrifugation. Microcosm codes are as in Figure 13.

Taxon-specific EFs confirmed these first indications, but also revealed distinct population-specific feeding preferences (Figure 18). rRNA of the amoeboid *Glaeseria* spp., for example, showed strong ^{13}C-enrichment especially under amendment of *A. globiformis* in both soils. Other amoeba including members of the *Schizoplasmodiida*, *Acanthamoeba, Dactylopodida* and the *Vampyrellidae* showed similar labelling patterns, but less pronounced. In contrast, rRNA of *Hartmannella* spp. and the amoeboid BOLA868 lineage appeared specifically labelled under *P. putida* amendment, especially in the rhizosphere. Other amoeba like *Vahlkampfia* and

Korotnevella spp. appeared specifically ^{13}C-labelled for *P. putida* treatments in bulk soil only. Other protists found to be enriched in heavy ^{13}C-rRNA, albeit less markedly, included the flagellate *Cercomonas* spp. and the *Centrohelida* (*Heliozoa*) especially in bulk soil, as well as *Pseodoplatyophyra* spp. (*Ciliates*) in the rhizosphere. A choanoflagellate taxon, *Salphingoeca* spp. was labelled, interestingly for *A. globiformis* in the rhizohsphere and *P. putida* in bulk soil. Several fungal taxa also showed enrichment in heavy ^{13}C-rRNA, i.e. members of the *Mucorales* in bulk soil of both *P. putida* and *A. globiformis* treatments. An algal taxon, *Chlamydomyxa* (*Stramenopiles*), also appeared highly enriched and abundant in heavy rRNA extracted from bulk soil.
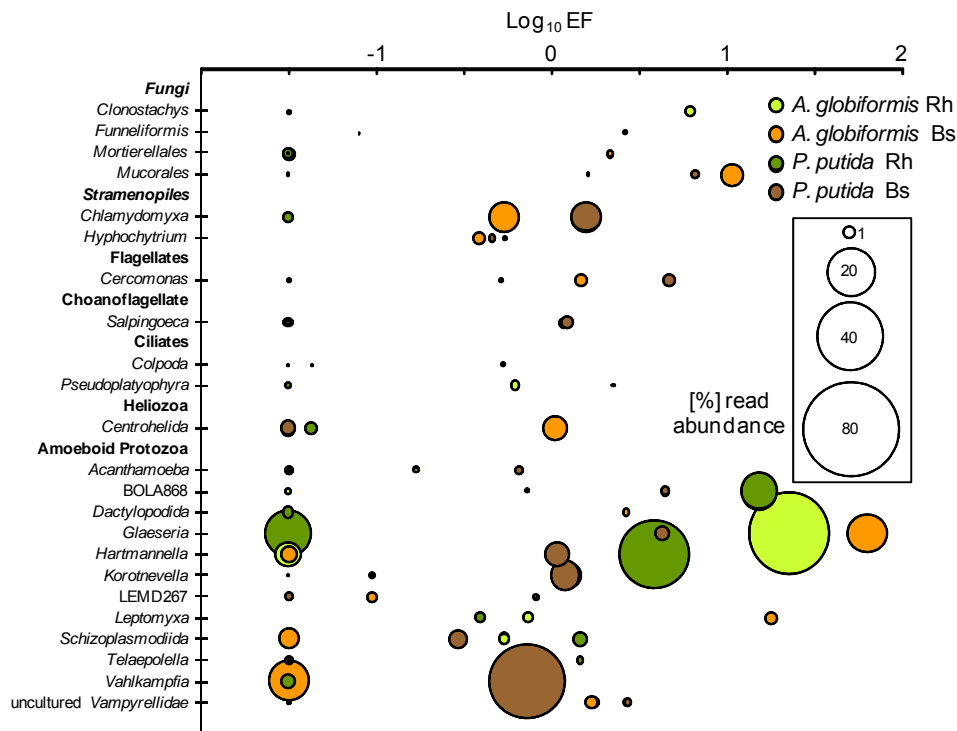
Figure 18. ^{13}C-labelled microeukaryotic taxa identified by SIP in soil microcosms after 8 d of incubation. All further details: see legend of Figure 16.

In summary, these findings show differential predatory mechanisms between bacterial and protozoan predators influenced by the nature of bacterial prey and by soil compartment (rhizosphere vs. bulk soil). In contrast to my first hypothesis, clear distinctions in the relevance of predation by protists vs. intrabacterial predation between bulk soil and rhizosphere were not observed. In the next step, I explored the translocation of topsoil root-associated bacterial populations to deeper soil horizons upon strong precipitation events.

3.2. Time-resolved transport of bacterial populations with seepage water after extreme precipitation in summer

To unravel the transport mechanisms of indigenous bacterial populations triggered by strong rainfall in the investigated agricultural soil, fresh seepage water was sampled over 24 h after a natural rain event. To further elucidate temporal bacterial transport patterns, an artificial rain experiment was conducted with fluorescently labelled bacteria amended to topsoil. In both cases, corresponding bulk soil at different depths, rhizosphere and rhizoplane samples near the lysimeters were also sampled. Flow cytometry was employed to provide quantitative assessment of transported bacteria, and T-RFLP fingerprinting together with amplicon sequencing were performed to analyse the composition of mobilised bacterial communities.

3.2.1. Seepage water and transported bacteria after a natural rain event

To investigate the mobilisation of indigenous bacterial populations triggered by rainfall in late summer, fresh seepage water was first sampled over 24 h after a natural rain event of ~30 mm (~5 L per lysimeter). Seepage water was taken in duplicates from two pairs of lysimeters located at depths of 35 and 65 cm. The mean soil temperature was 15°C at prevailing air temperature of 14.5°C on the sampling day. The mean water content (19.09.2012: 48 cm: 23±1 vol%, 58 cm: 25±1 vol%) was significantly lower than the mean annual water content (2010-2012; 48 cm: 26±3 vol%, 58 cm: 29±3 vol%). The two sampled plots (A and B) showed different seepage water characteristics over depth (Table 2). Lysimeters in plot A produced a larger seepage volume at 65 cm, while OC concentrations as well as that of nitrate and sulfate decreased with depth. In contrast, plot B showed an inverse trend, with a larger seepage volume collected at 35 cm, and higher concentrations of OC and anions in the lower depth water samples.

Bacterial communities in seepage water were compared to that in respective soil and root samples using principal component analysis (PCA) based on both T-RFLP and sequencing data sets. The spatial ordination of distinct samples in PCA plots was mirrored for both data sets (Figure 19). Seepage water samples were clearly separated from the bulk soil communities, especially along PC1s, which seemed to be influenced mostly by compartments. Rhizoplane bacterial communities were

further discriminated from the rhizosphere and bulk soil communities, and were placed closer to the seepage water samples along PC1 in both plots. The PC2s seemed to be mostly influenced by depth, which separated rhizoplane samples from rhizosphere, bulk soil and water samples at different depths. In general, replicated fingerprints and sequencing libraries were highly comparable, except that the fingerprints of bacterial communities in seepage water from the two 35-cm lysimeters appeared more variable along PC2.

Table 2. Seepage water volume and hydrochemical parameters (measured by Andreas Schmalwasser, group of Kai-Uwe Totsche, University of Jena) of the water samples taken after the natural rain event in September 2012. Duplicate lysimeters (A & B) were sampled in 35 and 65 cm depth each.

Lysimeter	Seepage volume [L]	pH	EC [µS cm^{-1}]	Nitrate [mg L^{-1}]	Sulfate [mg L^{-1}]
L35A	0.18	7.1	148	8.58	5.20
L65A	0.42	7.0	72	1.96	1.70
L35B	0.32	7.2	152	1.60	2.88
L65B	0.18	7.3	167	7.49	4.37
	TOC [mg L^{-1}]	DOC (< 0.45 µm) [mg L^{-1}]	POC (> 0.45 µm) [mg L^{-1}]	Hydrodynamic diameter [nm]	Zeta potential [mV]
L35A	94.74	2.92	91.82	1165	-16.6
L65A	16.88	2.67	14.21	p	-
L35B	7.09	2.61	4.48	p	-
L65B	18.47	3.33	15.14	982	-16.4

p – polydispersity of the sample resulted in no clear hydrodynamic diameter and zeta potential measurement

Sequencing suggested that the bacterial taxa representative for seepage water were mostly affiliated to the *Bacteroidetes* (*Chitinophagaceae*, *Cytophagaceae*, *Flavobacteriaceae* and *Sphingobacteriaceae*), and also the *Alphaproteobacteria* (*Sphingomonadaceae*), *Gammaproteobacteria* (*Moraxellaceae*) and *Verrucomicrobia* (*Verrucomicrobiaceae*), as shown in Figure 19b. Reads related to the *Comamonadaceae* (*Betaproteobacteria*) seemed to be characteristic for both the 65-cm seepage water samples and rhizoplane samples. Another lineage that appeared to be associated to rhizoplane samples was the *Pseudomonadaceae*

(*Gammaproteobacteria*). Reads affiliated to unclassified *Xanthomonadales* (*Gammaproteobacteria*) and *Hyphomicrobiaceae* (*Alphaproteobacteria*) were more important in rhizosphere and 10-cm bulk soil samples. In contrast, characteristic taxa found in bulk soil mostly belonged to the *Firmicutes* (*Bacillaceae*, *Clostridiaceae*, *Paenibacillaceae*, *Peptococcaceae* and *Planococcaceae*), the *Acidobacteria* (Subgroup 4 RB41 and Subgroup 6), the *Alphaproteobacteria* (*Rhodobiaceae* and *Xanthobacteraceae*), and also the *Gemmatimonadetes* (*Gemmatimonadaceae*), *Nitrospirae* (*Nitrospiraceae*) and *Planctomycetes* (*Planctomycetaceae*). Members of the *Firmicutes* appeared especially characteristic for bulk soil at the depth of 60-70 cm.
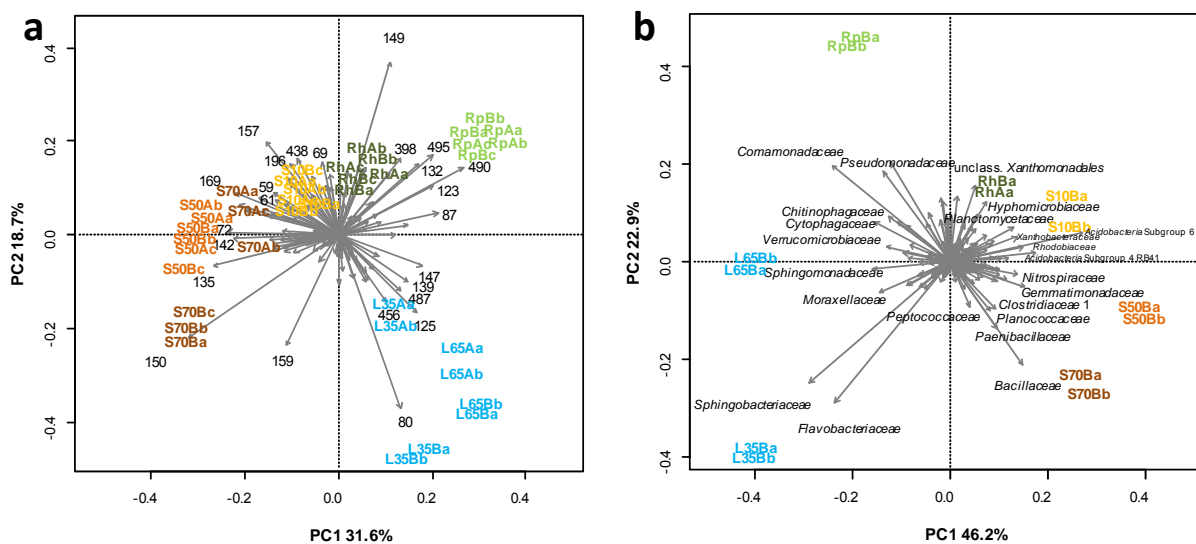
Figure 19. PCA biplots of T-RFLP (a) and amplicon sequencing (b) data sets of samples obtained after a natural rain event. Seepage water was sampled from two lysimeters, i.e. two pairs of 35 cm- and 65 cm-lysimeters (LA35, LA65 and LB35, LB65). S10, S50, S70: bulk soil samples from 0-10, 40-50 and 60-70 cm depth; Rh: rhizosphere; Rp: rhizoplane. Sample codes are shown in bold and in colors according to sampled compartments. Biological duplicates (a,b) of water samples and triplicates (a,b,c) of soil and rhizoplane samples were first analysed by T-RFLP (A), whereas duplicates (a,b) of water, soil and root samples from only one of the two lysimeters (LB) per depth were subject to amplicon sequencing (B). T-RFs (A) and taxa (B) are denoted by grey arrows, with selected discriminant T-RFs or taxa labelled or named, respectively.
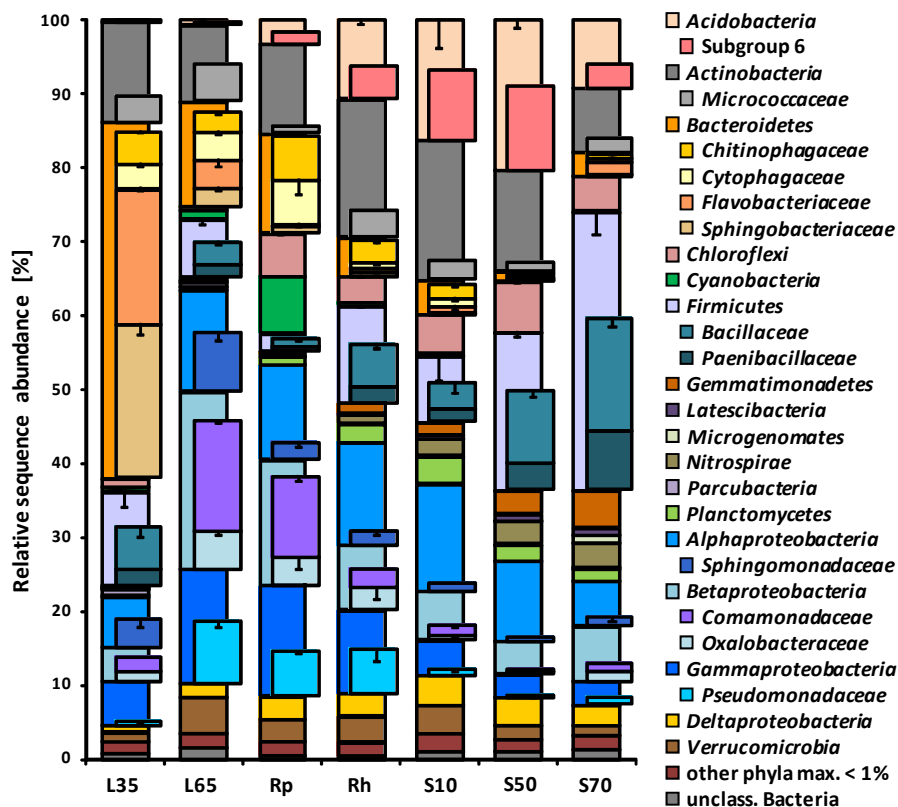
Figure 20. Relative sequence abundance for bacterial taxa obtained by amplicon sequencing of samples from the natural rain event. All phyla with average relative sequence abundance > 1% in at least one of the compartments were shown individually, as well as *Microgenomates* and *Parcubacteria* (< 1%, mentioned in text). Error bars (negative only) represent standard error (*n* = 2) of duplicate sequencing libraries. Selected abundant sub-phylum taxa are highlighted. Sample codes are as in Figure 19.

The comparison of taxon-level community composition of overall sequencing libraries substantiated these pronounced differences between the seepage water and bulk soil communities, as well as over depth (Figure 20). Reads of the *Flavobacteriaceae*, *Sphingobacteriaceae* and *Bacillaceae* were much more abundant in water at 35 cm (18%, 21% and 6%) than at 65 cm (4%, 2% and 3%). Families that appeared more frequent in seepage water at 65 cm included the *Sphingomonadaceae* (8% vs. 4%), *Comamonadaceae* (15% vs. 2%), *Oxalobacteraceae* (5% vs. 1%) and *Pseudomonadaceae* (8% vs.1%). Some of these abundant taxa in seepage water were also frequent on the rhizoplane, i.e. the *Chitinophagaceae* (L35: 4%, L65: 3%, Rp: 6%), *Cytophagaceae* (L35: 3%, L65: 4%, Rp: 6%), *Comamonadaceae* (Rp: 11%), *Oxalobacteraceae* (Rp: 4%) and *Pseudomonadaceae* (Rp: 6%), all of which were very low in relative abundance in bulk soils. Other taxa found in seepage water and

71

hardly observed in bulk soils included the *Flavobacteriaceae*, *Sphingobacteriaceae* and *Sphingomonadaceae*. In contrast, reads within the *Acidobacteria* and *Chloroflexi* were abundant in bulk soil and in the rhizosphere, but almost absent in seepage samples. Also, *Firmicutes* were predominant in rhizosphere and bulk soils, especially in soils at 40-50 cm and 60-70 cm depth, but lower in relative abundance in seepage waters (L35: 13%, L65: 8%, S50: 21%, S70: 38%).

3.2.2. Artificial rain experiment

To allow for a better experimental grasp of bacterial mobilisation with seepage water and to resolve possible temporal patterns in bacterial transport, an artificial rain experiment was conducted at the field site in Sept. 2014. The artificial rain experiment was carried out with six lysimeters, but seepage water was only obtained for two of the lysimeters (LC and LD) with an amendment of *A. globiformis* added to the artificial rain water. Seepage water could not be collected from the two other lysimeters amended with labelled bacteria and the two control lysimeters. Seepage water sampling at 35 cm depth for LC and LD lasted ~27 h and ~23 h, respectively, until no more seepage water appeared in the lysimeters. Six time-resolved water samples were collected for LC (LCT1-6; ~210 ml average vol.) and seven samples were obtained for LD (LDT1-6 ~250 ml average vol.; LDT7 contained only 22 ml of water and was omitted from molecular work). From the total applied water volume, i.e. 16 L per lysimeter, 1.25 L and 1.51 L (8-9%) were recovered in seepage. The pH of the seepage water was nearly constant for both lysimeters (LC: pH 6.9 ± 0.3; LD: pH 6.5 ± 0.2) over time, and slightly higher than the original pH of the artificial rain water (pH 6.1). The EC values increased to a maximum after ~0.5 L of total seepage volume (LC: 430 µS cm^{-1}; LD: 390 µS cm^{-1}), followed by a decrease to the original EC of the artificial rain water (335 µS cm^{-1}). The breakthrough curves of bromide as conservative tracer were distinct for the two lysimeters (Figure 21a). The curve for LC was characterised by increasing concentrations and a peak of 101 mg L^{-1} after 0.5 L seepage was produced, while similarly high concentrations of bromide immediately appeared in LD (0.2 L, 110 mg L^{-1}). Notable declines were observed after 4-5 fractions of seepage water (> 1 L in total) had been collected. The Br^{-} concentration of the artificial rain (151 mg L^{-1}) was not reached in seepage samples of LC (67%)

and LD (73%). In total, only ~4-6% of the amended bromide mass was recovered in seepage waters of LC and LD, respectively.

The fluxes of TOC and DOC also differed between both lysimeters over time (Figure 21b). LC showed an initial OC concentration of 18 mg L^{-1}, which then decreased to a constant level of ~10 mg L^{-1}. The contribution of particulate organic carbon (POC, > 0.45 μm) to TOC was initially high for LC (~43%), but then decreased with flow time to ~27% in LCT6). Initial TOC concentrations were slightly higher in LD (~21 mg L^{-1}), decreased transiently in fractions 3 and 4, but then increased to final concentrations around ~27 mg L^{-1}. Similarly, the POC content was initially much higher for LD (69% of TOC), transiently decreased to ~20%, and then increased again towards final seepage water fractions. Total cell counts fluctuated around ~10^7 cells ml^{-1} of seepage water (Figure 21c). Total cell counts and TOC export appeared correlated.

3.2.3. Mobilised bacteria after the artificial rain experiment

Bacterial communities recovered in successive seepage water fractions from the two lysimeters were again analysed by T-RFLP fingerprinting and amplicon sequencing. The spatial ordination of distinct samples in PCA biplots was also consistent for both data sets (Figure 22). The PC1s largely separated the seepage water communities recovered from LC and LD. Interestingly, the PC2s arranged the samples from LC and LD in comparable time-resolved patterns. The first water samples (LCT1 & LDT1) were always well-separated from subsequent samples. In both the fingerprinting and sequencing data sets, bacterial communities for early and late time points of seepage water recovery appeared related, while they were more distinct from the samples for intermediate fractions (LCT2-5, LDT3-5). The bacterial communities mobilised in LD generally showed a greater variation over time than in LC.
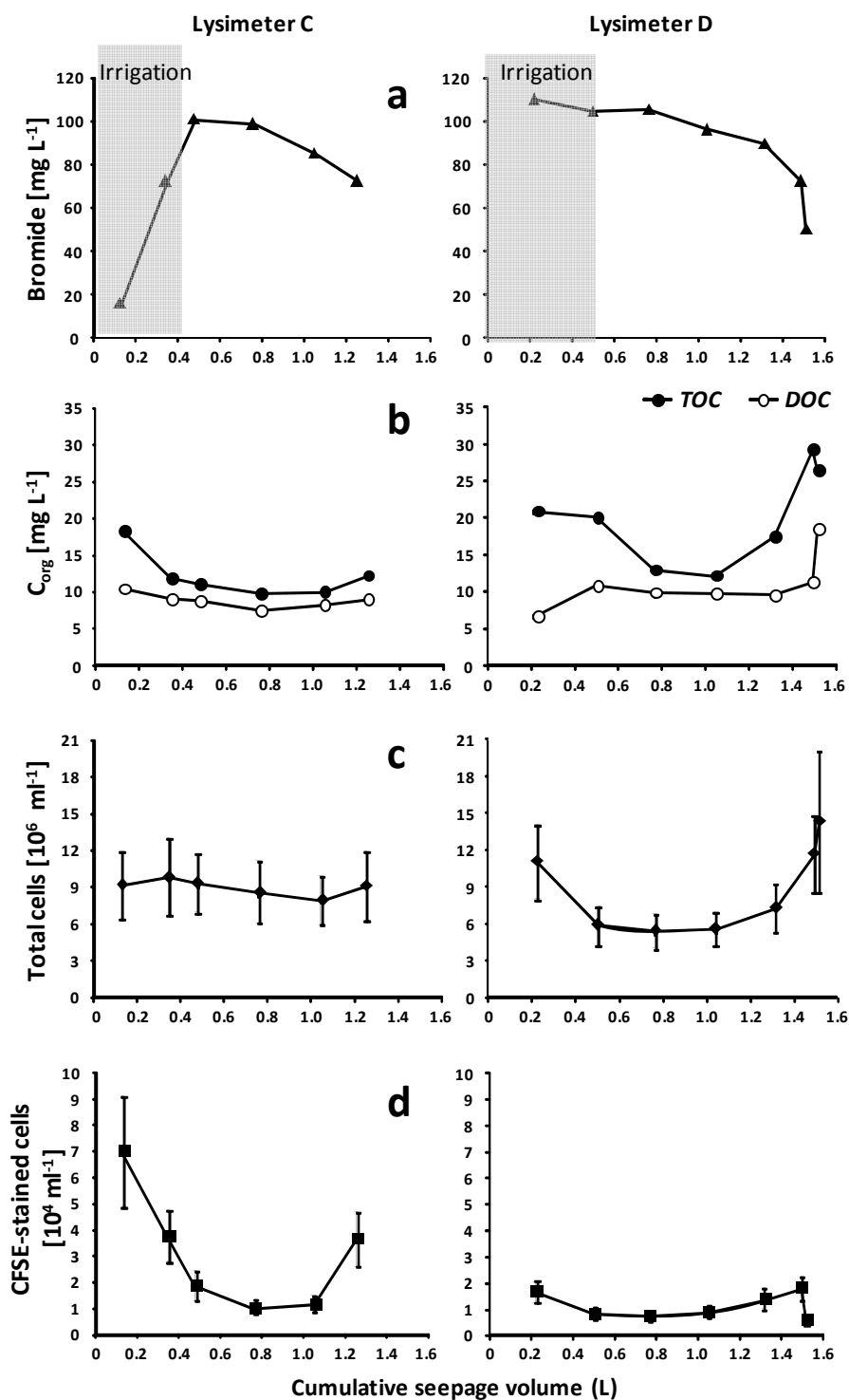
Figure 21. Concentration profiles of bromide (a), TOC and DOC (b), total bacterial cells (c) and CFDA/SE-stained cells (d) detected in seepage water fractions from LC and LD during the artificial rain experiment. Error bars represent standard error (*n* = 2) of duplicate measurements in (c) and (d), and are too small for visualization in (b, internal). Single measurements were conducted for (a).
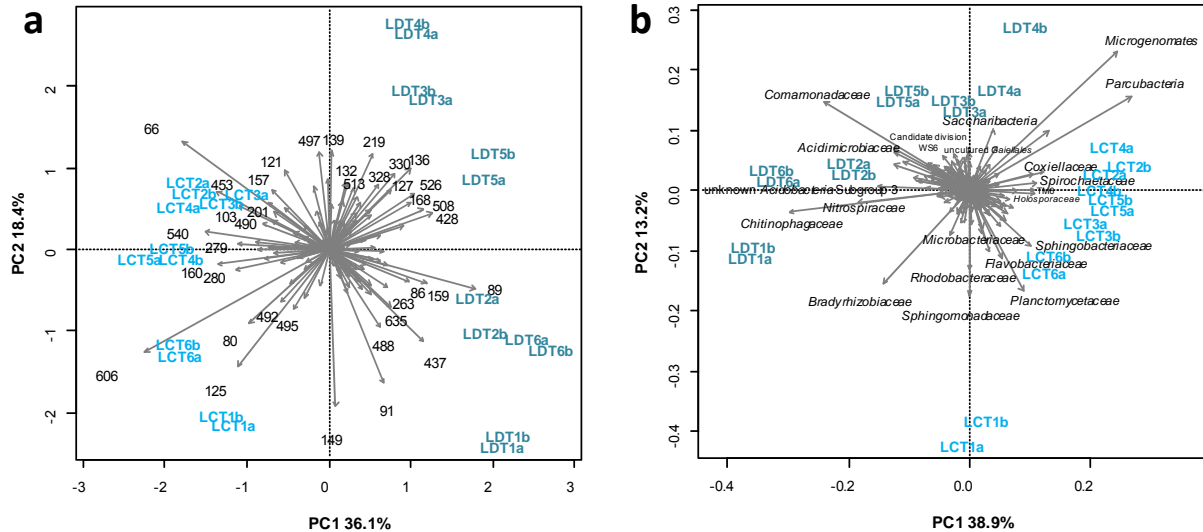
Figure 22. PCA biplots of bacterial communities in seepage water sampled during the artificial rain experiment based on T-RFLP (a) and amplicon sequencing (b) data. Water samples were collected from two lysimeters (LC and LD). All samples were subjected to fingerprinting and sequencing in biological duplicates. T-RFs (a) and taxa (b) are denoted by grey arrows, with selected relevant T-RFs or taxa labelled or named, respectively.

The PCA biplots helped to identify bacterial taxa characteristic for the different time points of seepage water collection in the two lysimeters (Figure 22b). While members of the *Bradyrhizobiaceae* (*Alphaproteobacteria*) seemed to be especially characteristic for initial seepage water samples, members of two candidate phyla, *Microgenomates* and *Parcubacteria*, appeared enriched in intermediate seepage fractions. Furthermore, members of the *Flavobacteriaceae*, *Sphingobacteriaceae* (both within the *Bacteroidetes*), *Planctomycetaceae* (*Planctomycetes*) and others appeared to be specifically associated with intermediate water samples of LC, while the *Chitinophagaceae* (*Bacteroidetes*), *Nitrospiraceae* (*Nitrospirae*), *Comamonadaceae* (*Betaproteobacteria*) and others appeared especially in respective fractions of LD (Figure 22b).

Overall taxon-level community dynamics in seepage water fractions after the artificial rain event and in respective rhizosphere, rhizoplane and bulk soil samples generally substantiated the marked distinctions between water and soil bacterial communities, as well as shifts in mobilised populations in seepage water over time (Figure 23). Members of the *Bacteroidetes*, the *Gammaproteobacteria* and the candidate phyla *Microgenomates, Parcubacteria*, SM2F11 and TM6, were of enriched abundance in seepage water samples, and much less abundant or almost absent in soil. In contrast,

the *Acidobacteria*, *Actinobacteria*, *Chloroflexi*, *Firmicutes* and *Gemmatimonadetes*, although abundant in bulk soils, were much less frequently detected in seepage waters.

The rhizoplane, rhizosphere and bulk soil samples showed highly similar overall communities between the two lysimeters, while the rhizoplane samples again appeared generally more similar to the seepage water samples (Figure 23). Consistent variations in relative sequence abundance during seepage water collection were observed for several bacterial taxa in both lysimeters. For example, mobilised *Chitinophagaceae*, while being generally more abundant in LD, were always more abundant in fractions 1 and 6 of both lysimeters. The alphaproteobacterial *Sphingomonadaceae* and *Bradyrhizobiaceae* showed a similar pattern, same as members of the *Comamonadaceae*, the latter only for LD. In contrast, reads within the *Microgenomates* and *Parcubacteria* showed a general increase in abundance between fractions 1 and 4 in both lysimeters, followed by slight decreases in relative abundance until the end of the seepage event. Members of the *Gammaproteobacteria* (*Coxiellaceae, Legionellaceae*) also steadily increased and were most abundant in intermediate water fractions collected from both lysimeters.

50 ml of live fluorescently labelled cells of *A. globiformis* at a concentration of ~2.8 × 10^9 cells ml^{-1} were amended to the topsoil above LC and LD during the artificial rain experiment. This corresponded to an amendment of ~6.2 × 10^7 cells per g_{dw} of topsoil (assuming a more or less even distribution throughout the first 2 cm of soil), and thus ~3% of the indigenous bacterial biomass (previously quantified at ~2.1 × 10^9 cells per g_{dw} in Dibbern *et al.*, 2014). The breakthrough curves of CFDA/SE-stained cells recovered in seepage water were much lower in concentration, in a range of 10^4-10^5 cells ml^{-1} (Figure 21d). The concentration of recovered labelled bacterial cells was always lower in LD seepage water than in LC, but fluxes in both lysimeters seemed to follow a similar pattern of slightly increased concentrations at the start and towards the end of the seepage process (similar as for TOC and total cells). Corrected for the total amount of exported bromide tracer retained in seepage water, only about ~0.6 and ~0.2% of the amended *A. globiformis* cells were recovered in LC and LD, respectively.
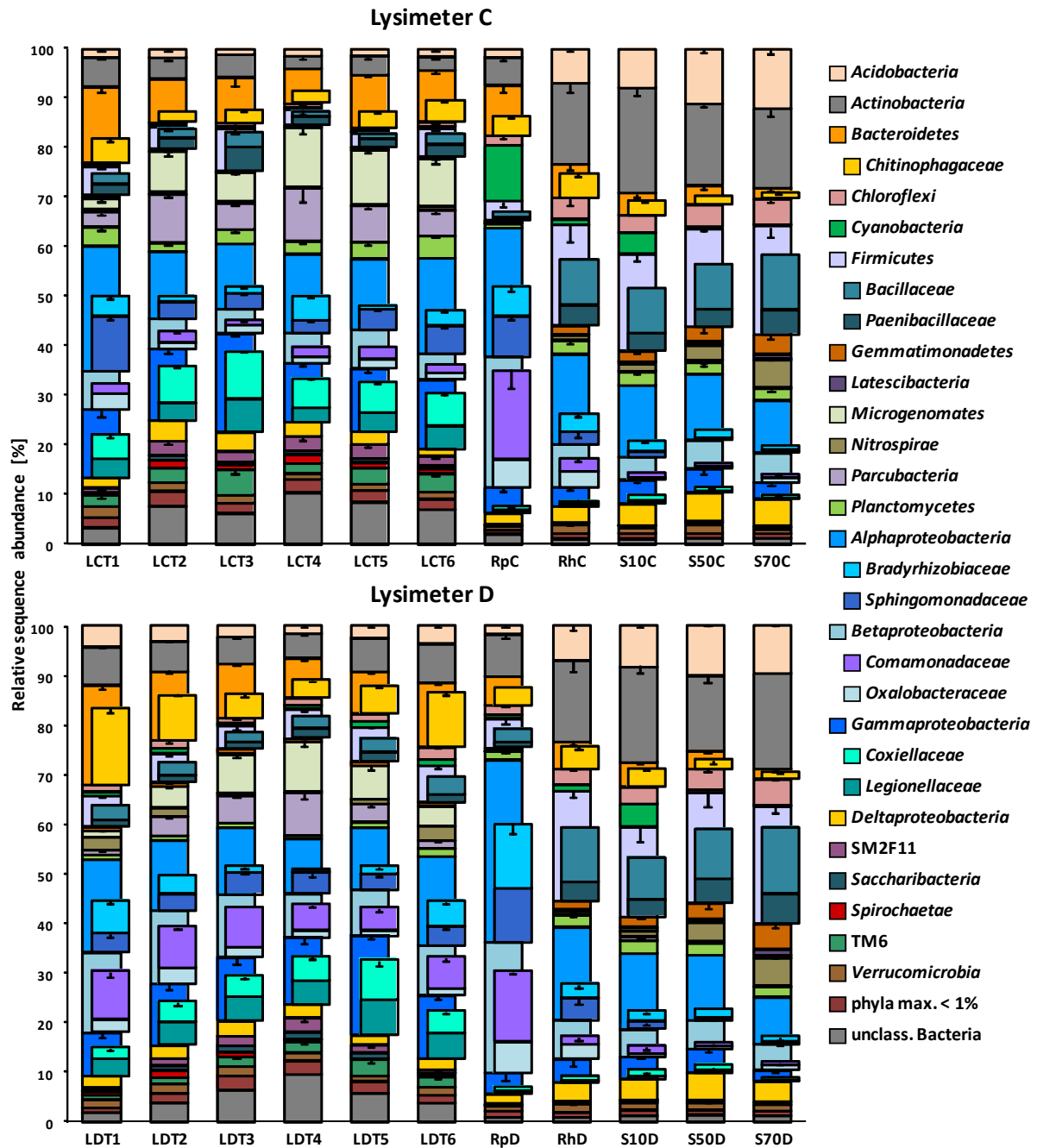
Figure 23. Relative sequence abundance for bacterial taxa obtained by amplicon sequencing of successive seepage water and soil samples during the artificial rain experiment. Error bars (negative only) represent standard error (*n* = 2) of duplicate sequencing libraries. Selected abundant sub-phylum taxa are highlighted. Sample codes and other details are as in Figure 19 and Figure 22.

In summary, my findings show that the transport of root-associated topsoil bacteria to deeper soil layers driven by extreme precipitation events exert stronger selection in summer in the presence of live root channels compared to winter. Consistent with my second hypothesis, a dynamic nature of microbiota mobilised between successive

fractions of collected seepage water was revealed, which has intriguing implications for various physiological characteristics of the translocated microbes. In the next step, soil bacterial populations were monitored in broader temporal and spatial scales to reveal their long-term distribution patterns.

3.3. Four-year monitoring of soil bacterial populations in the field

To investigate the diversity and distribution of soil bacterial communities in relation to plant species and litter amendment along a depth profile in the investigated field site, soil samples were obtained under distinct treatments at three different depths (0-10 cm, 40-50 cm and 60-70 cm) over four years in biological triplicates. Quantitative PCR, T-RFLP fingerprinting and amplicon pyrosequencing were employed to reveal the comprehensive characteristics of bacterial microbiota in the investigated soil.

3.3.1. Bacterial 16S rRNA gene abundances

Bacterial 16S rRNA gene quantities clearly decreased with soil depth (Figure 24). Litter amendment significantly elevated bacterial abundance in the topsoil in the last two years, although the effect was not significant in 2010 and 2011 (Figure 24; 2010: $F_{1,8} = 0.30$, $p = 0.60$; 2011: $F_{1,8} = 1.97$, $p = 0.20$; 2012: $F_{1,8} = 8.22$, $p = 0.02$; 2013: $F_{1,8} = 9.60$, $p = 0.01$). A plant species effect was hardly observed in the topsoil (Figure 24; 2010: $F_{1,8} = 4.21$, $p = 0.07$; 2011: $F_{1,8} = 2.04$, $p = 0.19$; 2012: $F_{1,8} = 2.87$, $p = 0.13$; 2013: $F_{1,8} = 0.88$, $p = 0.38$). In contrast, wheat-cropped plots exhibited a higher bacterial abundance compared to maize plots in the rooted horizon below the plough layer (40-50 cm), significantly visible in 2010, 2011 and 2013, while marginally in 2012 (Figure 24; 2010: $F_{1,8} = 12.19$, $p < 0.01$; 2011: $F_{1,8} = 8.70$, $p = 0.02$; 2012: $F_{1,8} = 5.07$, $p = 0.05$; 2013: $F_{1,8} = 2.54$, $p = 0.15$). A weak but significant plant effect was also observed in the root-free zone, but only in 2012 (Figure 24; 2012: $F_{1,8} = 8.85$, $p = 0.02$).
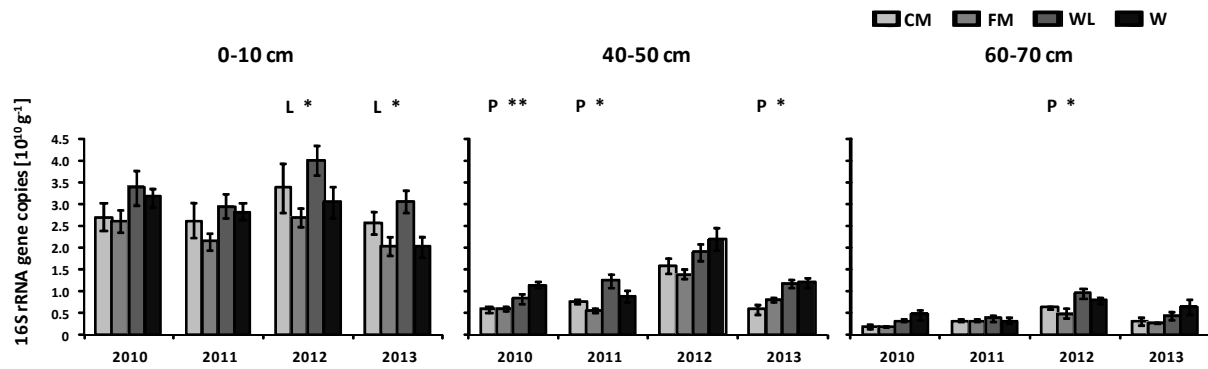
Figure 24. Bacterial 16S rRNA gene abundances at depths of 0-10 cm, 40-50 cm and 60-70 cm in corn maize (CM, maize with litter), fodder maize (FM, maize without litter), wheat with maize litter (WL) and wheat (W) treatments in September from 2010 to 2013. Error bars represent standard error (n = 3). Statistical significances are based on two-way ANOVA in relation to plant (P) and litter (L) at the investigated depths and sampling dates. $*p < 0.05$; $**p < 0.01$. Quantitative PCR was performed by Gabriele Barthel (Group of Molecular Ecology, IGÖ)

3.3.2. Bacterial community patterns

Redundancy analysis (RDA) was first performed on T-RFLP data to explore the overall pattern of bacterial communities related to depth and treatment (Figure 25). The first two RDA axes together accounted for 29.5% of the total variation. Bacterial communities at the three different depths were clearly separated (Figure 25; depth effect perMANOVA: $R^2 = 0.33$, $p < 0.001$). Some of the T-RFs characteristic for specific soil depth could be assigned to defined taxa based on *in silico* T-RF prediction from sequencing contigs obtained previously from the same soil (Dibbern *et al.*, 2014, Kramer *et al.*, 2016). For example, amongst the T-RFs mostly observed in topsoil, the T-RFs of 205 and 519 bp represented members of the *Cytophagaceae* and *Sphingobacteriaceae*, respectively; and T-RFs of both 80 and 86 bp were linked to *Flavobacteriaceae*. Some other T-RFs preferably found in the rooted zone were also affiliated previously: *Micrococcaceae* (61bp), *Chitinophagaceae* (89 bp), *Micrococcaceae* and *Micromonosporaceae* (both 159 bp). Among the T-RFs characteristic for the deeper soil, the 135 bp fragment was previously linked to the *Nocardiaceae,* and the 490 bp could be assigned to *Legionellaceae*, *Methylophilaceae*, *Oxalobacteraceae* and *Pseudomonadaceae*.

79

RDA also differentiated the replicated soil samples over the four years (Figure 25; year effect perMANOVA: R^2 = 0.11, p < 0.001). Moreover, plant species affected the structure of bacterial communities, as revealed by a slight separation of bacterial communities in maize plots from wheat plots (Figure 25) and perMANOVA analysis (R^2 = 0.02, p < 0.001). In contrast, a litter effect was hardly observed in overall comparison of the bacterial communities (Figure 25; litter effect perMANOVA: R^2 = 0.01, p = 0.13). However, depth-separated perMANOVA revealed specific discrimination between samples under treatments with and without litter input only for topsoil (0-10 cm: R^2 = 0.04, p < 0.001; 40-50 cm: R^2 = 0.01, p = 0.27; 60-70 cm: R^2 = 0.02, p = 0.19).
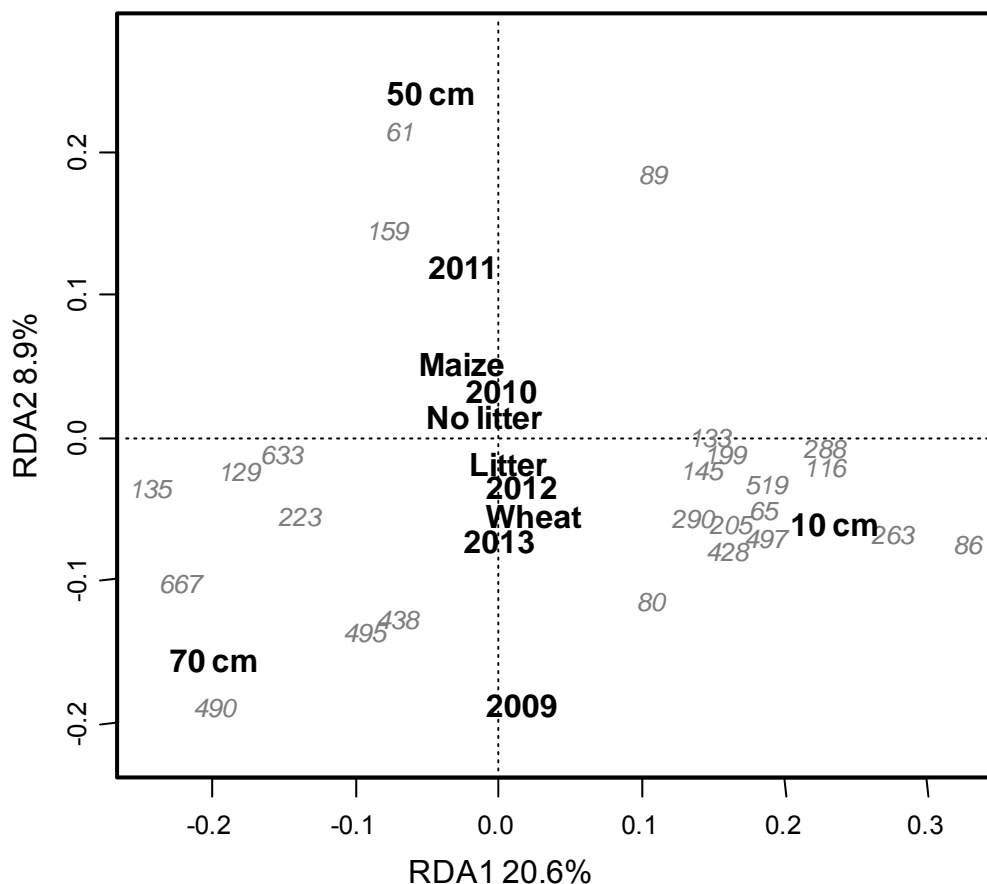
Figure 25. Redundancy analysis (RDA) ordination plot of the T-RFLP data in relation to depth (0-10 cm, 40-50 cm and 60-70), plant (maize and wheat), litter (litter and no litter) and year (2009 to 2013) as categorical explanatory variables. The first and second RDA axes are plotted on the x- and y-axis, respectively. Selected T-RFs are displayed in grey. Classes of the explanatory variables in black are plotted at the centroids of the samples within these classes.

3.3.3. Sequencing of the bacterial communities

Samples of the maize plots were subjected to bacterial 16S rRNA gene amplicon pyrosequencing. Samples from 2010 to 2013 were analysed in biological triplicates, while the 2009 amplicon libraries were not replicated. An overview of overall taxon-level community composition across all sequenced soil communities is shown in Figure 26. Distinctions in community composition were apparent by visual inspection for the different depths and time points. Reads within the *Bacteroidetes* and *Alphaproteobacteria* were always higher in relative abundance in topsoil (5.5 ± 2.6% and 15.7 ± 7.3%) compared to deeper soils (40-50 cm: 3.0 ± 1.6% and 12.3 ± 5.9%; 60-70 cm: 2.8 ± 1.3% and 9.9 ± 4.3%, respectively). On the contrary, reads affiliated to *Firmicutes* were more frequent below the plough layer (0-10 cm, 17.0 ± 8.2%; 40-50 cm, 21.5 ± 10.9%; 60-70 cm, 21.2 ± 11.9%) and *Betaproteobacteria* were especially abundant in the root-free zone (0-10 cm, 5.7 ± 3.0%; 40-50 cm, 5.2 ± 2.4%; 60-70 cm, 7.5 ± 3.4%, Figure 12). ANOVA revealed further significant OTU-level distinctions across depths, e.g. for reads affiliated to *Bacillus*, *Paenibacillus* and *Nitrospira* spp., *Acidobacteria* Subgroup 6, *Actinobacteria* MB-A2-108 and uncultured *Gemmatimonadaceae* (*Gemmatimonadetes*; Figure 26; Table 3).

Litter amendment also appeared to induce variation in relative abundance of specific taxa. For example, reads affiliated to *Bacillus* spp. were less abundant over depth in samples with litter input (CM, Figure 26; Table 3). In contrast, litter addition significantly elevated the relative abundance of uncultured *Acidimicrobiales* and *Burkholderia-Paraburkholderia* (*Beaproteobacteria*) across depth. *Flavobacterium* spp. were more abundant in CM samples in the top and rooted soils, whereas higher in relative abundance in FM samples in the root-free soil (Table 3). Other taxa showed a significant impact of litter addition specifically in topsoil: *Arthrobacter* (*Actinobacteria*) showed a higher relative abundance under CM treatment (1.0 ± 0.4% vs. 0.7 ± 0.4%; Mann-Whitney U-test, *p* = 0.04; Figure 26), whereas *Acidobacteria* RB41 (0.6 ± 0.2% vs. 1.0 ± 0.8%, *p* = 0.003), uncultured *Rhodobiaceae* (*Alphaproteobacteria*, 3.0 ± 0.8% vs. 3.5 ± 0.4%, *p* = 0.04) and uncultured *Gemmatimonadaceae* (1.6 ± 0.3% vs. 1.9 ± 0.3%, *p* = 0.04) were less abundant in CM vs. FM topsoil.
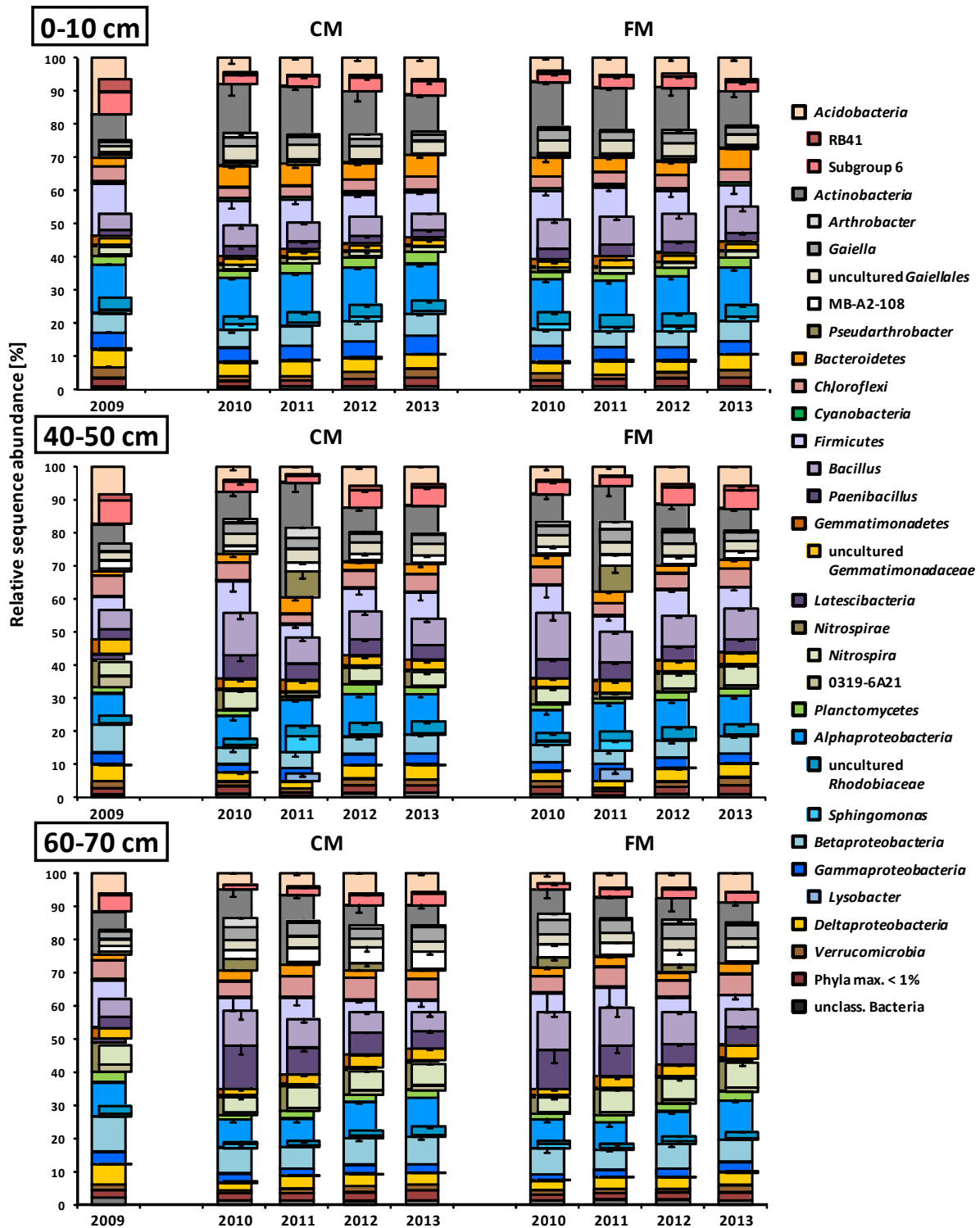
Figure 26. Relative sequence abundance for bacterial taxa obtained by amplicon sequencing of the investigated soil samples. All phyla with average relative sequence abundance > 1% in at least one soil compartment were shown. The 15 most abundant operational taxonomic units are highlighted. Values were averaged over biological triplicates except for 2009 with one single library per depth sequenced. Error bars (negative only) are given for selected taxa and represent standard error (n = 3). Sample codes are as in Figure 24.

Table 3. Two-way ANOVA results on relative sequence abundance in relation to depth, litter amendment and their interaction across years. Displayed are results for operational taxonomic units with average relative sequence abundance > 1% in at least one soil compartment. Statistically significant effects (p < 0.05) are highlighted in bold.

Operational Taxonomic Unit (OTU)	Depth (df = 2)		Litter (df = 1)		Interaction (df = 2)	
	F value	*p* value	*F* value	*p*	*F* value	*p* value
Bacillus	6.39	**< 0.01**	5.84	**0.02**	0.54	0.59
Paenibacillus	25.85	**< 0.001**	0.07	0.79	0.37	0.69
Pseudarthrobacter	3.77	**0.02785**	0.03	0.86	0.03	0.97
Nitrospira	68.74	**< 0.001**	0.27	0.61	0.02	0.98
Acidobacteria Subgroup 6	9.76	**< 0.001**	0.23	0.63	0.56	0.57
Actinobacteria MB-A2-108	75.32	**< 0.001**	0.04	0.84	0.72	0.49
Sphingomonas	3.15	**0.05**	0.17	0.68	0.93	0.40
uncultured *Gemmatimonadaceae*	28.38	**< 0.001**	2.31	0.13	0.15	0.86
uncultured *Gaiellales*	8.11	**< 0.001**	2.23	0.14	0.32	0.73
Gaiella	20.54	**< 0.001**	1.83	0.18	0.06	0.94
Acidobacteria RB41	8.30	**< 0.001**	3.55	0.06	1.46	0.24
uncultured *Rhodobiaceae*	47.65	**< 0.001**	0.46	0.50	1.57	0.22
Nitrospirales 0319-6A21	24.13	**< 0.001**	2.17	0.15	1.73	0.19
Lysobacter	4.18	**0.02**	0.28	0.60	0.10	0.90
Arthrobacter	1.24	0.30	2.21	0.14	0.06	0.95
uncultured *Nitrosomonadaceae*	7.67	**< 0.001**	0.54	0.46	0.62	0.54
Bradyrhizobium	11.91	**< 0.001**	0.38	0.54	0.32	0.73
Rhizobiales MNG7	88.81	**< 0.001**	1.28	0.26	0.31	0.74
uncultured *Chitinophagaceae*	89.24	**< 0.001**	2.19	0.14	0.53	0.59
uncultured *Anaerolineaceae*	44.12	**< 0.001**	0.43	0.51	2.54	0.09
Desulfurellaceae H16	4.86	**0.01**	0.77	0.38	0.15	0.86
Nocardioides	38.29	**< 0.001**	0.69	0.41	0.50	0.61
Agromyces	6.79	**< 0.01**	0.43	0.52	0.07	0.93
Geobacter	6.93	**< 0.01**	0.66	0.42	0.31	0.73
Latescibacteria	12.55	**< 0.001**	2.09	0.15	1.38	0.26
Oxalobacteraceae	51.93	**< 0.001**	1.68	0.20	0.79	0.46
Streptomyces	2.08	0.13	6.67	**0.01**	0.32	0.72
Burkholderia-Paraburkholderia	3.66	**0.03**	0.34	0.56	0.62	0.54
Flavobacterium	4.43	**0.02**	4.75	**0.03**	5.98	**< 0.01**
uncultured *Planctomycetaceae*	3.20	**0.05**	3.91×10^{-4}	0.98	3.14	**0.05**
uncultured *Xanthobacteraceae*	10.41	**< 0.001**	0.06	0.81	1.91	0.16
Acidobacteria Subgroup 17	14.60	**< 0.001**	0.85	0.36	0.96	0.39
Microlunatus	68.56	**< 0.001**	0.03	0.87	0.11	0.90
Verrucomicrobia OPB35 soil group	6.42	**< 0.01**	0.27	0.60	0.07	0.94
Betaproteobacteria SC-I-84	15.42	**< 0.001**	1.44	0.23	0.49	0.61
Candidatus Solibacter	34.86	**< 0.001**	0.70	0.41	0.35	0.70
uncultured *Acidimicrobiales*	11.53	**< 0.001**	5.47	**0.02**	0.09	0.92
Bryobacter	82.58	**< 0.001**	0.74	0.39	0.26	0.78
Acidibacter	46.93	**< 0.001**	5.47	**0.02**	5.31	**0.01**
Solirubrobacterales Elev-16S-1332	31.69	**< 0.001**	2.53	0.12	0.13	0.88
uncultured *Xanthomonadales*	8.28	**< 0.001**	0.10	0.76	0.81	0.45
Chthoniobacterales DA101 soil	2.03	0.14	0.13	0.72	0.02	0.98
Haliangium	16.42	**< 0.001**	1.69	0.20	3.64	**0.03**
Massilia	0.74	0.48	5.15×10^{-5}	0.99	0.61	0.55
Terrimonas	9.60	**< 0.001**	0.12	0.73	0.79	0.46
uncultured *Acidobacteriaceae*	3.23	**0.05**	1.26	0.27	0.72	0.49
Rhizobacter	1.52	0.23	1.65	0.20	0.55	0.58
Ktedonobacterales HSB OF53-F07	21.21	**< 0.001**	1.68	0.20	1.88	0.16
Acidobacteria Subgroup 11	28.73	**< 0.001**	0.02	0.88	0.14	0.87
Polaromonas	3.64	**0.03**	1.92	0.17	0.40	0.67
Pseudolabrys	6.36	**< 0.01**	0.89	0.35	0.19	0.83
Phyllobacterium	63.46	**< 0.001**	1.55	0.22	0.26	0.77
Chloroflexi KD4-96	4.14	**0.02**	0.29	0.59	0.10	0.90
Acidobacteria Subgroup 22	60.66	**< 0.001**	0.12	0.73	0.31	0.74

Several other intriguing patterns in taxa-specific abundances were observed between sampling dates. For example, in rooted soil below the plough layer, *Acidobacteria* was clearly lower in relative abundance in 2010 and 2011 compared to the other three years (2009, 16.8%; 2010-2013, CM: 7.7%, 8.4%, 9.8%, 11.0%; FM: 7.1%, 8.9%, 8.8%, 10.0%; Figure 26). A marked increase in *Actinobacteria* abundance, especially reads affiliated to *Pseudarthrobacter* spp. (2011, CM: 7.7 ± 3.7%, FM: 7.7 ± 3.1%; < 1.0% in the other years), was apparent for all 40-50 cm samples in 2011 (Figure 26). *Pseudarthrobacter* was much less abundant in other depths and all other sampling dates. A similar temporal pattern was found for reads affiliated to *Sphingomonas* and *Lysobacter* spp. in the same depth and year. *Acidobacteria* exhibited constantly increasing relative abundance over the years at 60-70 cm depth, whereas the opposite pattern was observed for *Firmicutes* in the same samples (Figure 26).

RDA was also applied across all sequencing data, to better resolve community distinctions across depth, treatments and time (Figure 27A). The first two RDA axes jointly explained 31.0% of the total variability of the bacterial communities. For the sequencing data, RDA1 seemed to be dominated by depth and differentiated the samples along soil profile (Figure 27A). PerMANOVA confirmed the significant influence of soil depth on bacterial community composition (R^2 = 0.28, p < 0.001). Reads affiliated to bacterial lineages within the *Acidobacteria* (*Bryobacter*, *Candidatus* solibacter), *Actinobacteria* (*Nocardioides*), *Bacteroidetes* (uncultured *Chitinophagaceae*), *Chloroflexi* (*Ktedonobacteria* C0119) and also the *Alphaproteobacteria* (uncultured *Rhodobiaceae*) appeared to be most representative for topsoil (Figure 27A). Reads related to *Phyllobacterium*, *Rhizobiales* MNG7 (both *Alphaproteobacteria*), *Actinobacteria* MB-A2-108 (*Actinobacteria*), *Oxalobacteraceae* (*Betaproteobacteria*), *Paenibacillus* (*Firmicutes*), *Ktedonobacterales* HSB OF53-F07, *Chloroflexi* P2-11E, uncultured *Anaerolineaceae* (*Chloroflexi*), *Acidobacteria* Subgroup 22, *Nitrospirales* 0319-6A21 and *Nitrospira* (*Nitrospirae*) were characteristic for soil at depth of 60-70 cm (Figure 27A). RDA2 seemed to be mostly influenced by sampling dates and largely separated the samples obtained in different years (Figure 27A; year effect perMANOVA: R^2 = 0.09, p < 0.001). Separation between the samples in CM plots with litter amendment and FM plots without litter,

however, was not visually apparent (Figure 27A; litter effect perMANOVA: R^2 = 0.01, p = 0.20).
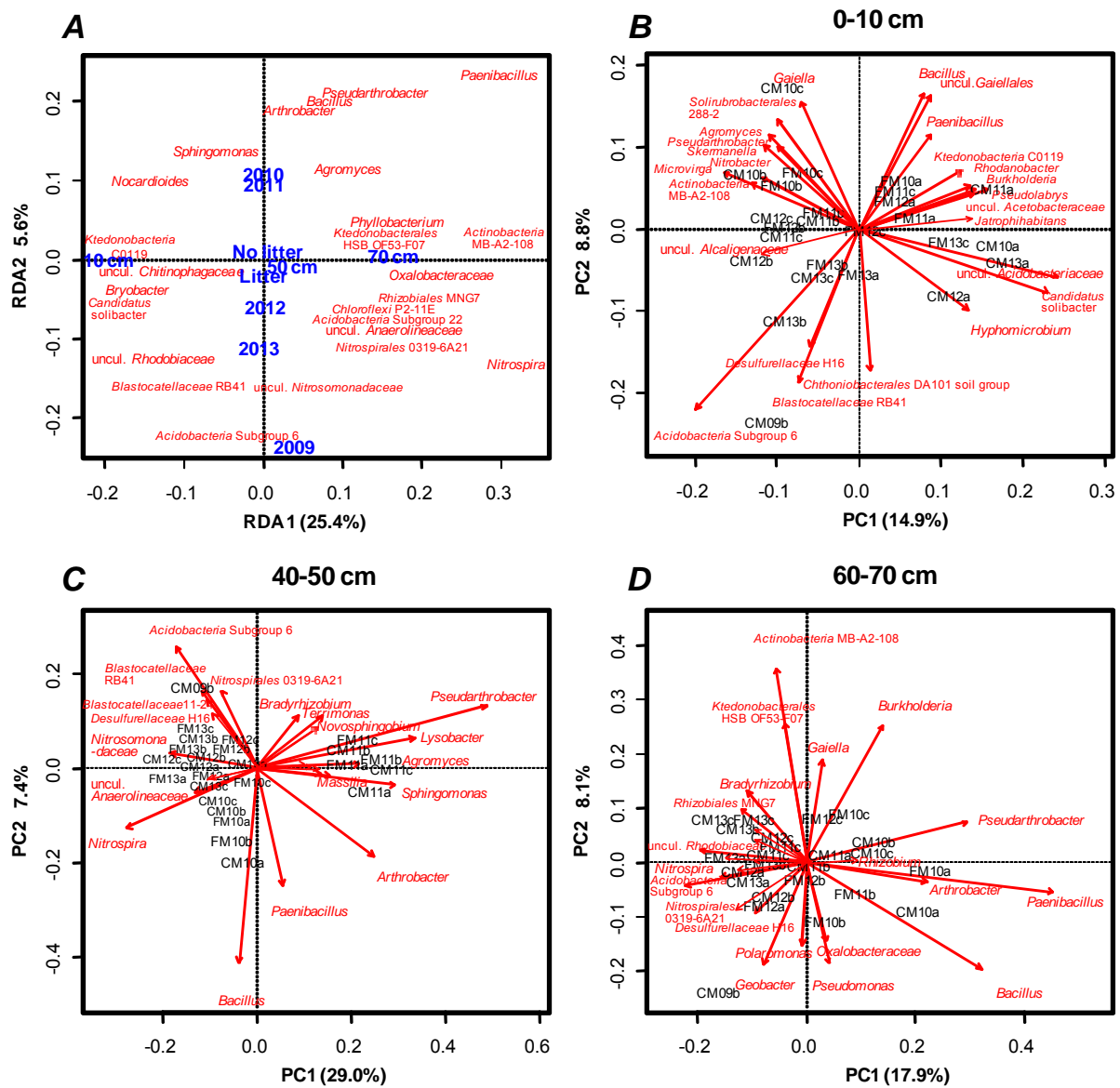
Figure 27. Ordination plots of the amplicon sequencing data. *A*, Redundancy analysis (RDA) plot of the sequencing data in relation to depth (0-10 cm, 40-50 cm and 60-70 cm), litter (litter and no litter) and year (2009 to 2013) as categorical explanatory variables across all depths. Selected operational taxonomic units (OTUs) are displayed in red. Class centroids of the explanatory variables are in blue. *B, C, D*, Principal component analysis (PCA) plots of the bacterial communities within each sampled soil depth. Selected OTUs are displayed in red with arrows indicating by length how well the corresponding OTUs are represented by the first two principal components. Individual soil samples are in black. Sample codes consist of treatment (corn maize, CM; fodder maize, FM), year (2009 to 2013, 09 to 13) and biological replicates (a, b and c).

At the same time, when statistics was done for depth-resolved data sets (depth-resolved perMANOVA), a significant litter effect was observed only for topsoil (0-10 cm: R^2 = 0.05, p = 0.03; 40-50 cm: R^2 = 0.04, p = 0.27; 60-70 cm: R^2 = 0.03, p = 0.90). This pattern was also reflected in depth-separated PCA plots (Figure 27B, C and D). Here, samples of the FM treatment formed a central cluster in PCA ordination, while CM samples were always more distant and thus seemed to undergo a larger dynamics over time (Figure 27B). Reads affiliated to unclassified *Gaiellales* (*Actinobacteria*), *Bacillus* and *Paenibacillus* (both *Firmicutes*) seemed to be characteristic for topsoil in the FM plots. On the contrary, samples at depths of 40-50 cm and 60-70 cm were hardly differentiated under treatment with vs. without litter input (Figure 27C and D). At the same time, major distinctions over time, like the increased abundance of *Pseudarthrobacter* spp. in 2011 at 50 cm depth were clearly resolved in PCA (Figure 27C).

3.3.4. Abundance and distribution of key bacterial food web constituents in the field

The distinct bacterial populations that were identified in SIP to be involved in specific carbon flows in the maize detritusphere (Kramer *et al.*, 2016), to utilise rhizodeposits (Hünninghaus *et al.*, submitted), or to act as micropredators in the field soil (this thesis) are summarized in Table 4. The different niches were mostly occupied by distinct bacterial populations with some exceptions, as several bacterial taxa were observed to be active in multiple functions.

Thus, the key bacterial food web members identified in microcosm experiments were tracked back to the field, to allow for an informed interpretation of their abundance and distribution *in situ*. Indeed, several of these bacterial taxa were also abundant in the field. *Arthrobacter* and *Flavobacterium* spp., for instance, both identified to actively degrade diverse detritusphere substrates, were amongst the most abundant bacterial genus-level lineages in the field. Moreover, several members of the *Actinobacteria*, the *Bacteroidetes* and the *Gammaproteobacteria*, either identified to be active in detritusphere carbon flows or in bacterial biomass turnover, were of consistently increased abundance in top soil.

Table 4. Key bacterial populations of the belowground food web: synthesis of detritusphere- (Kramer *et al.*, 2016), rhizosphere- (Hünninghaus *et al.*, submitted) and bacteria-labelling results and field abundance (this thesis).

Phyla & Classes	Genus- and Family-level	Labelling in SIP			Field abundance (‰)		
		Detritu-sphere	Rhizo-sphere	Micro-predation	0-10 cm	40-50 cm	60-70 cm
Actinobacteria					205.2	207.1	200.1
	Arthrobacter	++	++		8.5	11.8	11.8
	Humicoccus	++			2.5	0.3	0.3
	Kitasatospora	++			0.7	0.2	0.2
	uncl. *Micrococcaceae*	+			0.0	0.0	0.0
	Pseudonocardia		+		2.4	0.9	0.3
Bacteroidetes					53.2	29.0	26.8
	Cytophaga	+			0.4	0.0	0.1
	Flavisolibacter			++	3.5	0.5	0.4
	Flavobacterium	++			7.8	4.8	6.2
	Mucilaginibacter	+	++		0.7	0.1	0.1
	Ohtaekwangia	+	++		0.5	0.2	0.1
Planctomycetes					27.2	18.9	23.1
	Singulisphaera		++		2.2	1.0	0.8
Alphaproteobacteria					156.0	121.0	98.7
	Azospirillum		++		0.0	0.0	0.0
	Devosia			+	1.9	1.0	1.1
	Phenylobacterium			+	1.2	0.7	0.4
	Rhizobium			+	2.7	1.7	2.8
	Sphingobium		++	++	0.2	0.1	0.1
	Sphingomonas			++	14.3	14.1	8.3
Betaproteobacteria					56.7	54.5	77.2
	Massilia		++		2.7	3.1	2.1
	uncl. *Oxalobacteraceae*	+	+		0.4	0.3	0.5
	Rhizobacter		+		1.6	2.3	3.2
Deltaproteobacteria					43.0	35.3	37.6
	Byssovorax	++			0.0	0.0	0.0
	Cystobacter	++		++	0.0	0.0	0.0
	Cystobacteraceae	++		++	0.0	0.0	0.0
	Haliangium			++	8.3	5.3	5.3
	Phaselicystis			++	0.8	0.8	0.5
	Polyangiaceae	++			0.3	0.2	0.2
	Sandaracinus			++	0.2	0.1	0.0
	Sorangium	++			3.4	1.5	1.0
Gammaproteobacteria					46.2	34.6	25.8
	Arenimonas			+	2.4	0.8	0.4
	Cellvibrio	++			0.2	0.0	0.1
	Lysobacter			++	2.9	7.6	1.8
	Pseudomonas	+			0.4	1.0	2.6
	Rhodanobacter			++	3.2	0.1	0.1
	Thermomonas			++	0.1	0.0	0.0
	uncl. *Xanthomonadaceae*			++	0.5	0.5	0.6
Verrucomicrobia					20.4	16.5	14.9
	Opitutus		++		2.4	0.8	1.0

++ highly abundant or strongly enriched in labelled rRNA; + moderately detected in labelled rRNA. Colour codes for genus- and family-level average relative abundance in the sequencing libraries: red, > 0.5%; yellow, 0.1% - 0.5%; blue, < 0.1%

Comparably high abundance was also observed for *Sphingomonas* and *Haliangium* spp., both actively assimilating carbon derived from amended labelled bacterial biomass. Another potential predatory bacterial lineage, *Lysobacter* spp., was especially frequent in the rooted zone below the plough layer. In stark contrast, some key players with high activity as well as abundance in laboratory experiments were hardly observed in the field. Examples included *Kitasatospora*, *Ohtaekwangia* and *Cellvibrio* spp., all previously suggested to be specifically active in the detritusphere (Kramer *et al.*, 2016). Furthermore, *Sphingobium* spp. and *Mucilaginibacter* spp., all of which were previously placed in the detritusphere (Hünninghaus *et al.*, submitted), exhibited relative abundance below 0.2% across all libraries.

In summary, this last part of my thesis was engaged in providing comprehensive insights into long-term soil bacterial communities in the field. Under distinct treatments, plant and litter effect was revealed in rooted zone below the plough layer and the top soil, respectively, consistent with my hypothesis. Key bacterial populations identified in laboratory SIP experiments to be involved in various food web connections exhibited distinct distribution patterns in the field. These findings provide intriguing insights into link between bacterial communities and microbial function.

4. Discussion

To elucidate the roles of specific bacterial populations in belowground carbon flow and an exemplary soil food web, I conducted a ^{13}C-labelling microcosm experiment, field experiments with lysimeters as well as long-term monitoring at an arable field site planted with maize. Research questions towards intra-bacterial predation, vertical bacterial transport and long-term dynamics of soil bacterial communities *in situ* were addressed. I hypothesized that:

I)   Prey type as well as soil compartment could drive niche differentiation between bacterial micropredators and protozoa, and that intrabacterial predation by myxobacteria could be more relevant in bulk soil than in the rhizosphere.

II)   Transport of bacteria via preferential flow paths along root channels after strong precipitation events in dry summer could result in a rapid mobilisation of selective rhizosphere bacterial populations from top soil to deeper horizons. Dynamics in the composition of mobilised bacterial communities during seepage events could hint at distinct mechanisms of mobilisation and transport.

III)   Soil bacterial communities in the field respond to distinct plant and litter treatments, and that respective patterns in biomass and community distribution become increasingly apparent with the duration of given agricultural treatments.

The work within my thesis was centrally embedded in the research of the DFG FOR-918 (Carbon flow in belowground food webs assessed by isotope tracers). My research contributed to two overarching aims of the Research Unit: to identify keystone soil organisms and trophic links in a soil food web under different plant-derived resource inputs; and to integrate food web structure and carbon fluxes across microbial and faunal webs. To accomplish these goals, my thesis links the results of labelling experiments conducted in laboratory microcosms to microbial community analyses obtained in regular sampling campaigns, carried out together with the other subprojects of the Research Unit directly in the field.

4.1. Micropredator niche differentiation between bulk soil and rhizosphere depends on bacterial prey

Previous studies using nucleic acid-based SIP have unravelled microbial key players and interaction mechanisms for a number of food webs in soil (Murase & Frenzel, 2007, Drigo *et al.*, 2010, Kramer *et al.*, 2016). In the present thesis, secondary trophic interactions in the investigated soil microbial food web, or specifically the consumption of bacterial prey by competing guilds of micropredators were investigated. Marked distinctions in feeding preferences between bacterial and eukaryotic micropredators were revealed, driven by prey species and also by soil compartment.

4.1.1. Amendment and sequestration of bacterial prey

[13]C-labelled cells of *P. putida* and *A. globiformis* were amended as representative Gram-negative and Gram-positive bacterial prey. Both strains have been used previously in grazing experiments (Verhagen *et al.*, 1993, Eisenmann *et al.*, 1998), and close relatives of both have been identified as important components of the investigated soil microbiome (Dibbern *et al.*, 2014, Kramer *et al.*, 2016). Still, this rather limited selection of different prey types should not be expected to fully reflect the variety of ecological niches potentially realized by microbial predator-prey relationships in the investigated soil, but should still allow addressing the fundamental hypothesis (I) as explained above.

The similar relative abundance of both respective T-RFs after amendment (Figure 11) suggested that the two strains were successfully added in a comparable final abundance. However, it also suggested that rRNA of the amended biomass was much more abundant in the freshly amended soil than the ~2% of total bacteria as originally intended. While this could relate to biases in extracting rRNA from intrinsic soil microbiota vs. that of freshly amended cells (Wang *et al.*, 2012), it could also be attributed to a higher ribosome content of amended bacteria compared to intrinsic soil microbes, an under-quantification of the amended cells, or an over-estimation of the indigenous bacterial biomass. Quantitative DNA-targeted assays might help to resolve this, given that a genomic abundance of 5-7 *rrn* operons has been inferred for both *Pseudomonas* and *Arthrobacter* spp. (Stoddard *et al.*, 2015). Nevertheless,

as overall community structure before the amendment and after several days remained largely unchanged, the amendment did not seem to have altered indigenous bacterial communities beyond a degree that intrinsic food web functioning would no longer have been apparent.

The more rapid mineralization of *P. putida* compared to *A. globiformis* was not unexpected, as Gram-positive bacteria are generally known to be more resistant to protozoan grazing (Ronn *et al.*, 2002, Jousset, 2012) and also bacterial micropredators preferentially feed on Gram-negative bacteria (Rogosky *et al.*, 2006, Morgan *et al.,* 2010, Rotem *et al.*, 2014). Still, the drastically distinct kinetics of disappearance for both amendments in my experiment was unexpected. Choosing one "late" time point (8 d) for SIP analysis may have excluded the chance to detect transient early labelling of micropredators, especially for *P. putida*. but practically I had to focus SIP analysis on one time point. Furthermore, ^{13}C incorporation from *A. globiformis* may have been insufficient for trophic labelling at an earlier time of incubation, which is why the time point of 8 d was selected to address fundamental distinctions in micropredator prey preferences and niche segregation in this experiment.

4.1.2. Bacterial and microeukaryotic communities in rhizosphere vs. bulk soil

Total light rRNA did not suggest major distinctions in bacterial community composition for the different compartments after 8 d of incubation (Figure 13). This was surprising, since plants are known to express major selective pressures on rhizosphere microbiomes (Reinhold-Hurek *et al.*, 2015), as previously also confirmed directly at the investigated field site (Dibbern *et al.*, 2014). Potentially, the young age of the maize plants (~12 weeks) was insufficient to allow for the more pronounced development of a distinct rhizosphere microbiome in my experiment. Alternatively, the fact that the rhizosphere soil used was no longer under direct root influence during SIP incubation, albeit freshly harvested, could also have contributed to similar overall rRNA expression patterns.

Nevertheless, some minor distinctions in bacterial community composition were still apparent between compartments, such as the consistent detectability of rRNA of *Paucimonas* spp. in the rhizosphere, whereas scarcely observed in bulk soil. This

was consistent with previous findings by Dibbern *et al.* (2014) directly from the investigated field, where members of the *Oxalobacteraceae* (including *Paucimonas* spp.) were more abundant on the rhizoplane and in the rhizosphere than in bulk soil. Members of this genus have been previously reported to respond to plant secondary metabolites and to be of relevance in phytoremediation (Uhlik *et al.*, 2013).

In contrast to bacteria, profound variability was revealed for total light rRNA of microeukaryotes, depending mostly on soil compartment. For instance, ciliates of the genus *Gonostomum* were preferentially found in the rhizosphere of maize, similar as previously reported for the rhizosphere of several subtropical plants (Acosta-Mercado & Lynn, 2004). Interestingly, the rhizosphere also appeared enriched in amoeboid *Hartmanella* and kinetoplastid *Ichthyobodo* spp. Both are of pathogenic concern, either as vectors for pathogenic bacteria (Dobrowsky *et al.*, 2016) or directly for fish (Isaksen *et al.*, 2012). While especially the first have been frequently reported for agricultural soils (Takenouchi *et al.*, 2016), my observation adds to the discussion of the rhizosphere being a reservoir not only for bacterial (Berg *et al.*, 2013), but also for protistan pathogens. In bulk soil, *Vahlkampfia* spp. dominated the light rRNA libraries, especially when amended with *P. putida*. These protozoa have been previously reported for different soils (Takenouchi *et al.*, 2016, Tyml *et al.*, 2016), but the ecological relevance of such heterolobosean amoebae in soil food webs is still poorly understood. In summary, at least some of the original distinctions in microbial food web functioning between originally rooted vs. non-rooted soil were still apparent during SIP incubation.

4.1.3. Micropredator niche differentiation

The first intriguing finding amongst ^{13}C-labelled bacterial communities was the striking difference in diversity of labelled taxa in response to *P. putida* vs. *A. globiformis* amendments. Only a few selected *Myxococcales* assimilated C from amended *A. globiformis*. This very specific flow of ^{13}C to selected bacterial lineages strongly suggests that intrabacterial predation was involved. While the *Myxococcales* are an intensively investigated group of mostly facultative micropredators (Jurkevitch, 2007), the genus *Haliangium* has not been frequently reported from soils. Originally isolated from a marine environment and considered as halophilic (Fudou *et al.*, 2002), members of this genus have recently been detected in some soils (Fulthorpe *et al.*,

2008, Ding *et al.,* 2014) and were even discussed in a biocontrol context against fungal pathogens (Qiu *et al.,* 2012). The findings here demonstrate that *Haliangium* spp. are capable of predating on Gram-positive bacteria in soil.

A much larger diversity of myxobacterial lineages was indicated to be active in incorporating ^{13}C from *P. putida*. This included well-known soil myxobacteria such as the *Cystobacteraceae* (Dawid, 2000), and also several uncultured lineages. This was not unexpected, as myxobacteria have been consistently reported to preferentially prey on Gram-negatives (Morgan *et al.,* 2010). My results substantiate this prey preference for a considerable diversity of *Myxobacteria* in a complex natural soil microbiome. Also *Lysobacter* spp. appeared highly active in assimilating ^{13}C from *P. putida*, similarly as previously shown for a different soil amended with *E. coli* (Lueders *et al.,* 2006). Interestingly, labelling appeared more pronounced in the rhizosphere than in bulk soil in my experiment. Predatory behaviour of *Lysobacter* spp. in rhizosphere soils, to the best of my knowledge, has not been directly demonstrated before, but members of this genus are known as typical rhizosphere bacteria and also as biocontrol agents (Ciancio *et al.,* 2016).

For both *A. globiformis* and *P. putida* amendments, an unexpected diversity of microeukaryotes showed strong ^{13}C-labelling, suggesting a substantial flow of ^{13}C to microeukaryotes. As previously reported also for the detritusphere of the investigated soil (Kramer *et al.,* 2016), ^{13}C enrichment was found mostly in amoeboid protozoa, and prey-dependent distinctions were clearly apparent. Especially, rRNA of *Glaeseria* spp. appeared strongly labelled under *A. globiformis* amendment, irrespective of soil compartment. rRNA of *Glaeseria* spp. or closely related amoeba has recently been reported for a number of soils (Turner *et al.,* 2013, Geisen *et al.,* 2015). Their natural feeding preferences, however, have not been described. *P. putida*, in stark contrast, appeared preferentially predated by the closely related *Hartmannella* spp. in my experiment. These are known as typical free-living soil amoebae (Takenouchi *et al.,* 2016), but also as infectious agents in amoebic keratitis (Lorenzo-Morales *et al.,* 2007). To the best of my knowledge, such marked prey-dependent niche segregation for closely related amoeba in a complex soil microbiota has not been reported up to date.

One dominant amoeboid taxon with pronounced compartment-dependent activity was *Vahlkampfia* spp., which was exclusively labelled for *P. putida* in bulk soil. While the possible mechanisms explaining the apparent compartment-specific predation of this typical soil amoeba (Brown & De Jonckheere, 1999) remain unclear, they could possibly reflect slight differences in soil moisture (Rodriguez-Zaragoza *et al.*, 2005) between bulk soil and planted soil in my experiment, which despite best efforts, possibly were not fully avoidable during SIP incubation.

This first part of my thesis reveals pronounced niche differentiation between micropredators as driven by both bacterial prey and soil compartments. While intrabacterial predation was almost exclusive to Gram-negative prey and largely independent of soil compartment, both Gram-negative and Gram-positive bacterial prey was consumed by protistan predators, but with marked prey- and compartment-dependent niche differentiation. It has been repeatedly shown that protozoa with different prey preferences can alter the structure of soil bacterial communities (Ronn *et al.*, 2002, Murase *et al.*, 2006). However, in contrast to my initial hypothesis (I), clear distinctions between the importance of predation by protists versus intrabacterial predation between soil compartments were not observed. Key predators of amended bacteria in both rhizosphere and bulk soil were always represented within pro- and eukaryotic micropredators. Nevertheless, the strong prey preferences observed provide an important handle for the incorporation of competing intra-microbial predation routes into advanced soils food web models.

After focusing on the microbial food web interactions in the top soil, the next project of my thesis was aimed to investigate the translocation of rhizosphere and topsoil bacteria to deeper soil horizons with seepage water, potentially representing an underestimated link between microbial metacommunities in soil.

4.2. Successive transport of bacterial populations from plant-influenced top soil to deeper layers

With lysimeters installed in the field, I traced bacterial populations translocated from maize-influenced top soil to deeper soil horizons after extreme natural and artificial rain events in late summer. I aimed to address the dynamic composition of the

mobilised bacterial communities and reveal potentially distinct transport behaviour depending on populations and season. Seepage water was sampled in summer after a natural rainfall, and also in a simulated rain experiment to allow for better control of experimental conditions. During both sampling events, however, the difficulty of reliable seepage water collection in the field was illustrated by a considerable variability of seepage behaviour between lysimeters. After the natural rain event, Plot A seemed to be dominated by preferential flow, as indicated by a higher seepage volume and lower organic loads at 65 cm depth. In contrast, Plot B appeared to be more dominated by matrix flow, with lower seepage volumes and increasing solute concentrations over depth likely due to longer contact time between seepage water and solid phase. This illustrates the importance of local heterogeneities in hydraulic connectivity and differences in soil pore structure for seepage water formation (Cey *et al.*, 2009), even for the relatively homogeneous and regularly tilled agricultural soil at the site (Kramer *et al.*, 2012, Scharroba *et al.*, 2012). This considerable variability between lysimeters was even more apparent during the artificial rain experiment, where only two of the six installations produced seepage water at all. This could be attributed to the occurrence of diverted flow along the two compacted plow layers (at 20 and 30 cm depth) where a large share of the precipitation could have bypassed the lysimeters (Kramer *et al.*, 2012). Moreover, by assuming a mean soil porosity of 0.41 cm^{-3} cm^{-3} for the topsoil (Kramer *et al.*, 2012), the estimated pore volume of 35 L (14 L by assuming 25 vol% water content) in the upper 35 cm soil monoliths highlights the unsaturated flow conditions for the irrigation volume of 16 L. Therefore, it was not very surprising, that seepage water could not be collected from 4 out of 6 lysimeters, since a significant share of the irrigated water may have resulted in a recharge of the soil water storage at the end of the dry summer. However, the rapid arrival and high initial concentrations of the Br^- tracer, observed for LD, point to the activation of preferential flow (Jacobsen *et al.*, 1997, Cey *et al.*, 2009) along secondary macropores, most likely earthworm burrows or root-channels. Vice versa, the lower initial concentrations and slighty delayed arrival of Br^- suggested a larger contribution of matrix flow and resided soil water to seepage water in LC. It was expected, that the different contributions of preferential flow vs. matrix flow observed for the different lysimeters should also be reflected in transported microbiota.

4.2.1. Mobilised bacterial populations in summer vs. winter

In contrast to the expectation, systematic differences between the microbiota mobilised in LA/LD (more preferential flow) and LB/LC (more matrix flow) were not observed. Rather, as previously observed for decaying roots after snowmelt in winter (Dibbern *et al.*, 2014), mobilised bacterial communities always appeared highly influenced by rhizoplane communities, suggesting an importance of mobilisation via seepage flow along root channels also for live rhizosphere systems. Moreover, many dominant lineages mobilised in winter were consistently observed also in summer, such as members of the *Sphingobacteriaceae* (*Bacteroidetes*), the *Sphingomonadaceae* and *Bradyrhizobiaceae* (*Alphaproteobacteria*), the *Comamonadaceae* (*Betaproteobacteria*) and the *Legionellaceae* (*Gammaproteobacteria*). In summer, however, members of the *Bacteroidetes* (*Flavobacteriacea* and *Sphingobacteriaceae*) appeared much more enriched in seepage water. Members of both families have been previously reported as typical maize rhizosphere bacteria (Li *et al.*, 2014, Yang *et al.*, 2017). Their abundant detection in seepage water after extreme summer rainfall suggests a notable flushing effect along root channels, despite living roots are known to interact closely with associated microbes by releasing exudates, mucilage and border cells to increase the root-microbe bond (Haichar *et al.*, 2014) and counteract rhizopore water flow (Ghestem *et al.*, 2011).

Interestingly, members of the *Parcubacteria* and *Microgenomates*, both belonging to the candidate phyla previously named OD1 and OP11, respectively (Brown *et al.*, 2015), consistently appeared enriched in successive seepage water samples during the artificial rain experiment. They were not abundant in previous winter seepage (Dibbern *et al.*, 2014), but also detected in waters sampled after natural rain, albeit at much lower relative abundance (Figure 20). Since both lineages belong to the ultra-small bacteria and can pass through ~0.2 µm membranes (Luef *et al.*, 2015), it was first concerned whether they could have been introduced with the artificial rain water itself. Although the applied rain water was indeed filtered through 0.22 µm membranes, it was not checked before application for possible remaining microbial contamination, so conclusions will have to be made cautiously. However, an 'ex post' test of water originating from the same Milli-Q machine produced cell counts as low as ~10^2 ml^{-1}, approaching the detection limit. This was much lower than the ~10^7

cells ml^{-1} detected in seepage water after the artificial rain experiment, and thus could not have caused a notable contamination in seepage water sequencing libraries. Moreover, members of the *Parcubacteria* have been recently reported for several rhizosphere soils including that of maize (Correa-Galeote *et al.*, 2016, Dawson *et al.*, 2017). Therefore, my observation that these lineages may be selectively mobilised from oxic rhizosphere systems with seepage water adds a new perspective to their potential origin in the subsurface, where they are currently considered to be highly characteristic for anoxic groundwater habitats (Luef *et al.*, 2015, Nelson & Stegen, 2015).

4.2.2. Dynamics of the seepage water microbiota

Intriguing dynamics of seepage water microbiota were observed between successive fractions of seepage water sampled from the artificial rain experiment. Members of the *Chitinophagaceae*, *Sphingomonadaceae* and *Bradyrhizobiaceae* were amongst the populations with the most characteristic "early" and "late" patterns of mobilisation. Since the respective water fractions were also lowest in EC, close to the respective conductivity of the artificial rain water, it can be speculated that the mobilisation of these lineages was influenced by the comparably low ionic strength (Wang *et al.*, 2013, Choi *et al.*, 2017) of the artificial rain water. Higher concentrations of organic matter, which were also observed in early and late seepage water fractions, have also been reported to promote bacterial transport through soil (Jimenez-Sanchez *et al.*, 2015). In contrast, members of the *Parcubacteria*, *Microgenomates* and potentially pathogenic *Legionellaceae* were frequently observed in intermediate seepage fractions during transiently higher electrical conductivity. Cellular parameters like hydrophobicity (Wan *et al.*, 1994, Kim *et al.*, 2009) and surface charge (Bolster *et al.*, 2009) could have influenced mobilisation behaviour under such conditions. Alternatively, the contribution of matrix flow could have been higher in intermediate fractions, resulting in a potentially larger contribution of microbes mobilised from the soil matrix. Targeted transport experiments under controlled conditions with defined strain amendments will be necessary to further elucidate the possible regulators. In my experiment, nevertheless, the consistent observation of such mobilisation patterns between duplicate lysimeters demonstrates that different

factors controlling the detachment and mobilisation of distinct populations are effective within complex soil microbiota.

4.2.3. Low recovery of the amended *Arthrobacter globiformis*

A. globiformis cells were amended to the artificial rain experiment as a fluorescently labelled bacterial tracer. As already discussed above, members of this genus and closely related bacteria have been identified as abundant and functionally relevant in rhizosphere and bulk soil of the investigated field site (Kramer *et al.*, 2016, Hünninghaus *et al.*, submitted), which is why it was again considered as a selective, but representative microbial amendment to the soil. It is clear that a single bacterial strain will not reflect the full variety of conceivable bacterial transport behaviours effective at the site. Still, this tracer should provide an important first reference for quantifying bacterial efflux with seepage from the top soil.

Various other *Arthrobacter* strains have been used previously in bacterial transport experiments, mostly in laboratory studies (Gannon *et al.*, 1991, Wan *et al.*, 1994). *Arthrobacter* spp. typically feature lysine as diamino acids in the cell wall and are characterised by a growth cycle in which cells are rod-shaped in young cultures and coccoid in older cultures (Jones & Keddie, 2006). A low recovery of the *A. globiformis* amendment of only ~0.2 to ~0.6% in our artificial rain experiment was observed. Closely related strains have been shown to be characterised by a negative surface charge (Gannon *et al.*, 1991), which should increase transport behaviour through negatively charged soil particles. At the same time, *Arthrobacter* cells are relatively hydrophobic, which is why gas-water interfaces along the flow path can dramatically reduce cellular transport (Wan *et al.*, 1994). Nevertheless, considering maximal recovery rates of ~8% reported for *Arthrobacter* cells transported through 5 cm columns of a loam soil (Gannon *et al.*, 1991), the observed recovery in my experiment of up to ~0.6% at 35 cm depth of a natural Cambisol/Luvisol was not exceedingly low. This supports the idea that the application of labelled microbial strains isolated from or closely related to indigenous microbes can provide important insights on subsurface bacterial transport and microbial ecology (Fuller *et al.*, 2004).

In summary, selective bacterial transport, mostly along root channels occurred also in summer in the presence of living maize roots, which exerted an even stronger

selection on transported bacterial communities than the decaying roots in winter (Dibbern *et al.,* 2014). However, the recovery of amended bacterial cells and potential contribution to vertical carbon flux was low. Nevertheless, mobilised bacteria could potentially influence bacterial activity and induce shifts in communities in subsoils. Furthermore, an interesting dynamics of specific bacterial taxa during seepage events was consistently observed in two independent lysimeters, reflecting that general physiochemical characteristics of the seepage event must have regulated these patterns.

After disentangling microbial predation in the rhizosphere, as well as the vertical transport of root-associated bacterial populations to subsoil, the third part of my thesis was aimed to explore the long-term distribution patterns of soil bacterial communities in the field based on four years of consecutive monitoring.

4.3. Long-term dynamics of soil bacterial communities and key food web constituents in the field

A long-term agricultural field experiment was conducted within the frame of the DFG FOR-918, to investigate the long-term effects of carbon resource inputs and quality (determined by plant species and litter addition) on belowground food webs. This specific project contributed the investigation of the size and composition of soil bacterial communities depending on treatment, time and depth. High-throughput sequencing allowed for an in-depth examination of intrinsic soil bacteria, as well as their spatial distribution and temporal development in the investigated field soil. Previous studies on the same soil have identified specific bacterial populations that were actively involved in rhizosphere and detritusphere food webs (Kramer *et al.*, 2016, Hünninghaus *et al.*, submitted) in laboratory SIP experiments. Thus, it was possible to trace these identified specifically active populations, together with those secondary micropredators identified in my own SIP experiment (see section 3.1) back to the field, and query whether their specific functions as suggested in SIP experiments would also be reflected in respective distribution patterns in their natural habitat.

4.3.1. Plant and litter effect on overall bacterial communities

Soil bacterial communities in the rooted zone of maize and wheat plants were most clearly distinguished in overall quantity as well as in composition, thus substantiating my hypothesis (III) of a plant effect for the deeper root-influenced horizons (40-50 cm), but not for the top soil. The higher abundance of intrinsic bacteria in wheat-rooted-soil could be attributed to the larger root biomass of wheat compared to that of maize, as reported previously for this field (Kramer *et al.*, 2012). Microbial biomass has also been found to be elevated in rooted soil under wheat compared with the maize treatment, as assessed by the chloroform-fumigation-extraction method (Müller *et al.*, 2016). Interestingly, a quantitative plant effect was observed for the root-free zone (60-70 cm) in 2012, whereas it was absent for the rooted layer (40-50 cm) in the same year. Potentially, this could be connected to the transport of carbon resources from top soil to deeper soil layers with seepage water as discussed above. This is also supported by the observation of fresh maize-derived carbon in extractable organic carbon (EOC) pools obtained from the root-free zone of FM plots, which was higher than in the rooted horizon (Müller *et al.*, 2016). The EOC pool is assumed to represent the labile fraction of soil carbon and is therefore assumed to be an important substrate for soil microbial communities. Fungal communities in the same soil have also been observed to be higher in total biomass in the wheat-cropped plots compared to maize (Moll *et al.*, 2015).

Plant species also affected the bacterial community structure in my experiment, as revealed by T-RFLP fingerprinting. This was in line with many previous observations (Costa *et al.*, 2006, Haichar *et al.*, 2008, Berg & Smalla, 2009) and is suggested to relate to plant-specific root exudate profiles (Bais *et al.*, 2006, Garbeva *et al.*, 2008, Berg & Smalla, 2009). Carbon substrates of different quality are preferentially utilised by distinct bacterial groups (Kramer & Gleixner, 2008, Paterson *et al.*, 2008). Our results substantiated the strong influence of plant species on selecting for specific host-associated microbiomes, especially in their rhizosphere, but to some extent also in surrounding bulk soil compartments.

Topsoil bacterial communities were shown to be most clearly affected by litter inputs in my investigations, which was also in line with the initial hypothesis (III). Litter amendments clearly elevated the overall bacterial biomass and the effect became particularly pronounced after three years of consistent field treatments. For the same site, membrane fatty acids of both Gram-positive and Gram-negative bacteria have

been shown to be higher in CM plots with litter addition (Müller *et al.*, 2016) already in 2010. My qPCR data only substantiated a significant litter effect after 2011. Potentially, this delayed recapturing of the litter effect in bacterial rRNA genes could be method-related. The efficiency of PCR amplification can vary among samples, which could possibly have masked the differences in quantities of targeted genes between samples, and therefore also potential systematic effects (Buckeridge *et al.*, 2013). Bacterial community composition in the top soil was most clearly altered by litter addition, as revealed by both T-RFLP fingerprinting and by amplicon sequencing. Similar marked effects of litter amendment on top soil bacterial communities have been observed before (Baumann *et al.*, 2009, Pascault *et al.*, 2010).

4.3.2. Abundance and distribution of key bacterial food web constituents

Extensive laboratory experiments were conducted within the FOR-918 and also this thesis, to identify distinct microbial populations involved in specific carbon fluxes in the investigated soil and to understand their regulatory role in soil organismic food webs. Thus, SIP-microcosm experiments have been conducted to identify bacterial populations engaged in utilising carbon derived from live maize roots (Hünninghaus *et al.*, submitted), various maize litter-derived carbon substrates in the detritusphere (Kramer *et al.*, 2016) and, in my thesis, the consumption of living microbial biomass by different micropredators. In this final synthesis, I traced a number of the thus functionally categorized bacterial taxa back to the field, to elucidate whether their natural distribution patterns in the field would be consistent with their inferred contribution to food web functioning in the natural environment.

Arthrobacter spp. and *Flavobacterium* spp., for instance, both identified to be actively degrading diverse detritusphere carbon substrates, were amongst the most abundant bacterial lineages detected in the field. Occurrence of *Arthrobacter* and *Flavobacterium* spp. has been frequently reported in the rhizosphere and bulk soil of maize (Li *et al.*, 2014, Correa-Galeote *et al.*, 2016, Yang *et al.*, 2017). In accordance to their activity in the maize detritusphere found in SIP incubations (Kramer *et al.*, 2016), their relative abundance appeared higher in presence of maize litter amendments in the field. Furthermore, *Massilia* spp., members of the *Oxalobacteraceae* (both found to be active in the maize rhizosphere, *Lysobacter* spp.and *Haliangium* spp. (both identified as bacterial micropredators preying on the

Gram-negative strain) were also very abundant in the field. This suggests that at least for some of the bacterial populations extant in the field, their putative natural functions in ecological processes can be extrapolated from laboratory labelling experiments.

In stark contrast, some of the bacterial taxa observed to be highly active as well as abundant in SIP incubations, were hardly detected in the field. Examples include several detritusphere key players, *Kitasatospora*, *Ohtaekwangia* and *Cellvibrio* spp., as well as rhizosphere constituents such as *Sphingobium* and *Mucilaginibacter* spp., all of which exhibited relative abundances <0.2% across all amplicon libraries. Possibly, they were favoured in laboratory incubations and their potential activity and contribution to turnover processes in the field must be cautioned. SIP studies conducted directly in the field could possibly eliminate this caveat (DeRito *et al.*, 2005, Madsen, 2006), but would be subject to various other technical challenges in our context.

Other bacterial lineages, although not included in the taxa found to be root exudate or litter degraders, were abundant in the field, especially in deeper soils, especially *Bacillus* and *Paenibacillus* spp.. Such lineages could be assumed to thrive more on recalcitrant SOM, as fresh organic matter was used as amendments for all the SIP experiments investigated here. Indeed, for instance, *Bacillus subtilis* were found to be able to degrade complex aromatic compounds (Tam *et al.*, 2006), and proteomic analysis of related *Bacillus cereus* has revealed their capability of utilising SOM of various complexity (Luo *et al.*, 2007).

4.3.3. Connections of metacommunities over depth

As observed in this thesis and many other studies, distinct microbial communities were distributed down the soil profile (Fierer *et al.*, 2003, Agnelli *et al.*, 2004, Hansel *et al.*, 2008, Eilers *et al.*, 2012). My findings from the lysimeter experiments, however, imply a strong mechanism for translocation of microbes across community boundaries. Particularly, soil food webs in deeper soils may potentially be influenced by inputs of fresh bacteria from upper layers. Amongst the transported bacterial populations observed after rainfall, some are related to lineages previously identified to be keystone food web members. *Arthrobacter* spp. (*Micrococcaceae*) and

Pseudomonas spp. (*Pseudomonadaceae*) were identified as important sugar consumers (Kramer *et al.*, 2016). In deeper soils where recalcitrant soil organic matter prevails, it could be difficult for these bacteria to survive, and they probably would merely feed the subsoil food webs. Meanwhile, *Cytophaga* spp., *Ohtaekwangia* spp. (both *Cytophagaceae*), *Mucilaginibacter* spp. (*Sphingobacteriaceae*), *Flavobacterium* spp. (*Flavobacteriaceae*), *Oxalobacteraceae*, *Sphingobium* spp. and *Sphingomonas* spp. (*Sphingomonadaceae*), as suggested to be important degraders of complex detritusphere substrates derived from plant litter or bacterial biomass could probably find a chance to adapt to local conditions in subsoils. Numerous studies have reported survival of pathogenic bacteria in soil for considerable amount of time (Bradford *et al.*, 2013), e.g. at least over 19 weeks (Lau & Ingham, 2001). Future efforts should be made to assess the fate of indigenous topsoil bacteria mobilised to subsoil exposed to different resource and physical conditions. Also, investigations are needed to address the response to extreme precipitation events of intrinsic soil fungi, protists, nematodes and fauna, to elucidate whether event-driven mobilisation and efflux can be observed also for other trophic groups and level. To date, connections between organismic food webs of different soil depths are perceived to be patchy and irregular (Ferris, 2010, Scharroba *et al.*, 2012).

5. Conclusions and outlook

On the basis of an exemplary soil food web of an arable soil, my thesis showcases the fundamental importance of bacteria in soil food webs and carbon flow, and sheds light on several of the complex mechanisms involved. First, I provide direct evidence for intra-bacterial predation, especially by myxobacteria, and pioneering insights into the niche differentiation between bacterial and eukaryotic micropredators in the investigated soil. In contrast to my first hypothesis, I did not observe clear distinctions in the relevance of predation by protists vs. intrabacterial predation between bulk soil and rhizosphere, known as a hotspot of microbial activity. Thus, despite the different mineral and organic carbon content of the distinct compartments, neither bacterial nor protozoan micropredators seemed to be preferred. In spite of the fact that my SIP analyses did not include a strict quantitative comparison of population-level carbon fluxes (Hungate *et al.*, 2015, Uksa *et al.*, 2017), similar labelling intensities can at least be taken as an indicator of comparable predation activities. Future work is needed to more rigorously compare the quantitative importance of the two different trophic routes. This is, as far as I know, the first to show comparable cross-kingdom microbial predatory relevance. It would be highly interesting to extend this comparison to other systems, for example, aquatic ecosystems, where BALOs could be the prevailing prokaryotic predators (Jousset, 2012).

My work also shows that separate metacommunities and food webs over depth can be connected via vertical translocation of microorganisms, especially following recharge events. The transport of root-associated topsoil bacteria to deeper soil layers triggered by extreme precipitation events was more selective in summer in the presence of live root channels compared to winter. This is, to my best knowledge, the first study to demonstrate that the input of seepage water microbiota into subsoils can vary between seasonal events. Consistent with my second hypothesis, a dynamic nature of microbiota mobilised between successive fractions of collected seepage water was revealed, which has intriguing implications for various physiological characteristics of the translocated microbes (Bolster *et al.*, 2009, Kim *et al.*, 2009, Bradford *et al.*, 2013). For some populations originating from top soil, i.e. for the observed *Legionellaceae*, one should not overlook the pathogenic relevance of their mobilisation during extreme precipitation events and their fate in deeper soil and in groundwater. Numerous studies have demonstrated the leaching and spreading of

pathogens from agricultural soils to groundwater, especially under the application of manure (Bradford *et al.*, 2013, Oliver & Heathwaite, 2013). A better mechanistic understanding of microbial mobilisation and transport behaviour will be crucial for making predictions under scenarios of global change. With the increasing frequency and intensity of extreme precipitation events predicted (Min *et al.*, 2011), the impact of surface-borne microbiota and biodiversity on subsurface systems and groundwater may well require reconsideration (Küsel *et al.*, 2016). Thus, the pioneering work conducted in this thesis may initiate further research on soil microbiomes mobilised in seepage water.

Furthermore, the field experiment conducted at broader temporal and spatial scale showed a long-term regulation of soil bacterial communities by plant-derived substrate inputs. In accordance to my third hypothesis, depth and plant litter availability regulate soil bacterial communities. Several key bacterial lineages previously identified in laboratory labelling experiments to actively degrade rhizosphere or detritusphere carbon substrates, such as *Arthrobacter* spp. and *Flavobacterium* spp. were frequently observed with high abundance in the field, wheres others did not show expected distributions. This discrepancy between presence or abundance of particular organisms and microbial activity in biogeochemical processes is a primary challenge of studies attempting to link microbial communities to functions (Bier *et al.*, 2015). Possibly, such predictions may be more straightforward for specialist functions and populations, than for processes involving a huge diversity of distinct microorganism, e.g. the turnover of complex carbon substrates in the rhizosphere or detritusphere. This highlights the demand for comprehensive knowledge on mechanisms how microorganisms control biogeochemical processes and how they are influenced in turn.

This work essentially assists also in accomplishing the more overarching aims of the Research Unit, first by addressing intrabacterial vs. protozoa predation in rhizosphere and bulk soil, which adds intriguing perspectives to understanding soil food web trophic connectivities. One of the fundamental goals of microbial ecology studies is to aid in modelling and predicting ecosystem processes. Data generated in this thesis can contribute to an advanced population-based quantitative modelling of belowground carbon flow across all trophic levels involved in soil food webs, which was one of the long-term goals of the Research Unit FOR-918. Existing models of

soil carbon cycling and other biogeochemical processes include bacteria as a static and functionally homogeneous group. My thesis highlights the huge diversity, temporal dynamics, distinct spatial distribution and various functional capabilities of soil bacterial populations, suggesting that previous modelling concepts may be rather inappropriate. Indeed, incorporating information about microbial communities and genetic profiles into modelling of ecosystem processes can provide unique mechanistic insights into ecological and biogeochemical processes and also an advanced understanding of the roles of microbes in ecosystem functioning (Reed *et al.*, 2014). It is therefore imperative to integrate microbial community structure, specific functions and other relevant properties (Rousk, 2016) into ecosystem models, at an adequate level of increased model complexity.

6. References

Acosta-Mercado D & Lynn DH (2004) Soil ciliate species richness and abundance associated with the rhizosphere of different subtropical plant species. *J Eukaryot Microbiol* **51**: 582-588.

Agnelli A, Ascher J, Corti G, Ceccherini MT, Nannipieri P & Pietramellara G (2004) Distribution of microbial communities in a forest soil profile investigated by microbial biomass, soil respiration and DGGE of total and extracellular DNA. *Soil Biol Biochem* **36**: 859-868.

Aislabie J, McLeod M, Ryburn J, McGill A & Thornburrow D (2011) Soil type influences the leaching of microbial indicators under natural rainfall following application of dairy shed effluent. *Soil Res* **49**: 270-279.

Amann RI, Stromley J, Devereux R, Key R & Stahl DA (1992) Molecular and microscopic identification of sulfate-reducing bacteria in multispecies biofilms. *Appl Environ Microbiol* **58**: 614-623.

Amundson R (2001) The carbon budget in soils. *Annu Rev Earth Planet Sci* **29**: 535-562.

Anderson MJ (2001) A new method for non-parametric multivariate analysis of variance. *Austral Ecology* **26**: 32-46.

Anderson R, Wylezich C, Glaubitz S, Labrenz M & Jürgens K (2013) Impact of protist grazing on a key bacterial group for biogeochemical cycling in Baltic Sea pelagic oxic/anoxic interfaces. *Environ Microbiol* **15**: 1580-1594.

Bais HP, Weir TL, Perry LG, Gilroy S & Vivanco JM (2006) The role of root exudates in rhizosphere interactions with plants and other organisms. *Annual Review of Plant Biology* **57**: 233-266.

Banning EC, Casciotti KL & Kujawinski EB (2010) Novel strains isolated from a coastal aquifer suggest a predatory role for flavobacteria. *FEMS Microbiol Ecol* **73**: 254-270.

Baumann K, Marschner P, Smernik RJ & Baldock JA (2009) Residue chemistry and microbial community structure during decomposition of eucalypt, wheat and vetch residues. *Soil Biol Biochem* **41**: 1966-1975.

Bell T, Bonsall MB, Buckling A, Whiteley AS, Goodall T & Griffiths RI (2010) Protists have divergent effects on bacterial diversity along a productivity gradient. *Biol Lett* **6**: 639-642.

Beniston M & Stephenson DB (2004) Extreme climatic events and their evolution under changing climatic conditions. *Glob and Planet Change* **44**: 1-9.

Berg G & Smalla K (2009) Plant species and soil type cooperatively shape the structure and function of microbial communities in the rhizosphere. *FEMS Microbiol Ecol* **68**: 1-13.

Berg G, Alavi M, Schmid M & Hartmann A (2013) The rhizosphere as a reservoir for opportunistic human pathogenic bacteria. *Molecular Microbial Ecology of the Rhizosphere,* pp. 1209-1216. John Wiley & Sons, Inc.

Bernard L, Mougel C, Maron P-A*, et al.* (2007) Dynamics and identification of soil microbial populations actively assimilating carbon from ^{13}C-labelled wheat residue as estimated by DNA- and RNA-SIP techniques. *Environ Microbiol* **9**: 752-764.

Bier RL, Bernhardt ES, Boot CM*, et al.* (2015) Linking microbial community structure and microbial processes: an empirical and conceptual overview. *FEMS Microbiol Ecol* **91**: fiv113.

Blume E, Bischoff M, Reichert JM, Moorman T, Konopka A & Turco RF (2002) Surface and subsurface microbial biomass, community structure and metabolic activity as a function of soil depth and season. *Appl Soil Ecol* **20**: 171-181.

Bol R, Poirier N, Balesdent J & Gleixner G (2009) Molecular turnover time of soil organic matter in particle-size fractions of an arable soil. *Rapid Commun Mass Spectrom* **23**: 2551-2558.

Bolster CH, Haznedaroglu BZ & Walker SL (2009) Diversity in cell properties and transport behavior among 12 different environmental Escherichia coli isolates. *J Environ Qual* **38**: 465-472.

Bonkowski M (2004) Protozoa and plant growth: the microbial loop in soil revisited. *New Phytol* **162**: 617-631.

Bradford MA, Strickland MS, DeVore JL & Maerz JC (2012) Root carbon flow from an invasive plant to belowground foodwebs. *Plant Soil* **359**: 233-244.

Bradford SA, Morales VL, Zhang W, Harvey RW, Packman AI, Mohanram A & Welty C (2013) Transport and fate of microbial pathogens in agricultural settings. *Crit Rev Environ Sci Technol* **43**: 775-893.

Brown CT, Hug LA, Thomas BC, Sharon I, Castelle CJ, Singh A, Wilkins MJ, Wrighton KC, Williams KH & Banfield JF (2015) Unusual biology across a group comprising more than 15% of domain Bacteria. *Nature* **523**: 208.

Brown S & De Jonckheere JF (1999) A reevaluation of the amoeba genus *Vahlkampfia* based on SSU rDNA sequences. *Eur J Protistol* **35**: 49-54.

Buckeridge KM, Banerjee S, Siciliano SD & Grogan P (2013) The seasonal pattern of soil microbial community structure in mesic low arctic tundra. *Soil Biol Biochem* **65**: 338-347.

Buddrus-Schiemann K, Schmid M, Schreiner K, Welzl G & Hartmann A (2010) Root colonization by *Pseudomonas* sp. DSMZ 13134 and impact on the indigenous rhizosphere bacterial community of barley. *Microb Ecol* **60**: 381-393.

Cebrian J (1999) Patterns in the fate of production in plant communities. *Am Nat* **154**: 449-468.

Cey EE & Rudolph DL (2009) Field study of macropore flow processes using tension infiltration of a dye tracer in partially saturated soils. *Hydrol Process* **23**: 1768-1779.

Cey EE, Rudolph DL & Passmore J (2009) Influence of macroporosity on preferential solute and colloid transport in unsaturated field soils. *J Contam Hydrol* **107**: 45-57.

Chatzinotas A, Schellenberger S, Glaser K & Kolb S (2013) Assimilation of cellulose-derived carbon by microeukaryotes in oxic and anoxic slurries of an aerated soil. *Appl Environ Microbiol* **79**: 5777-5781.

Choi N-C, Choi J-W, Kwon K-S, Lee S-G & Lee S (2017) Quantifying bacterial attachment and detachment using leaching solutions of various ionic strengths after bacterial pulse. *AMB Express* **7**: 38.

Christensen S, Bjørnlund L & Vestergård M (2007) Decomposer biomass in the rhizosphere to assess rhizodeposition. *Oikos* **116**: 65-74.

Ciancio A, Pieterse CMJ & Mercado-Blanco J (2016) Harnessing useful rhizosphere microorganisms for pathogen and pest biocontrol. *Front Microbiol* **7**: 1620.

Cohen JE & Newman CM (1985) A stochastic theory of community food webs I. Models and aggregated data. *Proc R Soc Lond B Biol Sci* **224**: 421-448.

Cohen JE, Pimm SL, Yodzis P, Salda, xf & a J (1993) Body sizes of animal predators and animal prey in food webs. *J Anim Ecol* **62**: 67-78.

Correa-Galeote D, Bedmar EJ, Fernández-González AJ, Fernández-López M & Arone GJ (2016) Bacterial communities in the rhizosphere of amilaceous maize (*Zea mays* L.) as assessed by pyrosequencing. *Front Plant Sci* **7**: 1016.

Costa R, Götz M, Mrotzek N, Lottmann J, Berg G & Smalla K (2006) Effects of site and plant species on rhizosphere community structure as revealed by molecular analysis of microbial guilds. *FEMS Microbiol Ecol* **56**: 236-249.

Coyotzi S, Pratscher J, Murrell JC & Neufeld JD (2016) Targeted metagenomics of active microbial populations with stable-isotope probing. *Curr Opin Biotechnol* **41**: 1-8.

Culman SW, Bukowski R, Gauch HG, Cadillo-Quiroz H & Buckley DH (2009) T-REX: software for the processing and analysis of T-RFLP data. *BMC Bioinformatics* **10**: 171.

Dawid W (2000) Biology and global distribution of myxobacteria in soils. *FEMS Microbiol Rev* **24**: 403-427.

Dawson W, Hör J, Egert M, van Kleunen M & Pester M (2017) A small number of low-abundance bacteria dominate plant species-specific responses during rhizosphere colonization. *Front Microbiol* **8**: 975.

Dennis PG, Miller AJ & Hirsch PR (2010) Are root exudates more important than other sources of rhizodeposits in structuring rhizosphere bacterial communities? *FEMS Microbiol Ecol* **72**: 313-327.

DeRito CM, Pumphrey GM & Madsen EL (2005) Use of field-based stable isotope probing to identify adapted populations and track carbon flow through a phenol-degrading soil microbial community. *Appl Environ Microbiol* **71**: 7858-7865.

DeSantis TZ, Hugenholtz P, Larsen N, Rojas M, Brodie EL, Keller K, Huber T, Dalevi D, Hu P & Andersen GL (2006) Greengenes, a chimera-checked 16S rRNA gene database and workbench compatible with ARB. *Appl Environ Microbiol* **72**: 5069-5072.

Dibbern D, Schmalwasser A, Lueders T & Totsche KU (2014) Selective transport of plant root-associated bacterial populations in agricultural soils upon snowmelt. *Soil Biol Biochem* **69**: 187-196.

Dilly O, Bartsch S, Rosenbrock P, Buscot F & Munch JC (2001) Shifts in physiological capabilities of the microbiota during the decomposition of leaf litter in a black alder (*Alnus glutinosa* (Gaertn.) L.) forest. *Soil Biol Biochem* **33**: 921-930.

Ding G-C, Radl V, Schloter-Hai B, Jechalke S, Heuer H, Smalla K & Schloter M (2014) Dynamics of soil bacterial communities in response to repeated application of manure containing sulfadiazine. *PLoS One* **9**: e92958.

Dobrowsky PH, Khan S, Cloete TE & Khan W (2016) Molecular detection of *Acanthamoeba* spp., *Naegleria fowleri* and *Vermamoeba (Hartmannella)* vermiformis as vectors for *Legionella* spp. in untreated and solar pasteurized harvested rainwater. *Parasit Vectors* **9**: 539.

Drigo B, Kowalchuk GA, Knapp BA, Pijl AS, Boschker HTS & van Veen JA (2013) Impacts of 3 years of elevated atmospheric CO_2 on rhizosphere carbon flow and microbial community dynamics. *Glob Chang Biol* **19**: 621-636.

Drigo B, Pijl AS, Duyts H*, et al.* (2010) Shifting carbon flow from roots into associated microbial communities in response to elevated atmospheric CO_2. *Proc Natl Acad Sci U S A* **107**: 10938-10942.

Dumont MG & Murrell JC (2005) Stable isotope probing – linking microbial identity to function. *Nat Rev Microbiol* **3**: 499-504.

Eilers KG, Debenport S, Anderson S & Fierer N (2012) Digging deeper to find unique microbial communities: The strong effect of depth on the structure of bacterial and archaeal communities in soil. *Soil Biol Biochem* **50**: 58-65.

Eisenmann H, Harms H, Meckenstock R, Meyer EI & Zehnder AJB (1998) Grazing of a *Tetrahymena* sp. on adhered bacteria in percolated columns monitored by in situ hybridization with fluorescent oligonucleotide probes. *Appl Environ Microbiol* **64**: 1264-1269.

Ekelund F, Rønn R & Griffiths BS (2001) Quantitative estimation of flagellate community structure and diversity in soil samples. *Protist* **152**: 301-314.

Elfstrand S, Lagerlöf J, Hedlund K & Mårtensson A (2008) Carbon routes from decomposing plant residues and living roots into soil food webs assessed with ^{13}C labelling. *Soil Biol Biochem* **40**: 2530-2539.

Euringer K & Lueders T (2008) An optimised PCR/T-RFLP fingerprinting approach for the investigation of protistan communities in groundwater environments. *J Microbiol Methods* **75**: 262-268.

Feeney DS, Crawford JW, Daniell T, Hallett PD, Nunan N, Ritz K, Rivers M & Young IM (2006) Three-dimensional microorganization of the soil-root-microbe system. *Microb Ecol* **52**: 151-158.

Ferris H (2010) Contribution of nematodes to the structure and function of the soil food web. *J of Nematol* **42**: 63-67.

Fierer N, Schimel JP & Holden PA (2003) Variations in microbial community composition through two soil depth profiles. *Soil Biol Biochem* **35**: 167-176.

Foppen JWA & Schijven JF (2006) Evaluation of data from the literature on the transport and survival of *Escherichia coli* and thermotolerant coliforms in aquifers under saturated conditions. *Water Res* **40**: 401-426.

Fox J & Weisberg S (2011) *An R companion to applied regression*. Sage, Thousand Oaks (CA).

Fox O, Vetter S, Ekschmitt K & Wolters V (2006) Soil fauna modifies the recalcitrance-persistence relationship of soil carbon pools. *Soil Biol Biochem* **38**: 1353-1363.

Frankland JC (1998) Fungal succession – unravelling the unpredictable. *Mycol Res* **102**: 1-15.

Franz E, Semenov AV, Termorshuizen AJ, De Vos OJ, Bokhorst JG & Van Bruggen AHC (2008) Manure-amended soil characteristics affecting the survival of *E. coli* O157:H7 in 36 Dutch soils. *Environ Microbiol* **10**: 313-327.

Fritze H, Pietikäinen J & Pennanen T (2000) Distribution of microbial biomass and phospholipid fatty acids in Podzol profiles under coniferous forest. *Eur J Soil Sci* **51**: 565-573.

Fudou R, Jojima Y, Iizuka T & Yamanaka S (2002) *Haliangium ochraceum* gen. nov., sp. nov. and *Haliangium tepidum* sp. nov.: novel moderately halophilic myxobacteria isolated from coastal saline environments. *J Gen Appl Microbiol* **48**.

Fuller ME, Streger SH, Rothmel RK, Mailloux BJ, Hall JA, Onstott TC, Fredrickson JK, Balkwill DL & DeFlaun MF (2000) Development of a vital fluorescent staining method for monitoring bacterial transport in subsurface environments. *Appl Environ Microbiol* **66**: 4486-4496.

Fuller ME, Mailloux BJ, Zhang PF, Streger SH, Hall JA, Vainberg SN, Beavis AJ, Johnson WP, Onstott TC & DeFlaun MF (2001) Field-scale evaluation of CFDA/SE staining coupled with multiple detection methods for assessing the transport of bacteria in situ. *FEMS Microbiol Ecol* **37**: 55-66.

Fuller ME, Mailloux BJ, Streger SH, Hall JA, Zhang P, Kovacik WP, Vainberg S, Johnson WP, Onstott TC & DeFlaun MF (2004) Application of a vital fluorescent staining method for simultaneous, near-real-time concentration monitoring of two bacterial strains in an Atlantic coastal plain aquifer in Oyster, Virginia. *Appl Environ Microbiol* **70**: 1680-1687.

Fulthorpe RR, Roesch LFW, Riva A & Triplett EW (2008) Distantly sampled soils carry few species in common. *ISME J* **2**: 901-910.

Gannon JT, Manilal VB & Alexander M (1991) Relationship between cell surface properties and transport of bacteria through soil. *Appl Environ Microbiol* **57**: 190-193.

Garbeva P, Elsas JD & Veen JA (2008) Rhizosphere microbial community and its response to plant species and soil history. *Plant Soil* **302**: 19-32.

Geisen S, Koller R, Hünninghaus M, Dumack K, Urich T & Bonkowski M (2016) The soil food web revisited: Diverse and widespread mycophagous soil protists. *Soil Biol Biochem* **94**: 10-18.

Geisen S, Tveit AT, Clark IM, Richter A, Svenning MM, Bonkowski M & Urich T (2015) Metatranscriptomic census of active protists in soils. *ISME J* **9**: 2178-2190.

Gessner MO, Swan CM, Dang CK, McKie BG, Bardgett RD, Wall DH & Hättenschwiler S (2010) Diversity meets decomposition. *Trends Ecol Evol* **25**: 372-380.

Ghestem M, Sidle RC & Stokes A (2011) The influence of plant root systems on subsurface flow: implications for slope stability. *BioScience* **61**: 869-879.

Glavatska O, Müller K, Butenschoen O, Schmalwasser A, Kandeler E, Scheu S, Totsche KU & Ruess L (2017) Disentangling the root- and detritus-based food chain in the micro-food web of an arable soil by plant removal. *PLoS One* **12**: e0180264.

Gougoulias C, Clark JM & Shaw LJ (2014) The role of soil microbes in the global carbon cycle: tracking the below-ground microbial processing of plant-derived carbon for manipulating carbon dynamics in agricultural systems. *J Sci Food Agric* **94**: 2362-2371.

Grösbacher M, Spicher C, Bayer A, Obst M, Karwautz C, Pilloni G, Wachsmann M, Scherb H & Griebler C (2016) Organic contamination versus mineral properties: competing selective forces shaping bacterial community assembly in aquifer sediments. *Aquat Microb Ecol* **76**: 243-255.

Hünninghaus M, Dibbern D, Kramer S, Koller R, Pausch J, Schloter-Hai B, Urich T, Kandeler E, Bonkowski M & Lueders T (2018) Disentangling microbial carbon flows in rhizosphere and hyphosphere of maize. *PLoS One*, submitted.

Haichar FeZ, Santaella C, Heulin T & Achouak W (2014) Root exudates mediated interactions belowground. *Soil Biol Biochem* **77**: 69-80.

Haichar FeZ, Marol C, Berge O, Rangel-Castro JI, Prosser JI, Balesdent J, Heulin T & Achouak W (2008) Plant host habitat and root exudates shape soil bacterial community structure. *ISME J* **2**: 1221-1230.

Hansel CM, Fendorf S, Jardine PM & Francis CA (2008) Changes in bacterial and archaeal community structure and functional diversity along a geochemically variable soil profile. *Appl Environ Microbiol* **74**: 1620-1633.

Harcke E, Huttermann A & Kuhlwein H (1972) Studies on lytic activities of *Chondrococcus coralloides* (Myxobacterales). II. Identification of the bacteriolytic enzyme as a muramidase. *Arch Mikrobiol* **85**: 6-12.

Hartmann M, Lee S, Hallam SJ & Mohn WW (2009) Bacterial, archaeal and eukaryal community structures throughout soil horizons of harvested and naturally disturbed forest stands. *Environ Microbiol* **11**: 3045-3062.

Heimann M & Reichstein M (2008) Terrestrial ecosystem carbon dynamics and climate feedbacks. *Nature* **451**: 289-292.

Hendrick MHJ & Flury M (2001) *Uniform and preferential flow mechanisms in the vadose zone*. National Academy Press, National Research Council, Washington DC, 149-187.

Holtkamp R, van der Wal A, Kardol P, van der Putten WH, de Ruiter PC & Dekker SC (2011) Modelling C and N mineralisation in soil food webs during secondary succession on ex-arable land. *Soil Biol Biochem* **43**: 251-260.

Hungate BA, Mau RL, Schwartz E*, et al.* (2015) Quantitative microbial ecology through stable isotope probing. *Appl Environ Microbiol* **81**: 7570-7581.

Isaksen TE, Karlsbakk E, Repstad O & Nylund A (2012) Molecular tools for the detection and identification of *Ichthyobodo* spp. (*Kinetoplastida*), important fish parasites. *Parasitol Int* **61**: 675-683.

Ishii S, Ksoll WB, Hicks RE & Sadowsky MJ (2006) Presence and growth of naturalized *Escherichia coli* in temperate soils from Lake Superior watersheds. *Appl Environ Microbiol* **72**: 612-621.

Jacobsen OH, Moldrup P, Larsen C, Konnerup L & Petersen LW (1997) Particle transport in macropores of undisturbed soil columns. *J Hydrol* **196**: 185-203.

Jaesche P, Totsche KU & Kögel-Knabner I (2006) Transport and anaerobic biodegradation of propylene glycol in gravel-rich soil materials. *J Contam Hydrol* **85**: 271-286.

Janzen HH (2004) Carbon cycling in earth systems—a soil science perspective. *Agric Ecosyst & Environ* **104**: 399-417.

Jezbera J, Horňák K & Šimek K (2005) Food selection by bacterivorous protists: insight from the analysis of the food vacuole content by means of fluorescence in situ hybridization. *FEMS Microbiol Ecol* **52**: 351-363.

Jiang L & Morin Peter J (2005) Predator diet breadth influences the relative importance of bottom‐up and top‐down control of prey biomass and diversity. *The Am Nat* **165**: 350-363.

Jimenez-Sanchez C, Wick LY, Cantos M & Ortega-Calvo J-J (2015) Impact of dissolved organic matter on bacterial tactic motility, attachment, and transport. *Environ Sci and Technol* **49**: 4498-4505.

Johnke J, Cohen Y, de Leeuw M, Kushmaro A, Jurkevitch E & Chatzinotas A (2014) Multiple micro-predators controlling bacterial communities in the environment. *Curr Opin Biotechnol* **27**: 185-190.

Jones D & Keddie RM (2006) The genus *Arthrobacter. The Prokaryotes: Volume 3: Archaea Bacteria: Firmicutes, Actinomycetes,* (Dworkin M, Falkow S, Rosenberg E, Schleifer K-H & Stackebrandt E, eds.), pp. 945-960. Springer New York, New York, NY.

Jousset A (2012) Ecological and evolutive implications of bacterial defences against predators. *Environ Microbiol* **14**: 1830-1843.

Jurkevitch E (2007) Predatory behaviors in bacteria — diversity and transitions. *Microbe* **2**: 67-73.

Jurkevitch E, Minz D, Ramati B & Barel G (2000) Prey range characterization, ribotyping, and diversity of soil and rhizosphere *Bdellovibrio* spp. isolated on phytopathogenic bacteria. *Appl Environ Microbiol* **66**: 2365-2371.

Küsel K, Totsche KU, Trumbore SE, Lehmann R, Steinhäuser C & Herrmann M (2016) How deep can surface signals be traced in the critical zone? Merging biodiversity with biogeochemistry research in a central German Muschelkalk landscape. *Front in Earth Sci* **4**.

Kieft TL, Murphy EM, Haldeman DL*, et al.* (1998) Microbial transport, survival, and succession in a sequence of buried sediments. *Microb Ecol* **36**: 336-348.

Kim HN, Bradford SA & Walker SL (2009) *Escherichia coil* O157:H7 transport in saturated porous media: role of solution chemistry and surface macromolecules. *Environ Sci and Technol* **43**: 4340-4347.

Kim SB, Yavuz Corapcioglu M & Kim DJ (2003) Effect of dissolved organic matter and bacteria on contaminant transport in riverbank filtration. *J Contam Hydrol* **66**: 1-23.

Kleindienst S, Herbst F-A, Stagars M*, et al.* (2014) Diverse sulfate-reducing bacteria of the *Desulfosarcina/Desulfococcus* clade are the key alkane degraders at marine seeps. *ISME J* **8**: 2029-2044.

Knox OG, Killham K, Artz RR, Mullins C & Wilson M (2004) Effect of nematodes on rhizosphere colonization by seed-applied bacteria. *Appl Environ Microbiol* **70**: 4666-4671.

Kramer C & Gleixner G (2006) Variable use of plant- and soil-derived carbon by microorganisms in agricultural soils. *Soil Biol Biochem* **38**: 3267-3278.

Kramer C & Gleixner G (2008) Soil organic matter in soil depth profiles: Distinct carbon preferences of microbial groups during carbon transformation. *Soil Biol Biochem* **40**: 425-433.

Kramer S, Dibbern D, Moll J*, et al.* (2016) Resource partitioning between bacteria, fungi, and protists in the detritusphere of an agricultural soil. *Front Microbiol* **7**: 1524.

Kramer S, Marhan S, Ruess L*, et al.* (2012) Carbon flow into microbial and fungal biomass as a basis for the belowground food web of agroecosystems. *Pedobiologia* **55**: 111-119.

Lal R (2008) Carbon sequestration. *Philos Trans R Soc Lond B Biol Sci* **363**: 815-830.

LaMontagne MG, Schimel JP & Holden PA (2003) Comparison of subsurface and surface soil bacterial communities in California grassland as assessed by terminal restriction fragment length polymorphisms of PCR-amplified 16S rRNA genes. *Microb Ecol* **46**: 216-227.

Lane DJ (1991) 16S/23S rRNA sequencing. *Nucleic Acid Techniques in Bacterial Systematics,* (Stackebrandt E & Goodfellow M, eds.), pp. 115-175. John Wiley & Sons, New York.

Lau MM & Ingham SC (2001) Survival of faecal indicator bacteria in bovine manure incorporated into soil. *Lett Appl Microbiol* **33**: 131-136.

Leake JR, Ostle NJ, Rangel-Castro JI & Johnson D (2006) Carbon fluxes from plants through soil organisms determined by field $^{13}CO_2$ pulse-labelling in an upland grassland. *Appl Soil Ecol* **33**: 152-175.

Lee CG, Watanabe T, Sato Y, Murase J, Asakawa S & Kimura M (2011) Bacterial populations assimilating carbon from ^{13}C-labeled plant residue in soil: analysis by a DNA-SIP approach. *Soil Biol Biochem* **43**: 814-822.

Li X, Rui J, Mao Y, Yannarell A & Mackie R (2014) Dynamics of the bacterial community structure in the rhizosphere of a maize cultivar. *Soil Biol Biochem* **68**: 392-401.

Loeppmann S, Blagodatskaya E, Pausch J & Kuzyakov Y (2016a) Enzyme properties down the soil profile - A matter of substrate quality in rhizosphere and detritusphere. *Soil Biol Biochem* **103**: 274-283.

Loeppmann S, Blagodatskaya E, Pausch J & Kuzyakov Y (2016b) Substrate quality affects kinetics and catalytic efficiency of exo-enzymes in rhizosphere and detritusphere. *Soil Biol Biochem* **92**: 111-118.

Lorenzo-Morales J, Martínez-Carretero E, Batista N, Álvarez-Marín J, Bahaya Y, Walochnik J & Valladares B (2007) Early diagnosis of amoebic keratitis due to a mixed infection with *Acanthamoeba* and *Hartmannella*. *Parasitol Res* **102**: 167-169.

Lueders T, Manefield M & Friedrich MW (2004) Enhanced sensitivity of DNA- and rRNA-based stable isotope probing by fractionation and quantitative analysis of isopycnic centrifugation gradients. *Environ Microbiol* **6**: 73-78.

Lueders T, Wagner B, Claus P & Friedrich MW (2004) Stable isotope probing of rRNA and DNA reveals a dynamic methylotroph community and trophic interactions with fungi and protozoa in oxic rice field soil. *Environ Microbiol* **6**: 60-72.

Lueders T, Dumont MG, Bradford L & Manefield M (2016) RNA-stable isotope probing: from carbon flow within key microbiota to targeted transcriptomes. *Curr Opin Biotechnol* **41**: 83-89.

Lueders T, Kindler R, Miltner A, Friedrich MW & Kaestner M (2006) Identification of bacterial micropredators distinctively active in a soil microbial food web. *Appl Environ Microbiol* **72**: 5342-5348.

Luef B, Frischkorn KR, Wrighton KC*, et al.* (2015) Diverse uncultivated ultra-small bacterial cells in groundwater. *Nat Commun* **6**: 6372.

Luo Y, Vilain S, Voigt B, Albrecht D, Hecker M & Brözel VS (2007) Proteomic analysis of *Bacillus cereus* growing in liquid soil organic matter. *FEMS Microbiol Lett* **271**: 40-47.

Müller K, Kramer S, Haslwimmer H, Marhan S, Scheunemann N, Butenschön O, Scheu S & Kandeler E (2016) Carbon transfer from maize roots and litter into bacteria and fungi depends on soil depth and time. *Soil Biol Biochem* **93**: 79-89.

Madsen EL (2006) The use of stable isotope probing techniques in bioreactor and field studies on bioremediation. *Curr Opin Biotechnol* **17**: 92-97.

Manefield M, Whiteley AS, Griffiths RI & Bailey MJ (2002) RNA stable isotope probing, a novel means of linking microbial community function to phylogeny. *Appl Environ Microbiol* **68**: 5367-5373.

Marschner B, Brodowski S, Dreves A*, et al.* (2008) How relevant is recalcitrance for the stabilization of organic matter in soils? *J Plant Nutr Soil Sci* **171**: 91-110.

Martin MO (2002) Predatory prokaryotes: an emerging research opportunity. *J Mol Microbiol Biotechnol* **4**: 467-477.

Mawdsley JL, Bardgett RD, Merry RJ, Pain BF & Theodorou MK (1995) Pathogens in livestock waste, their potential for movement through soil and environmental pollution. *Appl Soil Ecol* **2**: 1-15.

Maxfield PJ, Dildar N, Hornibrook ERC, Stott AW & Evershed RP (2012) Stable isotope switching (SIS): a new stable isotope probing (SIP) approach to determine carbon flow in the soil food web and dynamics in organic matter pools. *Rapid Commun Mass Spectrom* **26**: 997-1004.

Milcu A, Partsch S, Scherber C, Weisser WW & Scheu S (2008) Earthworms and legumes control litter decomposition in a plant diversity gradient. *Ecology* **89**: 1872-1882.

Min S-K, Zhang X, Zwiers FW & Hegerl GC (2011) Human contribution to more-intense precipitation extremes. *Nature* **470**: 378.

Moll J, Goldmann K, Kramer S, Hempel S, Kandeler E, Marhan S, Ruess L, Krüger D & Buscot F (2015) Resource type and availability regulate fungal communities along arable soil profiles. *Microb Ecol* **70**: 390-399.

Moore JC & Walter DE (1988) Arthropod regulation of micro- and mesobiota in below-ground detrital food webs. *Annu Rev Entomol* **33**: 419-435.

Moore JC, McCann K & de Ruiter PC (2005) Modeling trophic pathways, nutrient cycling, and dynamic stability in soils. *Pedobiologia* **49**: 499-510.

Morgan AD, MacLean RC, Hillesland KL & Velicer GJ (2010) Comparative analysis of *Myxococcus* predation on soil bacteria. *Appl Environ Microbiol* **76**: 6920-6927.

Murase J & Frenzel P (2007) A methane-driven microbial food web in a wetland rice soil. *Environ Microbiol* **9**: 3025-3034.

Murase J, Noll M & Frenzel P (2006) Impact of protists on the activity and structure of the bacterial community in a rice field soil. *Appl Environ Microbiol* **72**: 5436-5444.

Murase J, Shibata M, Lee CG, Watanabe T, Asakawa S & Kimura M (2012) Incorporation of plant residue–derived carbon into the microeukaryotic community in a rice field soil revealed by DNA stable-isotope probing. *FEMS Microbiol Ecol* **79**: 371-379.

Nelson W & Stegen J (2015) The reduced genomes of *Parcubacteria* (OD1) contain signatures of a symbiotic lifestyle. *Front Microbiol* **6**: 713.

Nielsen UN, Ayres E, Wall DH & Bardgett RD (2011) Soil biodiversity and carbon cycling: a review and synthesis of studies examining diversity–function relationships. *Eur J Soil Sci* **62**: 105-116.

Oksanen J, Blanchet FG, Friendly M*, et al.* (2016) vegan: community ecology package.

Oliver DM & Heathwaite LA (2013) Pathogen and nutrient transfer through and across agricultural soils. *Environmental Toxicology: Selected Entries from the Encyclopedia of Sustainability Science and Technology,* (Laws EA, ed.) pp. 403-439. Springer New York, New York, NY.

Olsson PA & Johnson NC (2005) Tracking carbon from the atmosphere to the rhizosphere. *Ecol Lett* **8**: 1264-1270.

Orwin KH, Wardle DA & Greenfield LG (2006) Ecological consequences of carbon substrate identity and diversity in a laboratory study. *Ecology* **87**: 580-593.

Pascault N, Cécillon L, Mathieu O, Hénault C, Sarr A, Lévêque J, Farcy P, Ranjard L & Maron P-A (2010) In situ dynamics of microbial communities during decomposition of wheat, rape, and alfalfa residues. *Microb Ecol* **60**: 816-828.

Paterson E, Osler G, Dawson LA, Gebbing T, Sim A & Ord B (2008) Labile and recalcitrant plant fractions are utilised by distinct microbial communities in soil: Independent of the presence of roots and mycorrhizal fungi. *Soil Biol Biochem* **40**: 1103-1113.

Pausch J, Tian J, Riederer M & Kuzyakov Y (2012) Estimation of rhizodeposition at field scale: upscaling of a ^{14}C labeling study. *Plant Soil* **364**: 273-285.

Pausch J, Kramer S, Scharroba A*, et al.* (2016) Small but active – pool size does not matter for carbon incorporation in below-ground food webs. *Funct Ecol* **30**: 479-489.

Pendall E & King JY (2007) Soil organic matter dynamics in grassland soils under elevated CO_2 : Insights from long-term incubations and stable isotopes. *Soil Biol Biochem* **39**: 2628-2639.

Pilloni G, von Netzer F, Engel M & Lueders T (2011) Electron acceptor-dependent identification of key anaerobic toluene degraders at a tar-oil-contaminated aquifer by Pyro-SIP. *FEMS Microbiol Ecol* **78**: 165-175.

Pilloni G, Granitsiotis MS, Engel M & Lueders T (2012) Testing the limits of 454 pyrotag sequencing: Reproducibility, quantitative assessment and comparison to T-RFLP fingerprinting of aquifer microbes. *PLoS One* **7**: e40467.

Polis GA, Myers CA & Holt RD (1989) The ecology and evolution of intraguild predation: potential competitors that eat each other. *Annu Rev Ecol Syst* **20**: 297-330.

Poll J, Marhan S, Haase S, Hallmann J, Kandeler E & Ruess L (2007) Low amounts of herbivory by root-knot nematodes affect microbial community dynamics and carbon allocation in the rhizosphere. *FEMS Microbiol Ecol* **62**: 268-279.

Pollierer MM, Langel R, Körner C, Maraun M & Scheu S (2007) The underestimated importance of belowground carbon input for forest soil animal food webs. *Ecol Lett* **10**: 729-736.

Pruesse E, Quast C, Knittel K, Fuchs BM, Ludwig W, Peplies J & Glöckner FO (2007) SILVA: a comprehensive online resource for quality checked and aligned ribosomal RNA sequence data compatible with ARB. *Nucleic Acids Res* **35**: 7188-7196.

Qiu M, Zhang R, Xue C, Zhang S, Li S, Zhang N & Shen Q (2012) Application of bio-organic fertilizer can control *Fusarium* wilt of cucumber plants by regulating microbial community of rhizosphere soil. *Biol Fertil Soils* **48**: 807-816.

Quast C, Pruesse E, Yilmaz P, Gerken J, Schweer T, Yarza P, Peplies J & Glöckner FO (2013) The SILVA ribosomal RNA gene database project: improved data processing and web-based tools. *Nucleic Acids Res* **41**: D590-D596.

R Development Core Team (2011) A language and environment for statistical computing. R Foundation for Statistical Computing, Vienna, Austria.

Rønn R, McCaig AE, Griffiths BS & Prosser JI (2002) Impact of protozoan grazing on bacterial community structure in soil microcosms. *Appl Environ Microbiol* **68**: 6094-6105.

Reed DC, Algar CK, Huber JA & Dick GJ (2014) Gene-centric approach to integrating environmental genomics and biogeochemical models. *Proc Natl Acad Sci U S A* **111**: 1879-1884.

Reichenbach H (1999) The ecology of the myxobacteria. *Environ Microbiol* **1**: 15-21.

Reinhold-Hurek B, Bünger W, Burbano CS, Sabale M & Hurek T (2015) Roots shaping their microbiome: global hotspots for microbial activity. *Annu Rev Phytopatho* **53**: 403-424.

Rodriguez-Zaragoza S, Mayzlish E & Steinberger Y (2005) Vertical distribution of the free-living amoeba population in soil under desert shrubs in the Negev Desert, Israel. *Appl Environ Microbiol* **71**: 2053-2060.

Rogosky AM, Moak PL & Emmert EAB (2006) Differential predation by *Bdellovibrio bacteriovorus* 109J. *Curr Microbiol* **52**: 81-85.

Ronn R, McCaig AE, Griffiths BS & Prosser JI (2002) Impact of protozoan grazing on bacterial community structure in soil microcosms. *Appl Environ Microbiol* **68**: 6094-6105.

Rotem O, Pasternak Z & Jurkevitch E (2014) *Bdellovibrio* and like organisms. *The Prokaryotes: Deltaproteobacteria and Epsilonproteobacteria,* (Rosenberg E, DeLong

EF, Lory S, Stackebrandt E & Thompson F, eds.), pp. 3-17. Springer Berlin Heidelberg, Berlin, Heidelberg.

Rousk J (2016) Biomass or growth? How to measure soil food webs to understand structure and function. *Soil Biol Biochem* **102**: 45-47.

Ruess L & Ferris H (2004) Decomposition pathways and successional changes. Vol. 2 (Cook R & Hunt D, eds.), pp. 547-556. E.J. Brill, Leiden, Netherlands.

Rumpel C & Kögel-Knabner I (2011) Deep soil organic matter—a key but poorly understood component of terrestrial C cycle. *Plant Soil* **338**: 143-158.

Sadaka N & Ponge J-F (2003) Soil animal communities in holm oak forests: influence of horizon, altitude and year. *Eur J Soil Biol* **39**: 197-207.

Scharroba A, Dibbern D, Hünninghaus M*, et al.* (2012) Effects of resource availability and quality on the structure of the micro-food web of an arable soil across depth. *Soil Biol Biochem* **50**: 1-11.

Scheu S (2002) The soil food web: structure and perspectives. *Eur J Soil Biol* **38**: 11-20.

Scheu S & Setälä H (2002) Multitrophic interactions in decomposer food-webs. *Multitrophic Level Interactions,* (Hawkins BA & Tscharntke T, eds.), pp. 223-264. Cambridge University Press, Cambridge.

Scheu S, Ruess L & Bonkowski M (2005) Interactions between microorganisms and soil micro- and mesofauna. *Microorganisms in Soils: Roles in Genesis and Functions,* (Varma A & Buscot F, eds.), pp. 253-275. Springer Berlin Heidelberg, Berlin, Heidelberg.

Scheunemann N, Maraun M, Scheu S & Butenschoen O (2015) The role of shoot residues vs. crop species for soil arthropod diversity and abundance of arable systems. *Soil Biol Biochem* **81**: 81-88.

Schimel JP & Schaeffer SM (2012) Microbial control over carbon cycling in soil. *Front Microbiol* **3**: 348.

Schmidt MWI, Torn MS, Abiven S, *et al.* (2011) Persistence of soil organic matter as an ecosystem property. *Nature* **478**: 49-56.

Seccareccia I, Kost C & Nett M (2015) Quantitative analysis of *Lysobacter* predation. *Appl Environ Microbiol* **81**: 7098-7105.

Sen TK (2011) Processes in pathogenic biocolloidal contaminants transport in saturated and unsaturated porous media: a review. *Water Air Soil Pollut* **216**: 239-256.

Simon A, Bindschedler S, Job D, Wick LY, Filippidou S, Kooli WM, Verrecchia EP & Junier P (2015) Exploiting the fungal highway: development of a novel tool for the in situ isolation of bacteria migrating along fungal mycelium. *FEMS Microbiol Ecol* **91**: fiv116.

Stoddard SF, Smith BJ, Hein R, Roller BRK & Schmidt TM (2015) rrnDB: improved tools for interpreting rRNA gene abundance in bacteria and archaea and a new foundation for future development. *Nucleic Acids Res* **43**: D593-D598.

Stolp H & Starr MP (1963) *Bdellovibrio bacteriovorus* gen. et sp. n., a predatory, ectoparasitic, and bacteriolytic microorganism. *Anton Leeuw* **29**: 217-248.

Stumpp C, Lawrence JR, Hendry MJ & Maloszewski P (2011) Transport and bacterial interactions of three bacterial strains in saturated column experiments. *Environ Sci Technol* **45**: 2116-2123.

Suzuki MT & Giovannoni SJ (1996) Bias caused by template annealing in the amplification of mixtures of 16S rRNA genes by PCR. *Appl Environ Microbiol* **62**: 625-630.

Takenouchi Y, Iwasaki K & Murase J (2016) Response of the protistan community of a rice field soil to different oxygen tensions. *FEMS Microbiol Ecol* **92**: fiw104.

Tam LT, Eymann C, Albrecht D, Sietmann R, Schauer F, Hecker M & Antelmann H (2006) Differential gene expression in response to phenol and catechol reveals different metabolic activities for the degradation of aromatic compounds in Bacillus subtilis. *Environ Microbiol* **8**: 1408-1427.

Todorovic RG, Stemmer M, Tatzber M, Katzlberger C, Spiegel H, Zehetner F & Gerzabek MH (2010) Soil-carbon turnover under different crop management: Evaluation of RothC-model predictions under Pannonian climate conditions. *J Plant Nutr Soil Sci* **173**: 662-670.

Totsche KU, Jann S & Kögel-Knabner I (2007) Single event-driven export of polycyclic aromatic hydrocarbons and suspended matter from coal tar-contaminated soil. *Vadose Zone J* **6**: 233-243.

Turner TR, Ramakrishnan K, Walshaw J, Heavens D, Alston M, Swarbreck D, Osbourn A, Grant A & Poole PS (2013) Comparative metatranscriptomics reveals kingdom level changes in the rhizosphere microbiome of plants. *ISME J* **7**: 2248-2258.

Tyml T, Skulinová K, Kavan J, Ditrich O, Kostka M & Dyková I (2016) Heterolobosean amoebae from Arctic and Antarctic extremes: 18 novel strains of *Allovahlkampfia, Vahlkampfia* and *Naegleria. Eur J Protistol* **56**: 119-133.

Uhlik O, Musilova L, Ridl J, Hroudova M, Vlcek C, Koubek J, Holeckova M, Mackova M & Macek T (2013) Plant secondary metabolite-induced shifts in bacterial community structure and degradative ability in contaminated soil. *Appl Microbiol Biotechnol* **97**: 9245-9256.

Uksa M, Buegger F, Gschwendtner S*, et al.* (2017) Bacteria utilizing plant-derived carbon in the rhizosphere of *Triticum aestivum* change in different depths of an arable soil. *Environ Microbiol Rep* **9**: 729-741.

Vance-Chalcraft HD, Rosenheim JA, Vonesh JR, Osenberg CW & Sih A (2007) The influence of intraguild predation on prey suppression and prey release: a meta-analysis. *Ecology* **88**: 2689-2696.

Vandenkoornhuyse P, Mahé S, Ineson P, Staddon P, Ostle N, Cliquet J-B, Francez A-J, Fitter AH & Young JPW (2007) Active root-inhabiting microbes identified by rapid incorporation of plant-derived carbon into RNA. *Proc Natl Acad Sci U S A* **104**: 16970-16975.

Verhagen FJM, Duyts H & Laanbroek HJ (1993) Effects of grazing by flagellates on competition for ammonium between nitrifying and heterotrophic bacteria in soil columns. *Appl Environ Microbiol* **59**: 2099-2106.

von Lützow M, Kögel-Knabner I, Ludwig B, Matzner E, Flessa H, Ekschmitt K, Guggenberger G, Marschner B & Kalbitz K (2008) Stabilization mechanisms of organic matter in four temperate soils: Development and application of a conceptual model. *J Plant Nutr Soil Sci* **171**: 111-124.

Wan J, Wilson JL & Kieft TL (1994) Influence of the gas-water interface on transport of microorganisms through unsaturated porous media. *Appl Environ Microbiol* **60**: 509-516.

Wang Y, Hayatsu M & Fujii T (2012) Extraction of bacterial RNA from soil: challenges and solutions. *Microbes Environ* **27**: 111-121.

Wang Y, Bradford SA & Šimůnek J (2013) Transport and fate of microorganisms in soils with preferential flow under different solution chemistry conditions. *Water Resour Res* **49**: 2424-2436.

Wardle DA & Yeates GW (1993) The dual importance of competition and predation as regulatory forces in terrestrial ecosystems: evidence from decomposer food-webs. *Oecologia* **93**: 303-306.

Warren PH & Lawton JH (1987) Invertebrate predator-prey body size relationships: an explanation for upper triangular food webs and patterns in food web structure? *Oecologia* **74**: 231-235.

Weiss TH, Mills AL, Hornberger GM & Herman JS (1995) Effect of bacterial cell shape on transport of bacteria in porous media. *Environ Sci Technol* **29**: 1737-1740.

Winderl C, Anneser B, Griebler C, Meckenstock RU & Lueders T (2008) Depth-resolved quantification of anaerobic toluene degraders and aquifer microbial community patterns in distinct redox zones of a tar oil contaminant plume. *Appl Environ Microbiol* **74**: 792-801.

Woodward G & Hildrew AG (2002) Body-size determinants of niche overlap and intraguild predation within a complex food web. *J Anim Ecol* **71**: 1063-1074.

Yang Y, Wang N, Guo X, Zhang Y & Ye B (2017) Comparative analysis of bacterial community structure in the rhizosphere of maize by high-throughput pyrosequencing. *PLoS One* **12**: e0178425.

Yilmaz P, Parfrey LW, Yarza P, Gerken J, Pruesse E, Quast C, Schweer T, Peplies J, Ludwig W & Glöckner FO (2013) The SILVA and "All-species Living Tree Project (LTP)" taxonomic frameworks. *Nucleic Acids Res* **42**: D643-D648.

Zhang L & Lueders T (2017) Micropredator niche differentiation between bulk soil and rhizosphere of an agricultural soil depends on bacterial prey. *FEMS Microbiol Ecol* **93**: fix103.

Zhang L, Lehmann K, Totsche KU & Lueders T (2018) Selective successional transport of bacterial populations from rooted agricultural topsoil to deeper layers upon extreme precipitation events. *Soil Biology & Biochemistry* **124**:168-178.

Zhang L, Dibbern D, Schloter-Hai B & Lueders T (2018) Depth and plant litter as regulators of bacterial community composition over four years of maize cultivation in an arable soil (in preparation).

Publications and authorship clarifications

<u>Accepted manuscripts</u>

1. **Zhang L** & Lueders T (2017) **Micropredator niche differentiation between bulk soil and rhizosphere of an agricultural soil depends on bacterial prey**. *FEMS Microbiology Ecology* 93: fix103.

2. **Zhang L**, Lehmann K, Totsche KU & Lueders T (2018) **Selective successional transport of bacterial populations from rooted agricultural topsoil to deeper layers upon extreme precipitation events**. *Soil Biology & Biochemistry* 124:168-178.

<u>Pending manuscripts</u>

3. **Zhang L**, Dibbern D, Schloter-Hai B & Lueders T (2018) **Depth and plant litter as regulators of bacterial community composition over four years of maize cultivation in an arable soil** (in preparation).

1.   Zhang & Lueders: The experiment was planned by Lu Zhang and Tillmann Lueders. I conducted the experiment, applied cell counting using flow cytometry, and measured CO_2 production. The EA-IRMS analysis for biomass labelling was performed by Ramona Brejcha (Research Unit of Environmental Isotope Chemistry, HMGU). I also extracted soil RNA, performed rRNA-SIP analyses, and generated and analysed the bacterial and eukaryotic T-RFLP fingerprinting and amplicon sequencing datasets. Sequencing was done by IMGM (Martinsried). I wrote most parts of the manuscript. Tillmann Lueders revised and edited large parts of the manuscript. Parts of the manuscript were used in the introduction, methods, results and discussion of this thesis (Chapters 1.3.2, 2.2, 3.1 and 4.1).

2.   Zhang *et al.*: The experiments were planned by Lu Zhang and Tillmann Lueders, together with Andreas Schmalwasser and Kai Uwe Totsche (University of Jena). Kai Uwe Totsche and Andreas Schmalwasser installed the lysimeters. I

produced fluorescently labelled bacteria and conducted the artificial rain experiment with Andreas Schmalwasser who prepared the artificial rain water. Seepage water and soil samples were obtained by Lu Zhang and Andreas Schmalwasser. I performed cell counting using flow cytometry with the water samples. I also applied T-RFLP fingerprinting and amplicon sequencing to the water and soil samples and analysed the data. Sequencing was done by Katrin Hörmann (Group of Molecular Ecology, IGÖ) and Brigitte Schloter-Hai (Comparative Microbiome Analysis, COMI) at the Helmholtz Zentrum München for natural rain event samples, and by IMGM (Martinsried) for the artificial rain experiment samples. Andreas Schmalwasser performed the physiochemical water analyses, and Katharina Lehmann provided data analyses. The manuscript was mostly written by Lu Zhang and Tillmann Lueders. Katharina Lehmann and Kai Uwe Totsche contributed to writing of the hydrological part of the manuscript. Parts of the manuscript appear in the introduction, methods, results and discussion of this thesis (Chapters 1.4, 2.3, 3.2 and 4.2).

3.   Zhang *et al.*: Soil was sampled in the experimental arable field from joint sampling by all members of the Research Unit FOR-918. Olaf Butenschön (University of Göttingen) was responsible for field site management and leading of the field sampling compaigns, and all the other collaborative research groups (https://www.biologie.hu-berlin.de/de/gruppenseiten/oekologie/dfg)   were   also involved in soil sampling. I extracted soil DNA, generated the T-RFLP fingerprinting datasets. Sequencing was done by Katrin Hörmann (Group of Molecular Ecology, IGÖ) and Brigitte Schloter-Hai (Comparative Microbiome Analysis, COMI) at the Helmholtz Zentrum München for 2009 samples, and by IMGM (Martinsried) for the rest of the samples. Uni- and multivariate statistics for data analysis were applied by me. The qPCR assessments were performed by Gabriele Barthel (Group of Molecular Ecology, HMGU). I wrote the first draft of the manuscript. Tillmann Lueders revised and edited large parts of the manuscript. Parts of the manuscript were used in the introduction, methods, results and discussion of this thesis (Chapters 1.2, 2.1, 3.3 and 4.3).

Full list of scientific communications

Published manuscripts

1. Zhang L, Jungblut AD, Hawes I, Andersen DT, Sumner DY & Mackey TJ (2015) Cyanobacterial diversity in benthic mats of the mcmurdo dry valley lakes, Antarctica. *Polar Biol* 38: 1097-1110.
2. Zhang L & Lueders T (2017) Micropredator niche differentiation between bulk soil and rhizosphere of an agricultural soil depends on bacterial prey. *FEMS Microbiol Ecol* 93: fix103.
3. Zhang L, Lehmann K, Totsche KU & Lueders T (2018) Selective successional transport of bacterial populations from rooted agricultural topsoil to deeper layers upon extreme precipitation events. *Soil Biol Biochem* 124:168-178

Conference presentations

1. Zhang L, Dibbern D, Schmalwasser A, Totsche KU & Lueders T (2013) Selective vertical mobilisation of microbes in agriculture soils after rainfall. Poster at VAAM, Bremen.
2. Zhang L, Dibbern D & Lueders T (2013). Spatial and temporal dynamics of keystone bacterial food web members in an arable soil: from SIP microcosms back to the field. Talk at GfÖ, Potsdam.
3. Zhang L, Dibbern D & Lueders T (2014). 5-year tracking of overall soil bacterial communities and keystone bacteria involved in plant-derived carbon in a maize field. Poster at VAAM 2014, Dresden.
4. Zhang L & Lueders T (2015). Transport of plant-associated bacterial populations in an agriculture soil upon rainfall. Poster at VAAM 2015, Marburg.
5. Zhang L & Lueders T (2016). Micropredator niche differentiation in bulk soil and rhizosphere of an agricultural soil. Talk at Workshop on "Soil Food Webs", HU Berlin 2016.

Acknowledgements

Appendix

Table A1. Bacterial 16S rRNA gene abundances in bulk soil samples from the long-term field experiment assessed using qPCR as shown in Figure 24. CM: corn maize; FM: fodder maize; WL: wheat with maize litter; W: wheat.

		0-10 cm		40-50 cm		60-70 cm	
		gene copies [g^{-1}]	SE	gene copies [g^{-1}]	SE	gene copies [g^{-1}]	SE
2010	CM	2.70E+10	3.09E+09	5.95E+09	6.18E+08	2.06E+09	3.84E+08
	FM	2.61E+10	2.47E+09	6.01E+09	5.57E+08	1.95E+09	2.61E+08
	WL	3.38E+10	4.00E+09	8.26E+09	1.14E+09	3.40E+09	4.37E+08
	W	3.15E+10	2.11E+09	1.15E+10	5.97E+08	4.76E+09	1.22E+09
2011	CM	2.62E+10	3.97E+09	7.62E+09	3.55E+08	3.38E+09	3.58E+08
	FM	2.13E+10	1.83E+09	5.74E+09	3.27E+08	3.35E+09	2.75E+08
	WL	2.95E+10	2.72E+09	1.24E+10	1.60E+09	3.87E+09	5.45E+08
	W	2.83E+10	1.76E+09	8.84E+09	1.22E+09	3.42E+09	5.81E+08
2012	CM	3.36E+10	5.59E+09	1.58E+10	1.73E+09	6.46E+09	3.41E+08
	FM	2.69E+10	2.11E+09	1.40E+10	1.12E+09	4.94E+09	1.14E+09
	WL	3.99E+10	3.45E+09	1.90E+10	1.80E+09	9.51E+09	1.26E+09
	W	3.03E+10	3.43E+09	2.19E+10	2.69E+09	8.02E+09	6.77E+08
2013	CM	2.56E+10	2.56E+09	5.95E+09	9.54E+08	3.26E+09	7.95E+08
	FM	2.04E+10	1.91E+09	8.13E+09	5.98E+08	2.79E+09	2.01E+08
	WL	3.06E+10	2.54E+09	1.18E+10	1.11E+09	4.56E+09	9.13E+08
	W	2.01E+10	2.34E+09	1.20E+10	1.10E+09	6.38E+09	1.59E+09

Table A2. Number of 454 reads and average read lengths produced in sequencing of bacterial 16S and eukaryotic 18S rRNA genes from the day 8 SIP gradient fractions.

Sample	Fraction of picotitre plate	Total amplicons per pool	Total reads	Average length total reads [bp]	Quality trimmed reads	Average length trimmed reads [bp]
Bacterial 16S						
A.g. Rh ^{13}C heavy	1/4	25	4479	583	4479	512
A.g. Bs ^{13}C heavy	1/4	25	7643	566	7643	517
A.g. Rh ^{12}C heavy	1/4	25	7873	499	7873	426
A.g. Bs ^{12}C heavy	1/4	25	5026	490	5026	423
A.g. Rh ^{13}C medium	1/4	25	2699	504	2699	424
A.g. Bs ^{13}C medium	1/4	25	3181	487	3181	411
A.g. Rh ^{12}C medium	1/4	25	3421	497	3421	423
A.g. Bs ^{12}C medium	1/4	25	4127	485	4127	417
A.g. Rh ^{13}C light	1/4	25	3154	496	3154	418
A.g. Bs ^{13}C light	1/4	25	3546	474	3546	404
A.g. Rh ^{12}C light	1/4	25	3668	495	3668	422
A.g. Bs ^{12}C light	1/4	25	3861	482	3861	414
P.p. Rh ^{13}C heavy	1/4	25	9333	492	9333	419
P.p. Bs ^{13}C heavy	1/4	25	3520	473	3520	401
P.p. Rh ^{12}C heavy	1/4	25	2861	479	2859	405
P.p Bs ^{12}C heavy	1/4	25	8267	493	8267	420
P.p. Rh ^{13}C medium	1/4	25	8588	497	8588	424
P.p. Bs ^{13}C medium	1/4	25	3850	476	3850	405
P.p. Rh ^{12}C medium	1/4	25	3285	477	3285	408
P.p. Bs ^{12}C medium	1/4	25	6839	490	6839	419
P.p. Rh ^{13}C light	1/4	25	3586	492	3586	418
P.p. Bs ^{13}C light	1/4	25	2922	476	2922	406
P.p. Rh ^{12}C light	1/4	25	2407	477	2407	407
P.p. Bs ^{12}C light	1/4	25	2201	491	2201	418
Eukaryotic 18S						
A.g. Rh ^{13}C heavy	1/4	24	6706	492	6706	440
A.g. Bs ^{13}C heavy	1/4	24	6082	491	6081	438
A.g. Rh ^{12}C heavy	1/4	24	7337	491	7337	435

A.g. Bs ¹²C heavy	1/4	24	8308	485	8308	434
A.g. Rh ¹³C medium	1/4	24	8141	492	8141	436
A.g. Bs ¹³C medium	1/4	24	6909	495	6909	447
A.g. Rh ¹²C medium	1/4	24	8716	494	8715	439
A.g. Bs ¹²C medium	1/4	24	7248	497	7248	448
A.g. Rh ¹³C light	1/4	24	5463	497	5463	441
A.g. Bs ¹³C light	1/4	24	6730	496	6730	446
A.g. Rh ¹²C light	1/4	24	8556	501	8556	445
A.g. Bs ¹²C light	1/4	24	8600	493	8600	441
P.p. Rh ¹³C heavy	1/4	24	9133	506	9132	454
P.p. Bs ¹³C heavy	1/4	24	5663	485	5663	441
P.p. Rh ¹²C heavy	1/4	24	9720	494	9720	447
P.p. Bs ¹²C heavy	1/4	24	9693	467	9693	427
P.p. Rh ¹³C medium	1/4	24	8958	495	8958	445
P.p. Bs ¹³C medium	1/4	24	6893	497	6893	449
P.p. Rh ¹²C medium	1/4	24	6261	493	6259	437
P.p. Bs ¹²C medium	1/4	24	9313	467	9313	429
P.p. Rh ¹³C light	1/4	24	10880	502	10879	456
P.p. Bs ¹³C light	1/4	24	9425	499	9425	449
P.p. Rh ¹²C light	1/4	24	10328	499	10328	451
P.p. Bs ¹²C light	1/4	24	9308	474	9308	438

Table A3. Number of 454 reads and average read lengths produced in sequencing of bacterial 16S rRNA genes in seepage water, root and soil samples from the field lysimeter experiments.

Sample	Fraction of picotitre plate	Total amplicons per pool	Total reads	Average length total reads [bp]	Quality trimmed reads	Average length trimmed reads [bp]
Natural rain event samples						
Seepage B 35cm a	1/4	24	2635	487	2561	423
Seepage B 35cm b	1/4	24	3663	316	2228	418
Seepage B 65a	1/4	24	3092	470	2897	418
Seepage B 65b	1/4	24	3667	344	2456	415
LB rhizoplane a	1/4	24	4475	460	4293	398
LB rhizoplane b	1/4	24	5233	343	3792	388
LA rhizosphere	1/4	24	2755	467	2582	415
LB rhizosphere	1/4	24	3881	477	3743	405
Bulk soil B 10 cm a	1/4	24	3056	485	2972	412
Bulk soil B 10 cm b	1/4	24	2921	426	2496	413
Bulk soil B 50 cm a	1/4	24	3100	466	2870	420
Bulk soil B 50 cm b	1/4	24	2477	438	2130	418
Bulk soil B 70 cm a	1/4	24	2733	504	2704	417
Bulk soil B 70 cm b	1/4	24	3388	474	3168	422
Artificial rain experiment samples						
LC T1 a	1/4	25	4172	510	4172	431
LC T2 a	1/4	25	4734	506	4732	426
LC T3 a	1/4	25	5545	496	5545	419
LC T4 a	1/4	25	4211	505	4210	426
LC T5 a	1/4	25	6133	506	6133	429
LC T6 a	1/4	25	6442	509	6442	431
LC T1 b	1/4	22	3769	481	3769	409
LC T2 b	1/4	25	3967	487	3967	407
LC T3 b	1/4	25	3415	480	3415	407
LC T4 b	1/4	25	3227	487	3227	409
LC T5 b	1/4	25	3572	489	3572	413
LC T6 b	1/4	25	4383	488	4383	409
LD T1 a	1/4	25	6338	504	6338	420

LD T2 a	1/4	25	4921	501	4921	417
LD T3 a	1/4	25	3694	507	3694	429
LD T4 a	1/4	25	4695	502	4695	425
LD T5 a	1/4	25	4650	503	4650	427
LD T6 a	1/4	25	3790	497	3790	418
LD T1 b	1/4	25	3913	486	3913	404
LD T2 b	1/4	25	2475	480	2475	404
LD T3 b	1/4	25	4346	484	4346	411
LD T4 b	1/4	25	3767	485	3767	408
LD T5 b	1/4	25	4472	485	4472	411
LD T6 b	1/4	25	3863	480	3863	398
Bulk soil A 10 cm a	1/4	22	8827	478	8826	411
Bulk soil A 10 cm b	1/4	22	7955	479	7955	410
Bulk soil B 10 cm a	1/4	22	7172	475	7172	408
Bulk soil B 10 cm b	1/4	22	7569	473	7569	404
Bulk soil A 50 cm a	1/4	25	4864	498	4864	421
Bulk soil A 50 cm b	1/4	22	7336	479	7336	410
Bulk soil B 50 cm a	1/4	25	2529	480	2528	406
Bulk soil B 50 cm b	1/4	22	6116	469	6115	398
Bulk soil A 70 cm a	1/4	22	7079	476	7079	410
Bulk soil A 70 cm b	1/4	22	6045	473	6045	405
Bulk soil B 70 cm a	1/4	22	6334	474	6334	408
Bulk soil B 70 cm b	1/4	22	6274	467	6274	400
LA rhizoplane a	1/4	22	7011	475	7011	407
LA rhizosphere a	1/4	22	8173	476	8173	408
LA rhizoplane b	1/4	22	8514	478	8514	409
LA rhizosphere b	1/4	25	3091	480	3091	410
LB rhizosphere a	1/4	22	6701	480	6700	407
LB rhizoplane a	1/4	22	7008	474	7007	403
LB rhizosphere b	1/4	22	6449	474	6449	404
LB rhizoplane b	1/4	24	3720	470	3720	391

Table A4. Number of 454 reads and average read lengths produced in sequencing of bacterial 16S rRNA genes in bulk soil samples from the long-term field experiment.

Sample	Fraction of picotitre plate	Total amplicons per pool	Total reads	Average length total reads [bp]	Quality trimmed reads	Average length trimmed reads [bp]
0-10 cm						
2009 15 maize	1/4	24	6251	442	6158	267
2010 11 CM	1/4	24	4288	474	4288	406
2010 14 FM	1/4	24	4974	474	4974	404
2010 15 CM	1/4	24	4453	469	4453	401
2010 16 FM	1/4	24	4620	475	4620	404
2010 17 CM	1/4	24	5386	473	5386	405
2010 20 FM	1/4	24	5106	475	5106	408
2011 11 CM	1/4	24	6235	473	6235	404
2011 14 FM	1/4	24	4598	471	4598	402
2011 15 CM	1/4	24	5345	476	5345	408
2011 16 FM	1/4	24	5110	473	5110	404
2011 19 CM	1/4	24	5165	476	5165	406
2011 20 FM	1/4	24	4483	465	4483	396
2012 11 CM	1/4	24	4963	474	4963	404
2012 14 FM	1/4	24	5053	475	5053	407
2012 15 CM	1/4	24	4649	478	4649	404
2012 16 FM	1/4	24	4010	469	4010	402
2012 17 CM	1/4	24	3788	471	3788	401
2012 20 FM	1/4	24	4628	471	4628	401
2013 11 CM	1/4	24	5052	476	5052	406
2013 14 FM	1/4	24	6400	476	6400	408
2013 15 CM	1/4	24	4598	475	4598	405
2013 16 FM	1/4	24	6539	474	6539	406
2013 17 CM	1/4	24	4460	472	4460	399
2013 20 FM	1/4	24	4322	472	4322	403
40-50 cm						
2009 15 maize	1/4	24	5869	438	5791	261
2010 11 CM	1/4	24	3510	469	3510	405

2010 14 FM	1/4	24	4300	467	4300	399
2010 15 CM	1/4	24	4230	462	4230	396
2010 16 FM	1/4	24	4208	467	4208	394
2010 17 CM	1/4	24	3038	466	3038	401
2010 20 FM	1/4	24	4630	472	4630	403
2011 11 CM	1/4	24	3122	467	3122	399
2011 14 FM	1/4	24	2413	465	2413	392
2011 15 CM	1/4	24	4036	467	4036	398
2011 16 FM	1/4	24	4333	467	4333	397
2011 19 CM	1/4	24	4281	473	4281	403
2011 20 FM	1/4	24	3652	465	3652	394
2012 11 CM	1/4	24	4062	466	4062	400
2012 14 FM	1/4	24	3833	466	3833	399
2012 15 CM	1/4	24	3717	469	3717	395
2012 16 FM	1/4	24	3058	462	3058	396
2012 17 CM	1/4	24	2904	465	2904	393
2012 20 FM	1/4	24	3468	466	3468	397
2013 11 CM	1/4	24	4846	469	4846	399
2013 14 FM	1/4	24	4080	467	4080	399
2013 15 CM	1/4	24	4197	467	4196	399
2013 16 FM	1/4	24	5240	468	5240	401
2013 17 CM	1/4	24	4547	463	4547	391
2013 20 FM	1/4	24	3921	466	3921	399

60-70 cm

2009 15 maize	1/4	24	6422	440	6305	266
2010 11 CM	1/4	25	4380	471	4380	413
2010 14 FM	1/4	25	4863	472	4863	410
2010 15 CM	1/4	25	4609	468	4609	405
2010 16 FM	1/4	25	4373	474	4373	405
2010 17 CM	1/4	25	5127	471	5127	409
2010 20 FM	1/4	25	6050	477	6050	412
2011 11 CM	1/4	25	4633	469	4633	407
2011 14 FM	1/4	25	4276	468	4276	402
2011 15 CM	1/4	25	5413	475	5413	411

139

2011 16 FM	1/4	25	5786	471	5786	409
2011 19 CM	1/4	25	6144	475	6144	410
2011 20 FM	1/4	25	3946	466	3946	399
2012 11 CM	1/4	25	5183	469	5183	406
2012 14 FM	1/4	25	3991	472	3991	408
2012 15 CM	1/4	25	4472	478	4472	407
2012 16 FM	1/4	25	4580	470	4579	405
2012 17 CM	1/4	25	3965	470	3964	398
2012 20 FM	1/4	25	5306	472	5306	409
2013 11 CM	1/4	25	5838	472	5838	406
2013 14 FM	1/4	25	4656	474	4656	409
2013 15 CM	1/4	25	6060	474	6060	409
2013 16 FM	1/4	25	5487	471	5486	407
2013 17 CM	1/4	25	4055	468	4055	399
2013 20 FM	1/4	25	4435	472	4435	407